

Combining astrometric and radial velocity data for exoplanet detection

Viktor Holmelin

Lund Observatory
Lund University



2013-EXA75

Degree project of 60 higher education credits (for a degree of Master)
June 2013

Supervisors: David Hobbs and Lennart Lindegren

Lund Observatory
Box 43
SE-221 00 Lund
Sweden

Abstract

Context: The Gaia satellite will be provide astrometry with micro-arcsecond accuracy. This will allow for the determination of the orbital elements of exoplanets with measurable astrometric signature. Astrometry alone is not be able to disentangle an ambiguity in the orientation of planetary orbits, just as radial velocity is only able to give the mass of orbiting planets combined with multiplicative factor. Combining astrometry and radial velocity this can be resolved. Many different approaches exist of how to parameterize and solve the problem of finding the orbital parameters. This text takes a look at one parametrization and one method for solving the problem.

Aim: Define a model for the parametrization of the problem of finding the orbital elements for an exoplanet. This model should both describe the astrometric and radial velocity. Implement the model in *AGISLab* and determine how well it is able to retrieve the orbital elements.

Method: The problem was parameterized using Thiele-Innes parameters for describing the orientation and semi-major axis of the system. Further parameters were; mass ratio of the planet to the star, time of periapsis passage, eccentricity of the orbit and period. In addition, the astrometric parameters were also included; position, parallax and proper motion. Radial motion was not included. The Levenberg-Marquardt algorithm was used for the optimization. Boundaries on the planetary parameters were introduced, in order to prevent unrealistic solutions, through transformations. The transformation of the parameters was a standard trigonometric function. To estimate the formal errors on the optimized parameters, parametric bootstrapping was performed.

Result: The optimization works and provides sensible parameters, though the solution is very sensitive to the initial selection of parameters. Singular value decomposition of the matrix $\mathbf{J}^T\mathbf{W}\mathbf{J}$, the Hessian of the merit function, indicates that the problem is ill-conditioned so bootstrapping may be a better solution for computing formal errors on the parameters than calculating them from the square root of the diagonal elements of its inverse. Bootstrapping also indicates that the formal errors of the parameters are not normally distributed.

Conclusion: The method does work and allows for very easy combination of radial velocity and astrometric data. Due to the choice of parametrization and/or optimization procedure the method is unstable.

Populärvetenskaplig sammanfattning

I höst kommer rymdobservatoriet Gaia att sändas upp. Ett av dess mål är att mäta positionen av stjärnor med väldigt hög noggrannhet, denna positionsbestämning kallas astrometri. Gaias noggrannhet är såpass bra att det kommer bli möjligt att även mäta hur planeter när de färdas i sina banor runt stjärnor påverkar positionen av stjärnan. Astrometri kan inte ge en fullständig bild av hur planeten rör sig runt stjärnan utan kan endast se en projektion,

En annan metod för planetdetektion är radiell hastighet. Detta går ut på att man mäter hur snabbt en stjärna rör sig bort eller emot oss på grund av en planet i omloppsbanan. Denna metod kan inte heller ge en fullständig bild av hur planeten rör sig.

Genom att kombinera astrometri och radiell hastighet är det möjligt att ge en fullständig beskrivning av deras bana.

Här presenteras en metod att kombinera radiell hastighet och astrometri genom att utnyttja att några av parametrarna är desamma för de två tillvägagångssätten.

Dessvärre visar det sig att denna metod lider av några brister vilket gör att även om en beskrivning av planetbanan hittas är den väldigt osäker.

Contents

Abstract	iii
1 Introduction	1
1.1 Overview	1
1.2 History and Gaia	5
1.3 AGIS and AGISLab	10
1.3.1 AGIS	10
1.3.2 AGISLab	12
1.4 Brief overview of exoplanet detection	15
1.4.1 Radial Velocity	15
1.4.2 Astrometry	20
1.4.3 Timing	21
1.4.4 Micro-lensing	23
1.4.5 Direct Imaging	23
1.4.6 Transits	24
1.5 Other but similar investigations	24
1.5.1 Efficient fitting of multiplanet keplerian models to radial velocity and astrometry data	24
1.5.2 Double-blind test program for astrometric planet detection with Gaia	26
1.5.3 Unconstrained astrometric orbits for <i>HIPPARCOS</i> stars with stochastic solutions	26
1.5.4 Astrometric planet detection with Gaia, a short AGISLab study	27
1.5.5 Detectability of terrestrial planets in multi-planet systems: Preliminary report	28
1.5.6 Reduction of the astrometric binaries	28
1.5.7 A new algorithm for fitting orbits of multiple-planet systems to combined RV and astrometric data	29
1.6 Outline	29
2 Method	31
2.1 The system	31
2.2 Planetary model	32
2.3 Astrometric data	36
2.4 Radial velocity data	37
2.5 Levenberg-Marquardt	37
2.6 SVD and Bootstrapping	38

3	Results	41
3.1	Simple Bootstrap	41
3.1.1	Only astrometric variables	41
3.1.2	Astrometric and no orientation	45
3.1.3	Astrometric and orientation	49
3.2	Parametric bootstrap	52
3.2.1	Only astrometric variables	52
3.2.2	Astrometric and no orientation	55
3.2.3	Astrometric and orientation	57
3.3	Bootstrapping and including radial velocity	60
4	Conclusion	61
	Bibliography	63
A	Kepler's Laws	65
A.1	Ellipses	67
A.1.1	Cylindrical coordinates	70
A.2	A two body system	71
A.3	Kepler's Laws	80
A.3.1	First Law	80
A.3.2	Second Law	80
A.3.3	Third Law	80
A.3.4	Calculations of orbital period for artificial systems	81
B	Thiele-Innes Parameters	83
B.1	Rotations	83
B.1.1	Random points on the sphere	88
C	Levenberg-Marquardt	91
C.1	The problem	91
C.1.1	Gauss-Newton	92
C.1.2	Gradient descent	93
C.1.3	Levenberg-Marquardt	93
C.2	Partial derivatives	94
C.3	Optimization with boundary conditions	101
C.4	Optimization with penalties	101
C.5	How it was implemented	101
C.5.1	Boundaries for eccentricity	103
C.5.2	Semi-major axis	104
C.5.3	Thiele-Innes parameters	104
C.5.4	Period	104
C.5.5	Time of periapsis passage	105
C.5.6	Mass ratio	105
C.6	Construction of the Jacobian	105

D Testing of Code	109
D.1 Spread of observations points in time	109
D.2 Residuals when knowing the period	109

1 Introduction

Modern astrometry is still concerned with the same basic idea as the ancient predecessors, measuring the position of stars on the sky. As time has gone by, the precision and accuracy of the measurements and the brightness of the observed objects have changed. Objects which cannot be seen by the naked eye are now observed to a precision far surpassing previous measurements.

The increase in precision from Gaia will make it possible to measure the ever so slight wobble of a star induced by an orbiting planet. How this slight wobble is translated into parameters describing the orbit is the purpose of this project.

The Gaia mission is an *astrometry* mission primarily concerned with measuring the *position, distance* and *motion* of stars and other heavenly bodies such as asteroids, quasars etc. Launch of the spacecraft is planned to the latter part of 2013.

A introduction will be given to astrometry and Gaia. This is then followed by a short presentation of AGIS and AGISLab and their relation to Gaia. Different techniques for exoplanet detection are summarized. An overview of similar, to what is covered in this, works is given in the end.

1.1 Overview

This fall Gaia will be launched. It will be placed in orbit at the second Lagrange point, that is on the far side of the Earth as seen from the Sun. There it will slowly rotate and scan the sky, measuring the position of the stars. The accuracy will be good enough, that the ever so slight offset in the position of the star due to an orbiting planet will be measurable.

In Section 1.6 an overview is given of what will be presented in this thesis and the results of it. So it is possible to jump straight there, read it, and then come back here as an alternative route.

The motion around the Sun will have the effect that stars appear to move due to the parallax effect. For a given time the position of the star will then be the nominal position (taken as the position the star will have at mid-mission) with the addition of the parallax displacement. Further, the star will also move through space with a proper motion which will be measurable, and this proper motion also has to be taken into account when describing the position of the star. There will be a radial component of this proper motion, but to measure this means to measure the change in parallax over the mission and in general be very small so it will be

neglected from here on. In Figure 1.1 these effects are shown. The mid mission point is given by the coordinates (α_0, δ_0) . Due to the parallax ϖ and proper motion μ_{α^*} and μ_δ the star will appear to move in a spiral pattern.

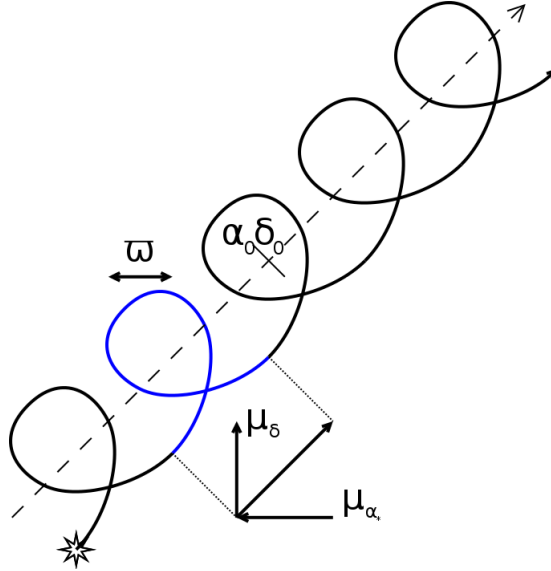


Figure 1.1: The position of the star will at some reference point in time (mid point of mission) be given by α_0 and δ_0 . Due to the motion of Gaia around the Sun, the position of the star will appear to trace out an ellipse. This is due to the parallax, and the half angle is given by ϖ . The star will also have a motion through space. The motion in right ascension and declination is given by μ_{α^*} and μ_δ respectively, where the $*$ on μ_{α^*} denotes that also the declination has been taken into account. There is also a radial motion, μ_R but this will generally be hard to measure as it would amount to measure the increasing or decreasing parallax as the star moves.

Next thing to describe is the orbit of the planet around the center of mass. This can be done through the semi major axis and eccentricity of the orbit, that is, the size and how elliptical the orbit is. What is also needed is something to describe where in the orbit the planet is for a given time. One way to define that is through the eccentric anomaly¹. To calculate the eccentric anomaly, Kepler's equation has to be solved. Unfortunately there is no analytical expression for the solution so instead some numerical solution has to be performed. Kepler's equation involves the period of the orbit, and the time of periapsis passage. The time of periapsis passage is the point in time when the planet is closest to the center of mass. With these parameters and expressions it is possible to describe the orbit of the planet in full.

When the planet orbits the center of mass, it will be tugging on the star so that too will make an orbit around the center of mass similar to the planet. The star's orbit will however be much smaller due to the much larger mass of the star, and it will be opposite to the orbit of the planet. In Figure 1.2 to the left the planet's orbit is described in the xy -plane, it will tug

¹In Figure A.1 the relation between the eccentric anomaly and the position of the planet in its orbit is further described, also the true anomaly is shown. The difference between the eccentric and true anomaly is that the true anomaly is an angle measuring the position of the planet in its orbit with the center of mass as vertex, whereas the eccentric anomaly is measuring the angle to a related position on the auxiliary circle. Still, it can be thought of as just a way to describe where the planet is in its orbit at a given time.

the star around in the same plane as to the right in the same figure. So from knowing how the planet moves it is possible to determine how the star will move.

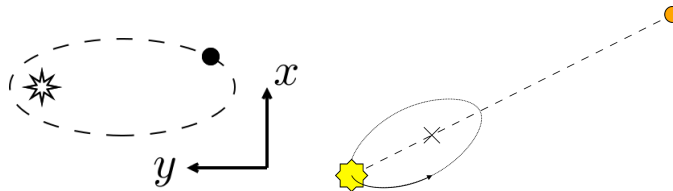


Figure 1.2: **Left:** Depiction of planet in orbit around a star. The focus of the ellipse describing the orbit is not centered on the star, instead it is at the center of mass of the system. **Right:** As the planet orbits the center of mass, it will tug on the star. The ellipse describing the motion of the star will be similar to the one for the planet, only scaled by the mass ration of the planet to the star. That is, if the star is one thousand times heavier than the planet, then the ellipse of the stars orbit will be one thousand times smaller than the ellipse of the planets orbit.

This tugging will introduce an additional offset of the stars position to be included in addition to the parallax and proper motion. In Figure 1.3 this is shown as a much enlarged effect. With no planet tugging the star would move according to the blue line, just the parallax and proper motion affecting its position. But as the planet moves, it will give this additional contribution to the position so the star will be moving on the red line.

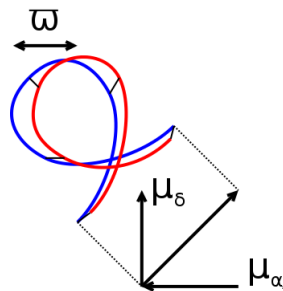


Figure 1.3: If the motion of the star due to the tugging of the planet from Figure 1.2 is super-imposed on the proper motion and parallax of the star from Figure 1.1, then there will be a slight contribution from the planet. Compared to just the parallax of the star, the tugging of the planet will include a factor for the mass ratio of the planet to the star and in general be much smaller than the parallax.

The orbit of the planet could be oriented in any way in relation to the observer. In Figure 1.4 three rotations are shown as one way to perform this orientation of the orbit in relation to the observer. If the observer is looking down at the star and planet along the Z -axis the orientation could be thought of as first creating the planets orbit in the XY -plane, performing one rotation around the Z -axis, followed by a rotation around the X -axis and finally once again around the Z -axis. This would result in the planets orbit being oriented to the observer in some particular fashion. This amounts to some linear transformation of the coordinates for the orbit from the xy -system to describe the position of the planet in the XYZ -system. Instead of using cos and sin terms of the three rotations, the transformations could be described by the Thiele-Innes parameters. Basically just six numbers describing the linear transformation.

Only six are needed as when describing the orbit of the planet initially it has $z = 0$, so any transformation of the z component is zero.

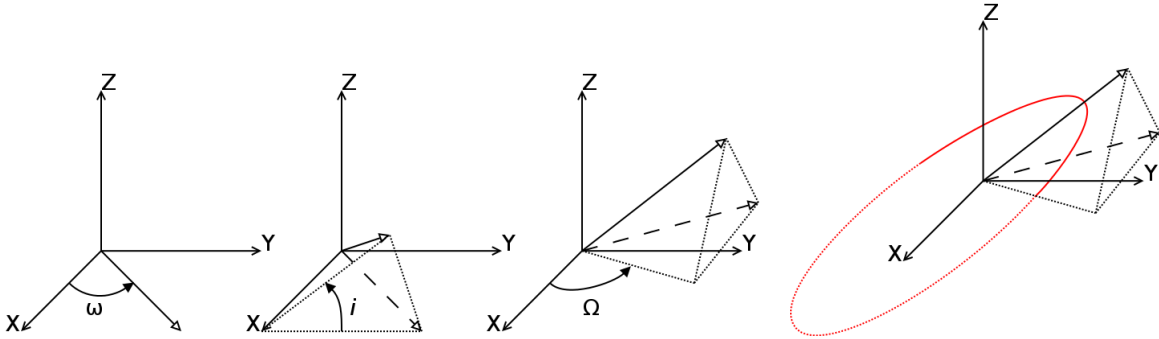


Figure 1.4: **Left:** The three pictures on the left describe a sequence of three rotations. These three rotations will orient the orbit with respect to the observer (looking down the Z -axis). **Right:** The orbit of the star around the center of mass in the XYZ -system. The full red line is when the star is “above” the XY -plane, and the dotted red line when it is “below”.

A number of different coordinate systems has been used to describe various things this far. In Figure 1.5 the relation between the different coordinate systems are shown. The observer is in the black XYZ -system in which the position to the star is given by α and δ , right ascension and declination respectively. The star is some distance away, which could be calculated from the measured parallax, in the gray XYZ -system. This gray XYZ -system is partially aligned with the normal triad $[p, q, r]$. The gray X -axis is parallel to the q -axis pointing in the direction of increasing declination, the gray Y -axis is parallel to the p -axis pointing in the direction of increasing right ascension, and the gray Z -axis is pointing in the opposite direction to the r -axis pointing in the radial direction to the star. It was in the gray XYZ -system that the planetary orbit was described, and also in the same which the offsets of the stars position was calculated due to the tugging of the planet. In addition to these, Gaia will have its own coordinate system where measurements will be made in. Due to the complicated scanning motion of Gaia, this system will not necessarily be aligned with any of the other systems so there will be a transformation to what coordinate position Gaia will measure for a star at a given time given by the scanning law of Gaia. Not more difficult, but a bit more convoluted as Gaia’s coordinates η and ζ will be functions of time, right ascension and declination.

With the description of how to go from a parametrization of the problem to calculated position, comparisons could be made to what is actually observed by Gaia. The goal is to find parameters describing the star and planet such that the calculated points are as close as possible to the ones actually measured by Gaia. The “measuring” takes place in AGISLab which is a realistic simulation of Gaia and in here it will take the place as true observations. With each observation there is an associated measurement error, this measurement error is used for calculating the weight of the observations, a small observation error result in a measurement which is given high importance or weight. The merit function is then defined as the weighted sum of square residuals, i.e., for a given set of parameters calculate the expected observations, take the difference with the true observation, square it and divide by the square of the measurement errors and finally sum up. In Figure 1.6 the general idea is shown. To the left the red line represents the measured motion of the star (leaving out the transformation to Gaia coordinates), the gray line represents the calculated positions for a given set of parameters. The calculated \mathbf{y} are compared

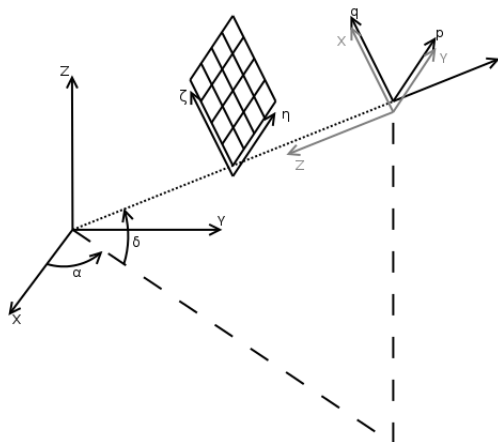


Figure 1.5: Relation between different coordinate systems. The stars orbit will be described in the gray XYZ -system. The observer (someone on earth) is in the black XYZ -system with direction to the star given by α and δ in right ascension and declination respectively. Gaia will be performing a complicated motion when scanning the sky, measuring the position of the star in its $\eta\zeta$ -coordinate system at a specific time.

to the true measured $\hat{\mathbf{y}}$ by taking the difference (again in Gaia coordinates the points are just one dimensional points and not as here depicted as a two dimensional point). The residuals are squared and divided by the square of the measurement error. This procedure is repeated for all points and summed up. To the right in the same Figure the merit function is plotted as a function of a single parameter. From an initial guess of parameter, updates to the parameter has to be made such that the merit function is minimized. Two different methods are the gradient descent and the Gauss Newton method. Gradient descent is to update the parameter by taking a step in the opposite direction to the gradient. Gauss-Newton approximates the function with a quadratic function which could be solved for the minimum, and using the minimum of the quadratic function as a updated parameter. By combining these two methods such that far away from the minimum of the merit function updates should be made according to the gradient descent method, and close to the minimum of the merit functions updates should be made according to the Gauss-Newton method the strengths of the two different methods can be utilized. One strategy for combining these two methods is called the Levenberg-Marquardt method.

1.2 History and Gaia

With increasing precision of measurements Friedrich Bessel was in the 19th-century (1807 wikipedia.org) able to determine the first *parallax*¹ to a star. That is, as Earth moves around the Sun, star seemed to move in a ellipse with respect to stars farther away.

Early on it was noted that some of the lights in the night sky moved and were called wanderers by the ancient Greeks. They were later determined to be bodies in the solar system,

¹Parallax is an angle with which an object appears to move with respect to the background when observed from two different points. A classical demonstration of this is to hold up one finger and look at it with one eye. Looking at it with the other eye and the finger appears to have moved with respect to the background. The angle eye-finger-eye is the parallax

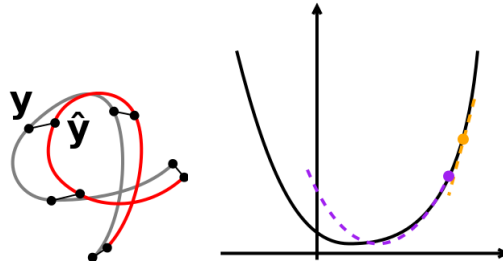


Figure 1.6: **Left:** The residuals are the difference between the measured point and the computed value. The goal is to find parameter such that the sum of weighted square residuals is minimized. **Right:** Depiction of the sum of weighted square residuals as a function of one parameter. Given an initial guess for parameter, the goal is to find the parameter which will give the least sum. One way is to update the parameter by moving in the opposite direction to the slope, the gradient descent method. Another is to approximate the function with a quadratic function and solving for the minimum of the quadratic function, the Gauss-Newton method. The Levenberg-Marquardt method is a combination of the two, behaving as the gradient descent when far away from the minimum (large changes in the function when changing parameter) and Gauss-Newton when close to the minimum.

planets. The stars were assumed *not* to move but now even stars can be measured to move, most notably Barnard's star with a motion of 10 seconds of arc¹ (as) per year. Even though that is a big number it would still take 180 years to pass over an angular distance equal to the diameter of the Moon's face.

To get an impression of what one second of arc is, or rather how small it is, imagine a ruler with markings for every millimeter. Place that ruler 200 meter away. Now, 1 millimeter at 200 meter away correspond to an angle of 1 second of arc ($60 * 60 * \arcsin(1/(200 \times 10^3))$)

One of the goals for Gaia will be to measure one billion stars. This is one of the stupefying numbers which will be littered around in the following pages. Though we might know that a billion is a thousand million, a "1" followed by nine "0"s, it is hard to get a conceptual grasp on a number of this size. As a comparison; a meter stick graduated at every millimeter has 1001 markings. If the meter stick were to be one kilometer it would have 1000001 markings. A thousand kilometers is a long distance and how that compares to one millimeter is not something easily done except in pure numbers. Some express amazement over some "primitive" cultures which do not have a distinction between 10 and 100, after all if you have more three you have a lot. So it is with these numbers, they are moving into the territory where our culture does not have a real distinction or conceptual grasp because we do not encounter them in ordinary life.

More along the same line is the precision with which Gaia will make measurements of position, or rather the position angles which will be calculated from the data provided by Gaia. The aim is to get down into the micro-arc second regime, that is in the millionths of an second of arc. Remember the comparison of a millimeter marking with the kilometer? In Figure 1.7 the accuracies of some astrometric catalogs are plotted as they have evolved over time and indicate that Gaia will take astrometry a big step forward, both in terms of number of stars and accuracy.

Now "Gaia" has been used in different meanings here and some clarification might be in

¹One second of arc is one sixtieth of a minute of arc. One minute of arc is one sixtieth of a degree. One degree is one three hundred and sixtieth of an full circle

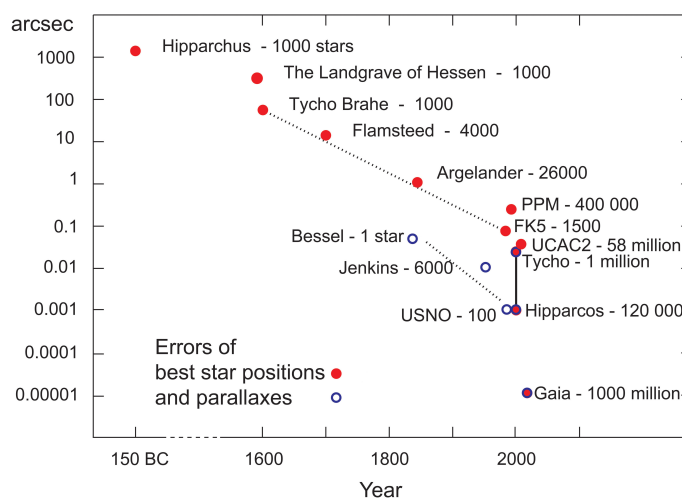


Figure 1.7: Evolution of the accuracy of astrometry over time. Interesting to note are the three last ones; Tycho, Hipparcos and Gaia which have both parallax and position. (Image E. Høg)

order. Gaia is the name of the spacecraft, the object that will be sent out in space to do measurements. The data it will provide, is not of much use until it has been processed into a usable form. To make it into a usable form considerations have to be made for how the spacecraft behaves when heated by the sun or some micro-meteorite (grain of sand) strikes while in space etc. to get precise measurements. The list of small things which have to be considered is long and to deal with that list in a reasonable time many people have been involved in the Gaia mission. This project is looking at a small part of what can be done with the data in relation to exoplanets, planets orbiting stars other than our own Sun. So there are two distinctions, the Gaia spacecraft and the Gaia mission. However, no further distinction will be made unless something specific is discussed related to either part.

If all goes according to plan then Gaia, the successor to Hipparcos, will be launched in the latter part 2013¹ atop a Soyuz-Fregatt from French Guyana. The first part, a Soyuz rocket, will take care of reaching low earth orbit. From there, the second stage will take Gaia further out to the second Lagrange point L_2 of the Sun and Earth. This is a point 1.5 million kilometers farther out than Earth from the Sun where the combined gravity from the Sun and Earth makes a test particle - in this case Gaia - orbit the Sun with the same period as Earth. Even though this is a large number, it is just one hundredth of the distance from the Sun to Earth. The point of this placement is that it is a stable environment. Placing satellites closer to Earth will mean that they also have to orbit Earth. For Gaia, due to the construction and operation, would mean that Earth would obstruct the view.

Gaia will stay here for the duration of the mission which is five years, slowly spinning around its own axis which will be tilted away from the Sun-Earth line. To explain how Gaia will scan the sky, Figure 1.8 gives a good overview. The way the scanning will be done is, as said before, Gaia will rotate slowly with four revolutions per day. The axis of rotation will not be aligned with the gravitational field, instead it will be 45° off from the Sun Earth line. So in addition to its rotation it will precess. One of this precessions will take roughly two months. As the Earth

¹ Currently scheduled for launch October 2013. The mission is in “PhaseD (Qualification and Production)”

moves around the Sun over they year, Gaia will follow. The result will be that the sky will be scanned in a spiral pattern. Not all parts of the sky will get the same number of visits, most observations will be made roughly 45° degree away from the ecliptic and least observations will be made in the ecliptic. Figure 1.9 show the number of times each part of the sky will be visited by Gaia.

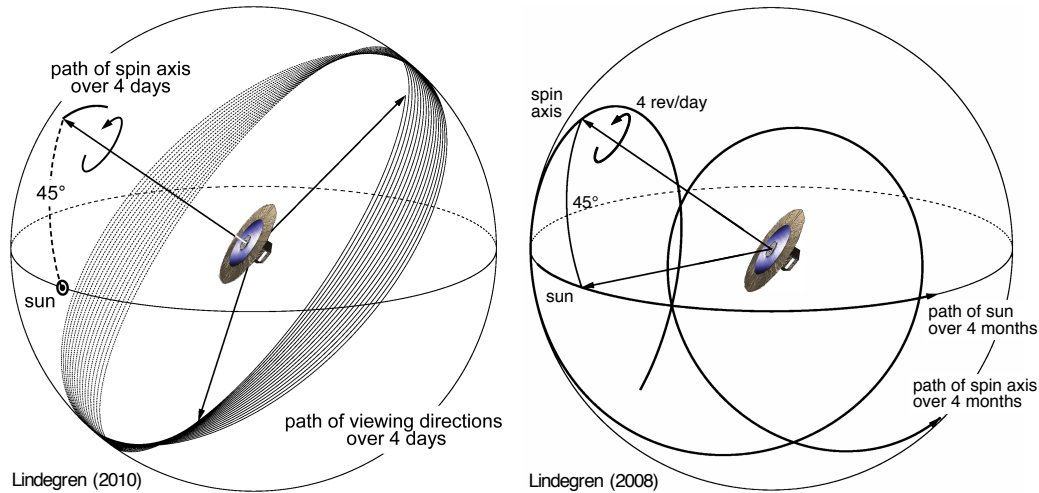


Figure 1.8: Overview of how gaia will scan the skies. **Left:** Gaia will be positioned with its spin axis oriented 45° away from the Sun which will cause it to precess. The period of the precession will be roughly two month. As the Sun changes position over the year this will result in the whole sky being scanned. **Right:** With a revolution for Gaia of roughly six hours the sky will be scanned in successive circles. As there is also a slow precession of the spin axis the circles will not be closed but instead form a spiral pattern covering a larger area of the sky. In addition with the motion around the Sun this will cover the whole sky. So there are three components which combined will make it possible to scan the whole sky; the spin of Gaia, the precession of the spin axis and the motion around the Sun. (Image L.Lindegren http://www.rssd.esa.int/SA/GAIA/images/image_gallery/Gaia_scanLaw_rotations.pdf)

The complicated motion of Gaia will also mean that a star will be measured a number of times as Gaia rotates. Eventually it will no longer pass through the field of view, and there will be a gap in time where no measurements are made of the star. So, the measurements of a star will be groups spaced out in time with roughly one hundred groups spaced out over the five year mission life time of Gaia. Figure 1.10 show this combination. The middle part of this figure show the number of “along scan” observations per source, these observations are grouped into groups according to Figure 1.9. Combining the number of along scan observations with the stellar density of the sky (top part of Figure 1.10) result in the number of along scan observations per deg^2 , which is shown in the bottom of Figure 1.10.

An overview of which parts of the Galaxy that Gaia will map out is in Figure 1.11. This overview was created by taking the Galaxy and on top, plot the expected density of stars Gaia will observe. As the number density of stars vary for different parts, and the extinction is varying in different directions, the density plot will not be symmetric even though the coverage of the scanning will be “symmetric”.

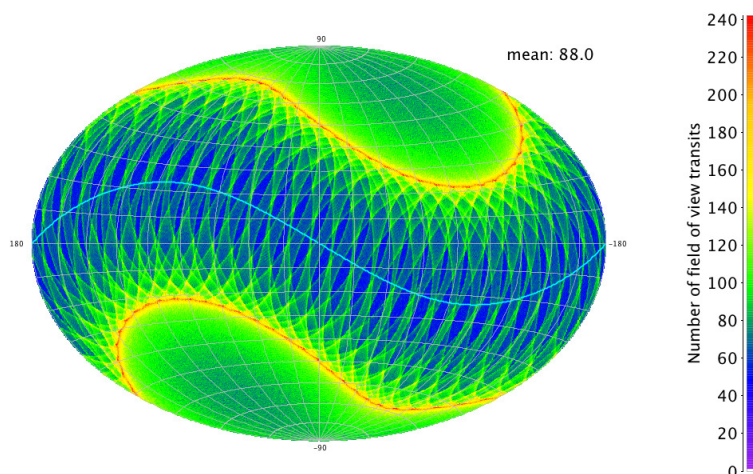


Figure 1.9: Number of field of view transits, or roughly how many times a certain area will be visited, for Gaia. The wavy light blue line correspond to the ecliptic. (Image Holl and Lindegren (2012))

One of the purposes of Gaia is to help create a new coordinate system¹. Over the years many different coordinate systems have been used which made sense for their time considering the precision or measurements possible.

Creating a coordinate system from the stars might seem like a good idea. After all, for most of the history of humanity they have been known to be fixed with a handful of them wandering about. Once in a while a new star appeared, moved considerably, but eventually faded away. Most importantly, the fixed stars stayed where they were. That was until the measurements became good enough to measure the motion of the stars and realizing all stars moved about. So this non-rotating coordinate system was not longer based on fixed stars. Bad for the coordinate system but very good for the understanding of things.

Another was to use the planets of the solar system and define it though their motion. The angular momentum of the full solar system is fixed so this makes it possible to create a dynamical definition in which the planets move with Keplerian motion.

A more refined system, still along the line of fixed stars, is to use quasars. These bright objects lie so far away that any motion they have can be neglected. Any changes is only through the refinement of the measurements. Still today this is done by measuring the position of the quasars with radio telescopes.

Once again, as precision gets better even the quasars will appear to move due to variability. Or rather their motion will be measurable. So go back two steps and replace the Solar system with the system of all quasars in the dynamical definition. Even though individual quasars might appear to move, overall they should not. This frame which is non-rotating could then be used as a coordinate system.

¹Based on a question asked in (Nov 2012) Stern und Weltraum but the construction of coordinate system goes back to the goals of Gaia (Perryman et al., 1997).

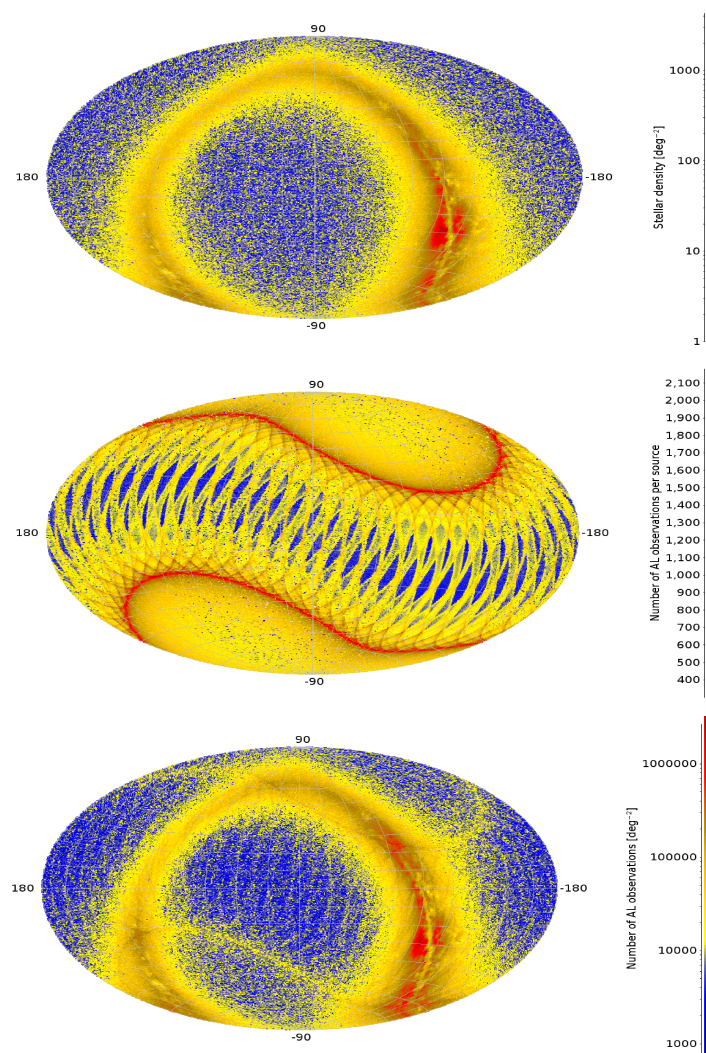


Figure 1.10: **Top:** The number of stars per square degree. The ring shape is the galaxy mid-plane. **Middle:** Number of along scan observations per source. **Bottom:** Number of along scan observations per square degree, or how many measurements per square degree which will be made for different parts of the sky. (Image Lindegren et al. (2012))

1.3 AGIS and AGISLab

1.3.1 AGIS

From the data collected by Gaia, five parameters pertaining to the position and motion of stars are the results of the reduction. Gaia will not make one observation of absolute position for a star but rather many observations of relative positions. This also assumes that the *attitude* (the direction that Gaia is pointing at a particular time) is known. However, as this is not the case the problem will be to determine the attitude and astrometric parameters of objects in an iterative fashion. This will be done in what is called AGIS (**A**strometric **G**lobal **I**terative **S**olution). What it all comes down to is minimize the difference between what is observed and

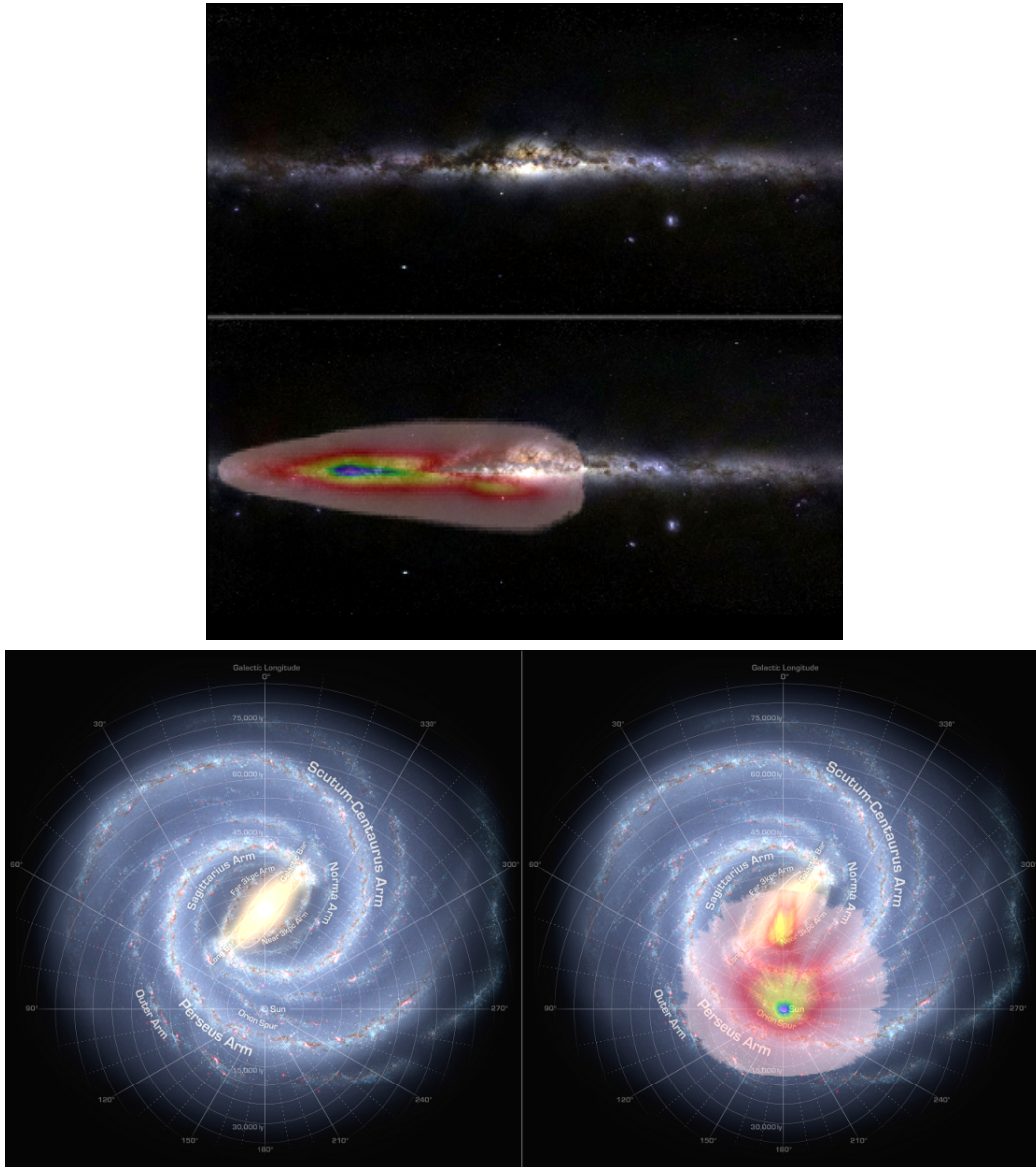


Figure 1.11: Overview of the extent to which Gaia will survey the galaxy. **Top:** Side view of the galaxy, top part shows just the galaxy and the bottom the colored overlay is what Gaia will observe in a density plot. This only shows the outer boundary of the density range which does not mean that Gaia only will observe thing within this range. **Bottom:** To the right is the same overview but from the top. The outcropping below and towards the center is Baade's window where the extinction is less and it is possible to see further. (Image X. Luri & the DPAC-CU2 http://www.rssd.esa.int/SA/GAIA/images/image_gallery/Overlay-Top-HiRes.png http://www.rssd.esa.int/SA/GAIA/images/image_gallery/Overlay-Side-HiRes.png)

what is expected to be observed based on a physical model.

Even though the data received will be pre-processed on board the Gaia satellite, the final data will be in excess of 1 petabyte. This is what will prohibit a direct solution and necessitate the iterative approach. The iteration will consist of; determine the astrometric parameters, deter-

mine the attitude of Gaia, determine instrument calibration and finally some global parameters which are constant over the mission.

1.3.2 AGISLab

AGISLab is similar to AGIS in the sense that they both produce an “Astrometric Global Iterative Solution”. However AGISLab can be viewed as a lightweight testing platform for performing realistic experiments in a scaled down fashion requiring fewer stars for performing the reduction¹. This makes it possible to develop and test new ideas and algorithms. As an example of this is the *velocity block* of AGISLab. This block determines the barycentric velocity of the Gaia spacecraft. It is implemented in AGISLab but it is not yet implemented in AGIS.

The noisy observations are generated *on the fly* instead of a pre-constructed data set of input observations, the true observations are pre-generated and stored. It starts out with a *true source*² this then has noise or other effects added to it creating the *running source*. The running sources are then handed over to the *source processor* which sets up the least-squares problem for the sources.

This procedure is similar in the other blocks; a true value is generated, to that true value random or systematic effects are added.

The least squares problem for the observations are combined with the least squares problems for the other blocks, and they are eventually solved with a conjugate gradient algorithm in an iterative manner.

The reason for going through all this trouble is that the *errors* can be calculated, that is the difference of the *solution* and the *true*. In the real mission this can obviously not be done making the estimation of the errors less straightforward.

How AGISLab works

As said before AGISLab generates data from parameters as well as trying to recover the parameters from the generated data. This might seem like crossing the river to get water, and indeed it is. It is the process of “crossing” which is to be investigated. If the parameters which generate the data are known, then it is possible to determine how good the recovered parameters are and what will happen if different errors and biases are added.

How is this implemented then? Figure 1.12 gives an overview of the different components in the two top “rows”. They each have their dedicated task which is separated from the others, and as the type of solution is of an iterative nature not all blocks are solved at the same time. Instead one block at a time is solved and combined in the *conjugate gradient* algorithm to get an optimal update.

Consider the two leftmost “columns” in Figure 1.12; source and attitude. Source refers to anything that Gaia will measure (e.g. stars, quasars) and attitude refers to where Gaia will be pointed. From the generators, containers for each type are generated containing the *true* sources and true attitude respectively. Errors, biases or anything else which might be of interest to investigate are added to the true values which create the *running* values. The running values are those which will get updated in each iteration, hopefully improving them by bringing them

¹Reducing the observations to physical parameters for the stars such as the five astrometric parameters; position, parallax and proper motion.

²“True” here is in the meaning of not taking into considerations any external effects

closer to the true values. Here also comes the possibility to compare the true to the running during the optimization and see how the errors evolve with each iteration. With the attitude and sources, observations can be generated and stored in observation containers. They however have to take into account the physical properties of Gaia and how external forces and influences will affect the measurements, this is done in the “Source Direction”. With the observations and the model it is possible to set up the least squares problem, this is done for each part in the *processors*. Each part is then solved giving updates, e.g. given the running attitude and the observations, the running sources are updated.

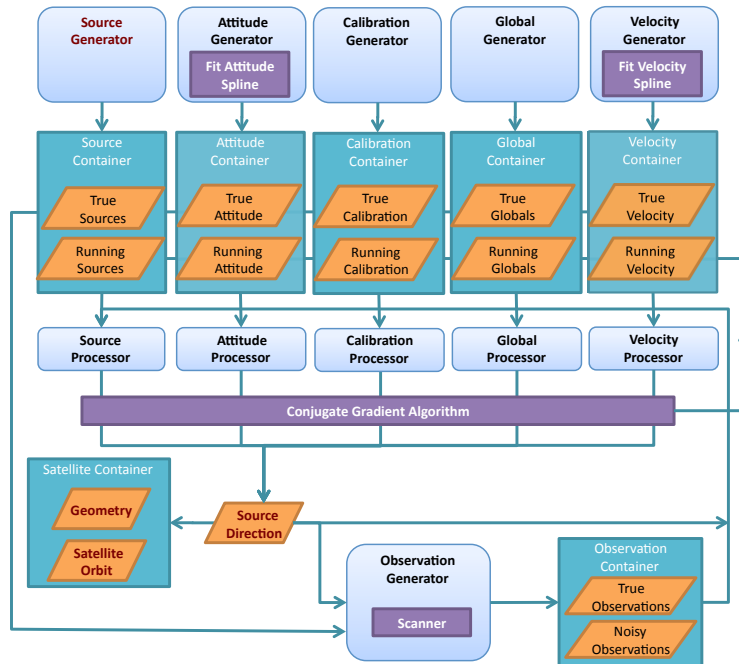


Figure 1.12: Overview of AGISLab showing the relation of different components. The relation to planets is in the “source” part where signatures of exoplanets are added in the source and the Levenberg-Marquardt algorithm is in the processor. Holl et al. (2012)

All this could have been done in AGIS with an addition of something to generate the observations, so going through all this trouble seems to be a bit un-necessary. The reason comes from AGIS being made to work on large data sets, after all it is made for reducing the real Gaia data. This will be a couple of hundred million primary sources each of which will be observed a number of times totaling an even greater number data points. This becomes prohibitive for doing experiments involving small *what if?*’s. Even scaling down the problem to use significantly less primary sources does not solve the problem, as doing tests usually involve running the experiment many times over for different conditions. This is where AGISLab comes in.

AGISLab uses a scaling parameter, S , to set the fraction of primary sources. A value of $S = 1$ will result in a run of a million primary sources and a value of $S = 0.01$ will result in a run of just one hundredth as many. Using one million primary sources is just enough for reconstruct the attitude, more complicated investigations will require many more primary sources quickly rendering small experiments prohibitive if they are to be run multiple times. So this scaling factor has some other effect then just reducing the number of primary sources (a much more

detailed discussion can be found in Holl et al. (2009), on which this is based).

Some physical processes takes a couple of years, eg. orbit of a planet. If the scaling parameter would affect the mission length, then the processes which could be followed over a full cycle would only be partially covered, eg. only a partial orbit. So the scaling parameter can not reduce the mission length.

More of these considerations have to be made to account for, for example; the number of transits for a given primary source, number of primary sources in the field of view at a given time and the mean number of transits. The reason for them are a bit more subtle, however, the result is that one way to honor these constraints without changing the operation of Gaia, is to change the focal length. This means that as the scale factor become smaller the field of view will get larger, but still the physical layout of Gaia and its operation will remain the same. As an example consider Figure 1.13, it depicts the focal plane of Gaia with the different CCDs. Only one star is shown crossing, but in reality more than one will be on the focal plane at any moment. Decreasing the scale factor would decrease the number of stars on the focal plane at any moment. So instead of changing making the CCD array larger, for example, to keep the same number of stars on the focal plane it is simpler to just change the focal length, effectively making the field of view larger. This then does not affect how fast a star is moving across the CCDs, how often it will move across but still the same number of stars would make the same number of crossings over a given time span, so the nominal mission length could also be kept constant.

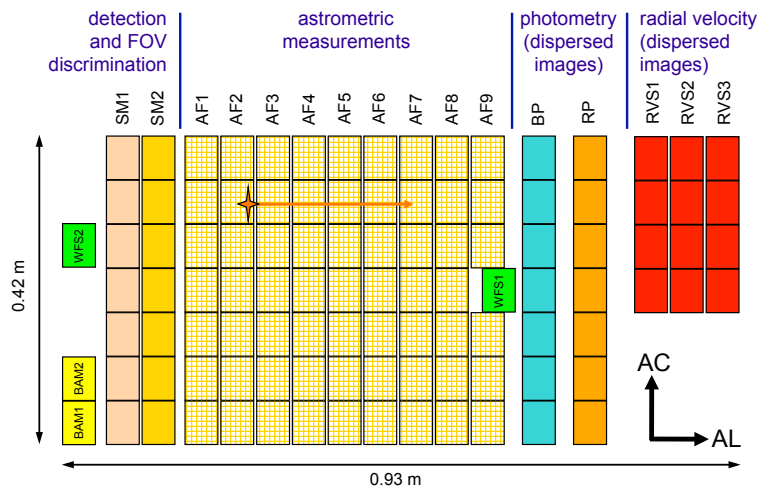


Figure 1.13: Depiction of how a star image will transit over the CCD plane of Gaia. Depending on the attitude of Gaia a star will enter on the left at a certain *across scan* position. The first two rows of CCD are the star mappers which determine if and how a star should be observed. As Gaia rotates the star will move to the right over the main block of CCDs for astrometric measurements. The relation of a star's true position on the sky and the transit time and location on this block is what AGIS will solve. AGISLab will do the same thing but for the purpose of testing ideas and techniques, such as adding a planetary signal to the star position. Holl and Lindegren (2012)

Integration into AGISLab

The integration of the planet detection is in the “source” part. True source data is loaded, such as proper motion, position and parallax. Whenever the position of the star is required, then in addition to how the proper motion has affected its position, the additional contribution of the planet has to be calculated. This means, that at the given time Kepler’s equation has to be solved for the eccentric anomaly so the position of the planet in its orbit can be calculated. With the position of the planet in its orbit and the orientation of the orbit the offset of the star, from the position it would have had if there was no planet, can be calculated. The offset of the star will be opposite to the position of the planet and the magnitude of the offset will be scaled with the mass relation of the planet/star. A lighter planet around a heavier star will, for a given orbital separation, give a smaller astrometric signature than a heavier planet around a lighter star. In the end a number of observations, or data points for the star, are obtained. If the attitude of Gaia is known then a optimization can be done. Initially there has to be some guess for what parameters were used for the planet, but still they have to be optimized. Together with the data points which represent the evaluation of the target function and the parameters the optimization step is set up in a Levenberg-Marquardt optimizer, this is in the “processor” for the source. If the optimization step for the planetary parameters succeed, the attitude can optionally be updated.

If in addition radial velocity is to be included an additional data set has to be loaded. Just as the positional offset of the star can be calculated from the orbit of the planet, the radial velocity¹ of the star can be calculated from the same orbital parameters. Instead of the position the time derivative of the position is used, using the same formulation of the problem. This simple combination of the two data sets in the same model is what makes it attractive.

1.4 Brief overview of exoplanet detection

The following is a short overview of some techniques for exoplanet detection. Most of the material is based on the book “The Exoplanet Handbook” by M.Perryman (Perryman, 2011), but also material from “Exoplanets” by S.Seager (Seager, 2011) is used.

The difficulty of detecting exoplanets is tied to the contrast of the exoplanet to the star. Even big Jupiter mass planet are lightweight compared to a star similar to the Sun, so any dynamical effect the planet will have on the star will be scaled by factor representing the mass ratio of the two. The same goes for the luminosity, even if a planet is hot and does emit in the infrared its host star will still outshine it.

But these problems, and many other, have been overcome to some degree. The number of planets detected is growing to a respectable pool and also the diversity of planet types is growing into a more representative sample. Likewise, the different techniques successfully employed to detect exoplanets has grown over time. In Figure 1.14 the position of discovered exoplanets is plotted together with what type of technique was used for the detection.

1.4.1 Radial Velocity

Measure how much the spectral lines of a star shift back and forth over time. Convert the measurements to radial velocity for the system and “[c]haracterization of the orbits of single

¹Here only the contribution of planets are included in the radial velocity

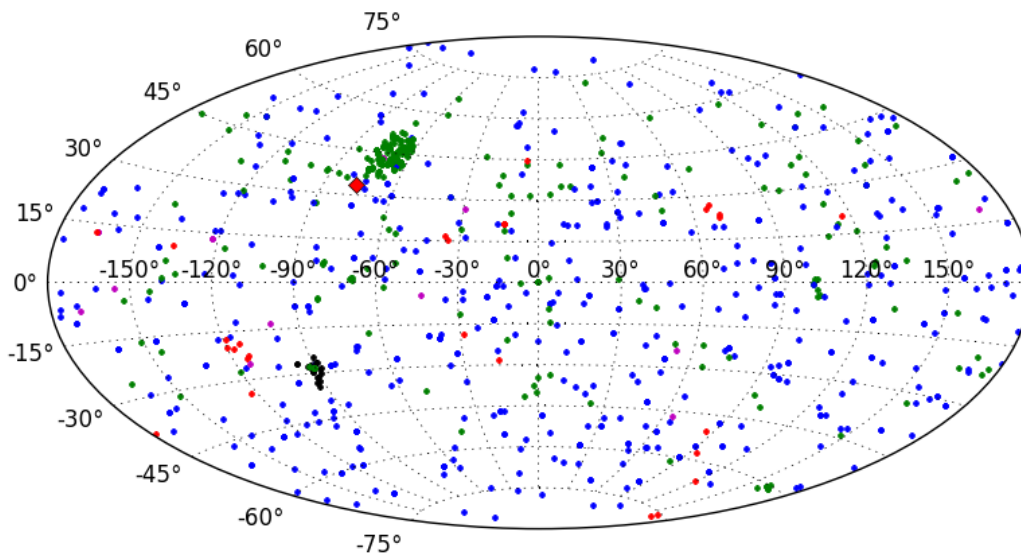


Figure 1.14: Exoplanets on the sky. The different method are; radial velocity - blue dots, imaging - red dots, transits - green, pulsar - magenta, micro-lensing - black dots and astrometry - red diamond. Kepler is looking in the direction of approximately 19 h and 45° which is the clump of green dots. In the similar direction is the only target classified as a astrometry detection, namely HD 176051 b which is a 1.5 M_J planet in an orbit of 1.7 AU. Source for data: <http://exoplanet.eu> (Retrieved on May 1'st)

unseen companions, such as exoplanets, is ultimately an exercise in the fitting of observed radial velocities to [...] orbital parameters" (Wright and Gaudi, 2013). In 1952 Otto Struve proposed (Struve, 1952) just this, to look for close in Jupiter-sized¹ planets which "would cause the observed radial velocity of the parent star to oscillate with a range of ± 0.2 km/s - a quantity that might be just detectable with the most powerful Coudé spectrographs in existence". In the same paper he also suggested to look for eclipses in the same type of systems.

However, it had to wait until 1995 when Mayor and Queloz (Mayor and Queloz, 1995) published a paper titled "A Jupiter-mass companion to a solar-type star". In this paper they published the first account of a radial velocity detection of a exoplanet. It was of a planet with mass $M_2 \sin i = 0.47 M_J$ which orbited the quite Sun like star 51 Peg. The accuracy of the instrument was such that it could measure radial velocities with an accuracy of 13 m/s, which was somewhat better than the spectrographs Struve suggested using. The radial velocity of the star was also quite large, $v \sin i = 2.2$ km/s and the orbital period of roughly 4.2 days. This

¹The radial velocity of the Sun due to Jupiter is around 13 m/s if viewed side on.

would mean that the planet was quite a large one on a small orbit. It was not expected for planets to have a period of only a few days but as the star was quiet and not chromospherically very active it would seem unlikely for this signal to be related to the rotation of the star.

In Figure 1.15 the trend of how the $M \sin i$ of radial velocity detections have evolved over time is shown. As it stands now it is possible to detect radial velocities which are below 1 m/s. Dumusque et al. (2012) presented results of a planet around α Centauri B with a semi amplitude of only 0.52 m/s, this translates into an Earth mass planet on a orbital period of only a few days.

Description of radial velocity

The radial velocity signal can then be calculated starting from Equation A.4. This radial vector has to be slightly modified as we are now looking at how the star is moving with respect to the center of mass. So it reads

$$R_1 = \frac{m_2}{m_1 + m_2} \frac{a(1 - e^2)}{1 + e \cos \nu}$$

with time derivative

$$\begin{aligned} \dot{R}_1 &= \frac{m_2}{m_1 + m_2} \frac{a_1(1 - e^2)}{(1 + e \cos \nu)^2} e \dot{\nu} \sin \nu \\ &= R_1 \frac{1}{1 + e \cos \nu} e \dot{\nu} \sin \nu \end{aligned}$$

The radial vector from the center of mass to the star can be expressed through the true anomaly

$$\mathbf{R}_1 = \begin{pmatrix} r_1 \cos \nu \\ r_1 \sin \nu \end{pmatrix}$$

The time derivative of this is then

$$\begin{aligned}
\dot{\mathbf{R}}_1 &= \begin{pmatrix} \dot{R}_1 \cos \nu - R_1 \dot{\nu} \sin \nu \\ \dot{R}_1 \sin \nu + R_1 \dot{\nu} \cos \nu \end{pmatrix} \\
&= \begin{pmatrix} \frac{R_1 e \dot{\nu} \sin \nu}{1 + e \cos \nu} - R_1 \dot{\nu} \sin \nu \\ \frac{R_1 e \sin^2 \nu}{1 + e \cos \nu} + R_1 \dot{\nu} \cos \nu \end{pmatrix} \\
&= \frac{R_1 \dot{\nu}}{1 + e \cos \nu} \begin{pmatrix} -\sin \nu \\ e + \cos \nu \end{pmatrix} \\
&= \frac{1}{a(1 - e^2)} \frac{m_2}{m_1 + m_2} r^2 \dot{\nu} \begin{pmatrix} -\sin \nu \\ e + \cos \nu \end{pmatrix} \\
&= \frac{1}{a(1 - e^2)} \frac{m_2}{m_1 + m_2} h \begin{pmatrix} -\sin \nu \\ e + \cos \nu \end{pmatrix} \\
&= \frac{1}{a(1 - e^2)} \frac{m_2}{m_1 + m_2} \sqrt{G(m_1 + m_2)a(1 - e^2)} \begin{pmatrix} -\sin \nu \\ e + \cos \nu \end{pmatrix} \\
&= \sqrt{\frac{Gm_2^2}{m_1 + m_2} \frac{1}{a(1 - e^2)}} \begin{pmatrix} -\sin \nu \\ e + \cos \nu \end{pmatrix}
\end{aligned}$$

This is a vector describing the velocity in the plane. It can be extended to describe the velocity vector in space by adding on the missing component

$$\dot{\mathbf{R}}_1 = \sqrt{\frac{Gm_2^2}{m_1 + m_2} \frac{1}{a(1 - e^2)}} \begin{pmatrix} -\sin \nu \\ e + \cos \nu \\ 0 \end{pmatrix}$$

This has to be rotated, or projected onto a vector, to represent the radial velocity which a observer will see. The matrix in Equation B.5 has the components, which means that $\dot{\mathbf{R}}_1$ is to be multiplied by

$$\mathbf{k} = \begin{pmatrix} \sin \omega \sin i \\ \cos \omega \sin i \\ \cos i \end{pmatrix}$$

So the radial velocity becomes

$$\begin{aligned}
v_{r,1} &= \mathbf{k}^T \dot{\mathbf{R}}_1 = \sqrt{\frac{Gm_2^2}{m_1 + m_2} \frac{1}{a(1 - e^2)}} (-\sin \nu \sin \omega \sin i + (e + \cos \nu) \cos \omega \sin i) \\
&= \sqrt{\frac{Gm_2^2}{m_1 + m_2} \frac{1}{a(1 - e^2)}} \sin i (e \cos \omega + \cos(\omega + \nu))
\end{aligned} \tag{1.1}$$

This also gives the *radial velocity semi-amplitude* of the star $K_1 = (v_{r,\max} - v_{r,\min})/2$ when $\omega + \nu = 0$ or π

$$K_1 = \sqrt{\frac{G}{m_1 + m_2} \frac{1}{a(1 - e^2)}} m_2 \sin i \quad (1.2)$$

So with the expression $v_{r,1}$ this connects the radial velocity to parameters of the orbit and masses of the bodies.

What is measured is the change in wavelength (Doppler shift) of some, or quite a few, spectral features. But leaving that aside for the moment all that has to be done is to calculate the shift in wavelength, relate it to the radial velocity which then could give the parameters of the orbit etc.

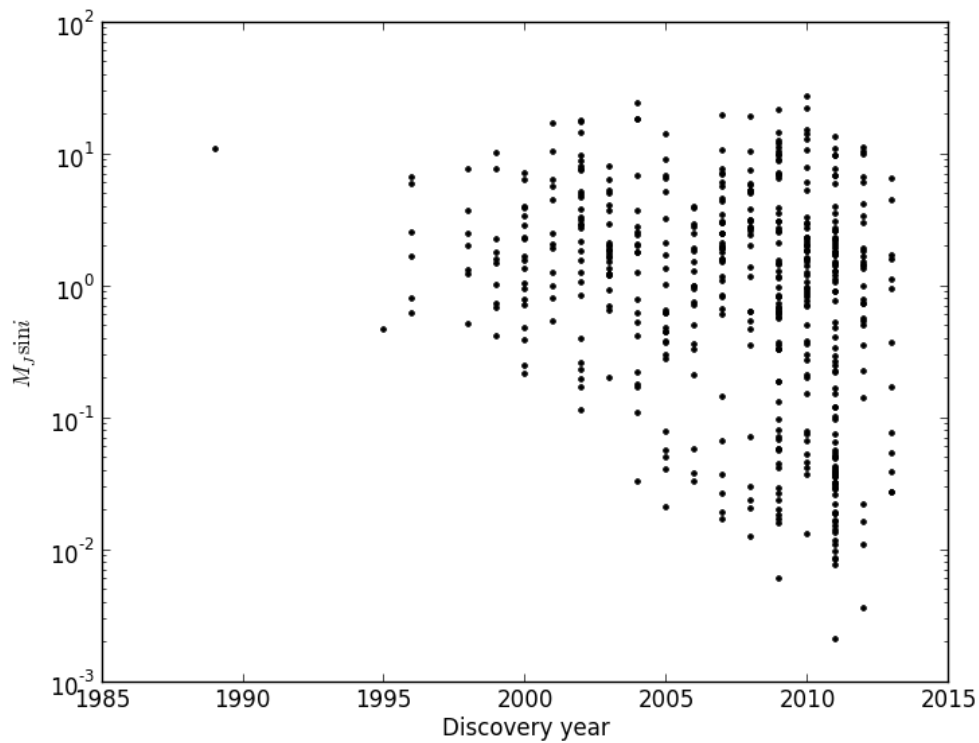


Figure 1.15: How the minimum mass of published exoplanets have evolved over time. With evolution of instruments lower mass planets can be detected. Source for data: exoplanets.org (Retrieved on May 1'st)

So in the simple case for non-relativistic Doppler shift the radial velocity become

$$v_r = \left(\frac{\lambda - \lambda_0}{\lambda_0} \right) c \quad (1.3)$$

This does not take into account that the system under observation might be moving, both radially and transversely, and even accelerating and rotating. Also, the motion and rotation of

Earth also has to be taken into account. Moreover, care has to be taken for gravitational redshift, stellar oscillations and granulations. The list of effects which has to be taken into account for just determining the Doppler shift keeps on growing the more precise the measurements become.

So from the measurements of the Doppler shift, together with some suitable parametrization of the problem what is left is to perform some optimization and thereby finding the parameters describing the system.

1.4.2 Astrometry

Astrometry has historically mainly considered the position of stars. With time the measurements improved allowing the determination of parallax, and eventually with increasing baselines in time the motion of stars. With Gaia the precision will be good enough to use astrometry for exoplanet detection.

Even though there were early claims of exoplanets detected by astrometry (Strand, 1943)¹ not any of them have been able to stand up to closer scrutiny over time. The techniques were a bit different from what is employed in Gaia as it was not possible to determine the position of many stars at the same time. Instead relative measurements were made between stars, if this relative distance appeared to change it was possible that one of the stars had an orbiting planet. Which of the two stars the planet belonged to could not be determined unless there was more input. Exactly this technique was employed for the above cited article.

So why should attention be made to a technique which have not really yet proven itself as a viable tool for exoplanet detection? The main point is not so much for the detection, today the number of confirmed planets have moved from the realm of detection into classification, but the point is that astrometry is able to measure parameters which are not possible with the other techniques.

An interesting applicability of astrometry measurements is in connection with pre-main sequence stars which have gas giants forming. The formation scenarios for the gas giants follow different time scales, and will provide astrometric signatures in relation to their mass. So it could be possible to connect the mass accretion with the age of the forming system.

Astrometry is also not as dependent on what kind of star the host star is. Even active stars can be observed and measured for planetary companions. This is a very strong limitation for radial velocity techniques as those require the star to be predictable and have nice absorption lines for the determination of the radial velocity. Transit techniques are also dependent on the stellar activity, the more quite the host star the easier it is to measure the light curve of the transit. A passing star spot does not move the photo-center of the star very much *How much does a star spot move the photo-center.*

One of the more important aspects of astrometric planet detection is that it is possible to measure the mass without the $\sin i$ ambiguity as is the case for radial velocity. Radial velocity only makes a one dimensional measurement, the motion of the star towards and away from the observer, this means that all the measurements of the mass have a term $\sin i$ included and thus only the minimum mass of the planet is quoted $m \sin i$. Astrometry on the other hand makes measurements in two directions which means that it is possible to avoid this ambiguity and get both the mass m of the planet and inclination of the orbit i .

¹This was of a 16 M_J companion but with “*an intrinsic luminosity so extremely low that we may consider it a planet*”, a mass which might seem a bit high for a planet today, but non the less very much smaller than a star

On the other hand astrometry is a very good compliment to radial velocity in that the astrometric signal increases with increasing semi major axis in contrast to radial velocity which has a signal decreasing with increasing semi major axis.

1.4.3 Timing

Timing is very well described by its name. Namely by measuring a periodic signal predictions can be made when the next signal will come, if the signal does not come when predicted there is probably something which has affected the system. If a model exist for the system emitting the signal, the delay/advancement can be used when testing why the signal was delayed.

As an simple example of this imagine a beacon emitting a signal with a regular period. If the object starts to move away the distance to it will be larger when the next signal is emitted so there will be a slight delay between the prediction and the observations. So in the beginning regular periods are measured but then all of a sudden the period increases a slight amount. An observer seeing this sudden increase in period between the measurements can still be able infer that the object has started to move if the model describing the system would have that as a possibility.

This is not a very realistic example but serves good as a stepping stone to a more realistic example; If a emission or absorption line is slightly shifted from what would be expected and the model is of a object moving away linearly, then this Doppler shift can be used to measure the velocity with which the object is moving.

Objects do not start moving away all of a sudden, but rather there is a force acting to cause the variation in the signal. Also just measuring the radial velocity with which a object is moving does not have much to do with exoplanets. But if, for example, there is an object emitting a periodic signal and the emitting object is moving in an orbit the delay will vary with orbital position, all depending on how fast it is moving away or towards the observer. Examples of objects which the timing is used as a measurement are pulsating stars, pulsars and eclipsing binaries. So if the model is of a orbiting planet causing the variation in the arrival of the signal this can be tested against what is really observed. This can be expressed through an equation (Equation 4.1 in Perryman (2011) and here reproduced in Equation 1.4). First off the change in arrival time is due to the finite speed of light c , then it is also proportional the semi-major axis of the orbit a and finally to the relative mass of the planet and object sending out the signal M_P/M_* and the orbital inclination $\sin i$ with respect to the observer. The larger the mass ratio the larger effect the orbiting planet will have, and larger orbits will give rise to larger changes in arrival time.

$$\tau_P = \frac{1}{c} a \frac{M_p}{M_*} \sin i \quad (1.4)$$

Currently there are 17 planets detected in 13 systems¹ detected by timing techniques

Pulsar timing

When massive stars (8-40 M_\odot) undergo core collapse in a supernova what is left is a neutron star. A pulsar is a rapidly rotating *neutron star* which have a magnetic field not aligned with

¹exoplanet.eu in January 2013

its rotational axis. A beam of electromagnetic radiation is created and shines radially out from the polar regions, acting like a light-house. If the orientation of the pulsar relative to Earth is fortunate they can be observed as a eerie periodic signal. The rotational period of these objects is very precise, and especially for millisecond pulsars the spin down rate can be as small as $3 \mu\text{s}$ per million year. Now this is dependent on the pulsar not accreting material thereby changing its period.

If a planet orbits a pulsar it will have an effect on the timing of the pulses; when the pulsar is being dragged towards Earth the period of the pulses will be slightly compressed and the opposite will happen as it is being dragged away. This was used to make the first confirmed¹ detection of an exoplanet in 1992 by Aleksander Wolszczan and Dale Frail (Wolszczan and Frail, 1992). Two planets were found, one of at least 2.8 Earth masses² and another of 3.4. A third planet was later on confirmed to also exist but initially it was just stated that it might exist. Its confirmation was done through slight variation in the timing due to interaction planet-planet and indicated a very low mass object of only $0.020M_{\oplus}$, that is on the same scale as the Moon. This planet-planet interaction also disfavored other non-planet explanations for the timing variation.

Pulsation timing

Related to the pulsar timing technique is pulsation timing. This technique also uses degenerate or evolved objects as sources for the signal, but for pulsation timing the star is in fact physically pulsating in contrast to a neutron star used for pulsar timing.

Objects not as heavy as the progenitors to neutron stars do not undergo supernova explosion but end up as a white dwarf. Still they are formed by degenerate matter but they never pass through the event that protons and electrons combine into neutrons, so only a core is left after they shed their envelope. Planets which are too far in will be slowed down and migrate inwards and planets which are not close enough to be engulfed by the expanding envelope will see a smaller mass as some of the mass is expelled out from the system. So these outer planets will move outward in response.

The end result is a very hot central object, the white dwarf, which may or may not have planets still orbiting it. When the white dwarf cools its photo-sphere will oscillate.

Some of these evolved objects also show remarkable stability (Kepler et al., 2005) with the white dwarf G117-B15A showing a change of period (215 seconds) on the order of $10^{-15} \text{ s s}^{-1}$. This period is the result of a $l = 1$ g-mode, or as the star cools the buoyancy of the inner regions change creating the force for the oscillation and the oscillation is basically the star sloshing back and forth.

Transit timing variation

A somewhat different technique is the *transit timing variation*. First of all it depends on having a transiting planet which will act as the generator for the signal. So if the system, at an initial glance, just consists of a single planet transiting, the time at which the transit occurs will be predictable and not show any variation. But if there is in addition another mass in the system

¹There is a distinction between confirmed and detected, and to make matters worse *confirmed* seem to mostly mean that the general consensus is that it is true

²The reason for saying that the mass is “*at least*” is related to the orbital inclination. As this is unknown it is not possible to say how massive the planets are but only to give a lower limit to their mass. Most often the mass is cited in the form of $M_{\oplus} \sin i$

in orbit around the star, not necessarily transiting, it will provide an additional force on the transiting planet shifting its expected transit time.

In Nesvorný et al. (2012) they look at the systems in the Kepler mission, namely KOI-872, for the search of exo-moons under the project “*Hunt for Exomoons with Kepler*”. Two transits are observed but there are also large variations in the transit time implying that there is another planet which does not transit but still affect one of the transiting planets. It is predicted to be in a resonant 5:3 orbit with the outer planet. As they are looking for exo-moons it could be imagined that the transit time variation could be due to a moon, but if it would be a moon there would also be variations in the transit duration. But no variations in the duration of the transit is seen.

This again shows the interplay with dynamical models and observations. Even though some events are not observed, such as a transit, the variations in the observations are best explained through the addition of an unseen object causing the variations.

Eclipsing Binaries

This is a binary system with low enough inclination so an eclipse occur. This eclipse will occur with a regular period if there are not external forces on the stars. However, if a third body is added, such as a planet in orbit around one of the stars, it will introduce an additional force and the signal will be either delayed or too early, i.e. dynamically very similar to transit timing variation but instead two stars taking part in the transit or eclipsing and the variation in time is not so much the planet changing the orbits of the star but instead affecting the system center of mass.

The duration of the eclipse is smaller than the orbital period of binary stars. The variation in the timing, or the signal, is even smaller than the transit so consequently there will be a difficulty with obtaining useful data. The more massive and farther out the orbiting planet is, the larger the effect it will have on the timing of the transits. On the other hand many observations are needed to be able to use statistical methods for extracting the signal, which mean a smaller orbit. These two are in opposition to each other so it is not as simple as just looking for the extreme situations.

1.4.4 Micro-lensing

The principle behind this technique is to have an alignment of two stars with the closer also harboring a planet. The planet will then affect the light from the farther star by gravity, resulting in an increased apparent flux. If the effect is not uniform, the irregularities can be used as the measurements of how the planet affects the light and thereby provide a way to model the system.

1.4.5 Direct Imaging

Direct imaging is very straightforward in theory, just look at the object with a good enough telescope and some technique for blocking out the light from the star. (Any stray light from the star entering the telescope will drown out light from the planet.) What would be seen is the reflected starlight or any radiation from the planet itself. However, as mentioned in the Introduction this is a problem due to the contrast between the star and planet. To date there has only been a few reported stars from this technique but the achievement is nonetheless impressive.

1.4.6 Transits

A very particular situation is when the orbit of a planet aligns such that it will pass in front of its host star as seen from Earth. This will cause a slight decrease in the amount of light observed coming from the star. As the system is very far away it does not matter how separated the planet is from its star, what matters is only how large the planet is in comparison to the star. So, for example, observing a Sun Jupiter system would roughly correspond to a decrease of one hundredth as the disc of Jupiter is roughly one hundredth of the Sun. It would not matter if Jupiter was orbiting as close as Mercury to the Sun or as far away as Neptune. However, the decrease is quite small so for each system many transits have to be recorded meaning that many more transits will be recorded from close in systems than systems with the planet far out, also the probability for a system aligning up so to make a transit is more probable with closer in planets.

If many objects of interest are to be observed the observations must be carried out continuously. A particularly good way to do this is to send up space-telescope which makes it possible to observe particular regions of the sky uninterrupted. One such spacecraft is the Kepler¹ which has been getting much attention lately due to the wide variety of and possible habitable systems observed. In particular observation of systems which have connection to Sci-Fi making it easy to popularize.

Some of the star's light will be blocked as the planet makes its transit, depending on what part of the star is being blocked the spectrum will look different. If the star is rotating the approaching limb will have slightly blue-shifted spectral features, whereas the other limb will have slightly red-shifted spectral features. The blocking of some of either the approaching or receding limb will have the effect of skewing spectral features, the Rossiter-McLaughlin effect. This makes it possible to glean information about the stellar rotation.

What is maybe most interesting with this technique is the possibility to obtain information about the atmospheres of exoplanets. As the planet passes in front of the star, some of the starlight will shine through the outer layers of the planet's atmosphere. The difference in the spectrum of only the star versus star and some transmission spectroscopy of the planetary atmosphere will make it possible to infer what type of molecules there are in the atmosphere of the planet.

1.5 Other but similar investigations

This is by no means an exhaustive overview of similar issues, as this project will deal with, done by others. Rather it is to be viewed as a short overview of different approaches to similar problems.

1.5.1 Efficient fitting of multiplanet keplerian models to radial velocity and astrometry data

A very similar approach as this project was already studied in Wright and Howard (2009) by combining radial velocity and astrometry to solve for the orbital elements of a system.

¹Not really a satellite as it does not orbit Earth but instead follows Earth with a slightly longer orbital period which means that Earth will catch up with it again in about 50 years

They start out with a discussion about how to partially linearize the problem in connection with radial velocity.

Their Equation 1 is

$$u(t) = \sum_{j=1}^n [K_j \cos(\omega_j + \nu_j(t)) + e_j \cos(\omega_j)] + \gamma + d(t - t_0)$$

Here $u(t)$ is the radial velocity at time t , γ is a time-independent offset and d is the trend parameters. K_j is the radial velocity semi-amplitude, as in Equation 1.2.

Expanding the first cosine term and re-arranging somewhat

$$u(t) = \sum_{j=1}^n [h_j \cos(\nu_j(t)) + c_j \sin(\omega_j)] + v_0 + d(t - t_0)$$

This gives the new linear parameters h_j , c_j and v_0 , from these the original parameters can be solved if necessary. However, some of the parameters still remain non-linear (period, eccentricity and time of periapsis passage) and require a separate solution.

By using explicit derivatives for the solution of the non-linear parameters they achieve a significant speedup, reducing the computation time to half or better.

Partial linearization gives a much better convergence ($\chi^2 - \chi_{\min}^2 < 2$ where χ_{\min}^2 is the best fit value and χ^2 is the model under test) success rate which is clearly shown in their Figure 1. With partial linearization the fraction of successful fits drop linearly with increasing number of standard deviations of initial fit from the best fit. Using fully non-linear models the fraction of successful fits drop to less than half when the initial guess is more than three standard deviations from the best fit.

For astrometry they choose the parametrization (Equation 49 and 50 in their paper)¹

$$\begin{aligned} \Delta\delta_k &= \sum_j (A_j X_{j,k} + F_j Y_{j,k}) + \Delta\delta_0 + \varpi\Pi_{\delta,k} + \mu_\delta(\tau_k - t_0) \\ \Delta\alpha_k \cos \delta &= \sum_j (B_j X_{j,k} + G_j Y_{j,k}) + \Delta\alpha_0 \cos \delta + \varpi\Pi_{\alpha,k} + \mu_\alpha(\tau_k - t_0) \end{aligned}$$

This parametrization is similar to the one used in this project. The two equations describe with the first sum the offsets due to a orbiting planet using Thiele-Innes parameters. Then comes the difference between the “true and nominal position at time t_0 ”, the effect due to parallax and finally the offset due to proper motion.

The way they combine astrometry and radial velocity data is to express the tangential (to the sky plane) offset of a star due to an orbiting body through a distance and angle. This as the parameters, (Thiele-Innes) used to describe this offset, will be the same as used to describe the radial velocity. Also this avoids the problem with a over-constrained solution and instead only use two Thiele-Innes parameters, C and H , instead of the four Thiele-Innes A , B , F and G .

¹See appendix B on Thiele-Innes parameters

$$\begin{aligned}
\rho_{\theta,k} &= \sum_j (A_j X_{j,k} + F_j Y_{j,k}) \cos \theta_k + (B_j X_{j,k} + G_j Y_{j,k}) \sin \theta_k \\
&\quad + (\Delta\delta_0 + \varpi\Pi_{\delta,k} + \mu_\delta(\tau_k - t_0)) \cos \theta_k \\
&\quad + (\Delta\alpha_0 \cos \delta + \varpi\Pi_{\alpha,k} + \mu_\alpha(\tau_k - t_0)) \sin \theta_k \\
&= \sum_j (H_j S_{j,k} + C_j T_{j,k} \\
&\quad + (\Delta\delta_0 + \varpi\Pi_{\delta,k} + \mu_\delta(\tau_k - t_0)) \cos \theta_k \\
&\quad + (\Delta\alpha_0 \cos \delta + \varpi\Pi_{\alpha,k} + \mu_\alpha(\tau_k - t_0)) \sin \theta_k
\end{aligned}$$

These H_j 's and C_j 's are linearly related to the h_j 's and c_j 's for radial velocity. Further $S_{j,k} = \cos(\Omega_j - \theta_k) \csc i_j X_{j,k} - \sin(\Omega_j - \theta_k) \cot i_j Y_{j,k}$ and $T_{j,k} = -\sin(\Omega_j - \theta_k) \cot i_j X_{j,k} - \cos(\Omega_j - \theta_k) \csc i_j Y_{j,k}$

1.5.2 Double-blind test program for astrometric planet detection with Gaia

This paper (Casertano et al., 2008) summarizes a quite extensive “double-blind” test campaign both for detectability and detection of exoplanets in a realist scenario with Gaia.

The part of most interest here is their “Test T2”. What this aims to establish is, for a known single planet system, the accuracy of the orbital determination. The orbital characteristics where, however, not known.

A sample of 50000 systems were created with orbital periods in the range of 0.2 to 12 years and astrometric signatures between 16 μas and 1.6 mas. From this sample two groups, or solvers, participated in the test to; an initial determination of parameters and then a orbital reconstruction.

Both solvers approach the problem through a hierarchical solution.

The result of this test is that the parameters can be reliably determined together with accurate error estimates. Still, however, a few percent of the systems do give incorrect solutions but are not identified through the error estimates.

1.5.3 Unconstrained astrometric orbits for *HIPPARCOS* stars with stochastic solutions

In this paper (Goldin and Makarov, 2006) they look at *acutal* data from Hipparcos. Both at data of known orbital solutions and “stochastic solutions”¹ of a further 1561 systems. The idea is that large errors (residuals between observed and computed position) may be contributed to a unseen companion. If an orbiting body is included in the solution the errors will be reduced as the errors in reality are a combination of signal and measurement errors.

The mathematical description is pretty much identical to what has been used in this project except they do not apply it to transformed² variables or use the same algorithm solving for the orbital parameters. The precision of the data, Hipparcos Intermediate Astrometric Data (HIAD), are around 10 mas for a single point, so the companions have to be at least as massive as a brown dwarf for detection.

¹Failures in the reduction of the data or large errors

²Here meaning that the variables are constrained through some mathematical transformations eg. $x \rightarrow \arctan x$.

Their choice of method for the reduction is a genetic optimization algorithm. This method does not rely on the partial derivatives of the objective function, but it has the advantage of better handling local minima. This means that the initial “population” will consist of many (30) random starting points for the optimization thereby side stepping the issue of selecting a single initial guess for the optimization. The larger the number of the initial population the greater the probability is that the optimization will indeed end up in the global minima, or at least close to it.

They also investigate the confidence interval of fitted parameters. To start they take the observed transit times and perform a reduction, both for a solution of only the five astrometric parameters and for a solution of all twelve parameters (5 astrometric, 7 “planetary” or in this case parameters describing the orbit of a companion star). This results in the residuals $\chi_{5,0}^2$ and $\chi_{12,0}^2$ respectively. Next step is to perturb the transit times with a normally distributed numbers reflecting the formal measurement errors and perform the same reduction again¹. This gives the values $\chi_{5,i}^2$ and $\chi_{12,i}^2$ respectively. Forming the expression in the equation below where Θ is a threshold function such that $\Theta_i(x) = 1$ for $x > 0$ and $\Theta_i(x) = 0$ otherwise.

$$p = \frac{1}{N} \sum_{i=1}^N \Theta_i \left(\frac{\chi_{5,i}^2}{\chi_{12,i}^2} - \frac{\chi_{5,0}^2}{\chi_{12,0}^2} \right)$$

This gives the probability that there is no extra companion.² If the null hypothesis is rejected then part of the same procedure as above is repeated, namely the transit times are slightly perturbed. The reduction is performed which results in a distribution of parameters. These distributions are then used for the creation of confidence intervals of the individual parameters.

From their treatment they propose a list of 65 candidate systems which are “good candidates for follow-up spectrographic studies”, these have proposed orbital fits at 99% confidence level and most of them had not been known as binary systems.

They also point out some problems which can arise when fitting for companions; If the period is longer than the mission length, then the contribution from an orbiting companion will look more like a straight segment which could easily be confused with proper motion. For high eccentricities the effective number of degrees of freedom goes up, which is to say that it is possible to find something looking like a global minimum if the eccentricity goes up.

In their paper they also provide most of the partial derivatives of the Thiele-Innes parameters, not the ones for radial velocity (C and H) though.

1.5.4 Astrometric planet detectability with Gaia, a short AGISLab study

This short technical note (Holl, 2011) uses AGISLab to determine the detectability of planets with Gaia. The technique for detectability is slightly different from the one used in for example Goldin and Makarov (2006). Here it is not so much if there is a additional signal in the measurement errors, but instead if it detection would be possible with Gaia. The parameters describing the orbiting body are assumed known and the residuals are compared. The criteria for detectability at α significance level is

¹Parametric bootstrapping

²To point out here is the difference between *detectability* and *detection* (see Holl (2011)). Detection is taken as the determination of the parameters and detectability as only an answer to the question if there is a companion or not.

$$\chi_{(a)}^2 \geq \chi_{(b)}^2 \Delta(N, \alpha)$$

where $\chi_{(a)}^2$ are the residuals for only the astrometric parameters and $\chi_{(b)}^2$ the residuals for the astrometric and *exactly* known orbital parameters. $\Delta(N, \alpha)$ is the delta Chi-square parameter for N parameters.

The conclusion is that indeed planets with a one year period will be harder to detect due to having the same orbital period as Gaia will have around the Sun. Also, depending on the distance and magnitude of the star, the gating scheme¹ in Gaia will have an effect. However, a 3 M_J planet could be detected as far out as 300 pc.

1.5.5 Detectability of terrestrial planets in multi-planet systems: Preliminary report

Similar in the concept as Casertano et al. (2008), that is, this experiment is carried out as a double blind test of realistic observations. The goal of this article (Traub et al., 2010) is to determine “if Earth-like planets can be detected in multi-planet systems, using astrometric and radial velocity observations”. However, it was more of a feasibility study for SIM Lite². The measurement principles for SIM Lite would be different from Gaia as it was planned as an interferometric instrument which would have it “visit” different stars a number of times during a short or long period. The result would be a positional accuracy around 0.1 μas , which is better than what is expected from Gaia.

For the radial velocity, accuracy was fixed at 1 m/s RMS per measurement. The radial velocity measurements were spaced with around one month between measurements over at least a 15 year period. They also include breaks in the measurements when the Sun would be in the way.

More considerations are made but they are more connected to the physical properties of the target star etc, and are not considered in the project.

The systems generated were “realistic” in the sense of composition of bodies and orbital parameters, and all had a distance of 10 pc.

Concerning false alarms only one of the groups participating in the detectability part was able to avoid any false alarms.

The conclusion is that, it would have been possible to detect terrestrial planets in multi-planet systems.

1.5.6 Reduction of the astrometric binaries

Another short technical note ((Pourbaix and Jancart, 2008)) take a look at the very similar problem, namely astrometric binaries. The model they employ is a grid search for the three parameters; eccentricity, period and time of periapsis as first step. This initial grid search is then used as the starting point for the optimization. A bit surprising is that, even if it is assumed that the orbits are circular, searching for period by χ^2 minimization is efficient for eccentric orbit.

¹CCD integration time due to apparent brightness of the star

²Space Interferometry Mission - Planned space telescope, but which due to budget cuts, was canceled in 2010.

1.5.7 A new algorithm for fitting orbits of multiple-planet systems to combined RV and astrometric data

In here (Catanzarite, 2010) a hierarchical fitting procedure is described, in which first the most significant signal (position, proper motion, parallax and the constant offset from the radial velocity data) is fitted and removed. Then the signal corresponding to the largest signal in a periodogram is removed. Once all the components have been found, they are used as starting guess for the final iteration, solving for all the parameters simultaneously.

1.6 Outline

The setting for this thesis is the launch of Gaia this fall combined with the accuracy of measurements. The class of possible star planet systems which will be possible to determine the orbital properties will be restricted by the magnitude of the star being in the range Gaia will be able to measure, the system not being too far away and the planet not being too small or on a too large orbit. Also there is not so much of an preferred direction for detection. All these combined, will make Gaia a good compliment to previous and on-going exo-planet hunts.

In this thesis a model will be derived describing the parametrization of the problem. Both the astrometric and the radial velocity part. Expressing both models in the same parameters will give an easier route to implementation. The model will then be implemented in Java and integrated into AGISLab. As initial step the astrometric part will be done and then the radial velocity part will be added. This so that a planetary signal can be added to the astrometric observations and also a simple generation of radial velocity data.

The same model will be used to try to recover the astrometric (position, proper motion, parallax and radial motion) as well as the planetary parameters. The result will be a way to solve for orbital parameter, both from only astrometric data and a combination of both astrometric and radial velocity. But also a way to add planetary signals, if so desired, to normal observations.

Just solving for the astrometric parameters, the parameters describing the motion of the star, is possible and works quite well. However, introducing parameters describing the orbit of the planet the solution become less well defined, i.e., large formal errors on parameters. Using all parameters describing the orbit of the planet, it is no longer possible to compute the formal errors and other techniques have to be employed to determine the errors of the parameters. This is done through bootstrapping and does prove possible to do.

Even though it is possible to find “best parameters” from the optimization the large formal errors would imply that those parameters - mainly the parameters related to the orientation of the orbit - are very uncertain. Basically any parameter value would give as good a solution as the optimum. One plausible reason for this is that some of the parameters are degenerated. Since it is not possible to calculate the formal errors when using all parameters due a problem of a matrix being singular¹ it implies that some of the parameters are redundant. This is also shown calculating the singular values of the matrix.

That it is not possible to calculate the formal errors is quite bad in the sense that this approach of solving the problem does not work. If necessary it is possible to get a grasp on how

¹The matrix $\mathbf{J}^T \mathbf{W} \mathbf{J}$ where \mathbf{J} is the Jacobian and \mathbf{W} is the weight matrix is used as an approximation of the Hessian when the optimization has converged. The inverse of this matrix is used in the calculation of the formal errors. If the matrix is singular, it is no longer possible to calculate the inverse and no formal errors can be calculated.

large the formal errors are from bootstrapping. A better solution would be to use a different parametrization of the problem, or to just reduce the number of parameters used. This would most likely be the best solution, and in addition not require too much extra work as most of the infrastructure is already in place, e.g., transformation of variables and partial derivatives.

Much details of the work are moved to the appendices, not because they are peripheral but if the details are of interest it is easier to jump to the appendix and then back, instead of jumping forward in the text.

In Appendix A a discussion about ellipses is used to create a parametrization for the mathematical expression of an ellipse. Newton's law is then used for a two body system (star and planet) to derive how they will orbit each other. This gives also Kepler's three laws; planets move on ellipses, the radius vector sweep out an equal area in equal time and the orbital period is proportional to the semi-major axis cubed. Kepler's equation is derived from which the eccentric anomaly is solved to describe where in its orbit the planet is.

Continuing on in Appendix B the relation between the Thiele-Innes parameters and rotating an orbit so it is viewed from an arbitrary angle is stated. This gives a way to go from just an ellipse describing the planetary orbit in a plane, to describe an orbit in a three dimensional coordinate system related to the observer. At the same time, the radial velocity is calculated from the time derivative of how the planet moves back and forth from the observer. This is the simultaneous description of astrometry and radial velocity.

Following in Appendix C the problem is defined; finding a set of parameters such that the merit function is minimized. The merit function is taken as the weighted square residuals from the calculated and measured positions of the stars. The Levenberg-Marquardt method is introduced as a way to find updates to the parameters for minimizing the merit function. The offset of the star due to the orbiting planet is also introduced which give the contribution to the astrometry part. Also, the time derivative of the radial offset is introduced which give the contribution to the radial velocity part. For the Levenberg-Marquardt method to work it needs the partial derivatives with respect to all the parameters, these are calculated. To keep the parameters in a sensible range, different boundary conditions are discussed and it is settled to use a transformation of the parameters. This means that the transformed parameters will be optimized, so all partial derivatives with respect to the transformed parameters are also calculated. The collection of all the partial derivatives result in the calculation of the Jacobian which is also used to calculate the formal errors on the optimized parameters from the Levenberg-Marquardt method.

2 Method

To begin the system used for the investigation, the template system, is described and motivated. After that follows a short summary of the modeling of the planetary system. This leads to the description of the problem together with the optimizer for optimizing the parameters, the Levenberg-Marquardt algorithm together with the Jacobian.

A successful optimization gives a set of parameters which, not necessary the same or close to those used to construct the system, will give “functional values” close to the observations. From the parameters the Jacobian can be calculate.

Knowledge of the measurement errors, lead to estimates on the formal errors of the parameters. This estimate is relying on a assumption which leads to a singular value decomposition of the inverse of the co-variance matrix $\mathbf{J}^T \mathbf{W} \mathbf{J}$.

Two other strategies, both bootstrapping, are then explored for calculating the formal errors of the parameters.

2.1 The system

Main considerations for choosing the system was that it should be able to be detected. That is, it should have a relative large astrometric signature $m_r \frac{a}{d} = \frac{m_p}{m_*} \frac{a}{d}$ where m_r is the mass ratio of the planet to the star, d the distance to the system and a the semi major axis of the orbit.

Barnard’s star was chosen. It has the required properties, and in addition it has large proper ($\mu_{\alpha*}$ and μ_δ) and radial motion (μ_R) if extending the modeling to include offsets due to planets in these terms is desired.

Properties for the planet were also chosen along these lines; a relatively massive planet on a not too wide orbit. The wider the orbit, the larger the astrometric signature. But at the same time, a too wide orbit will due to the limit of mission length look like a straight segment. The orientation of the orbit was set to 45° as this would give a good astrometric signal in addition to a good radial velocity signal. All the parameters are summarized in Table 2.1. In Figure 2.1 the mass of the planet (blue filled dot) is plotted in relation to the stellar mass with the size of the marker representing the magnitude of the host star. In the same figure, detected exoplanets are plotted. If the host-star does not have a listed magnitude it is plotted with a marker of just a dot. The selection of parameters puts the template system rather isolated in the parameter space of planet and stellar mass. But the main consideration here is not for realism, instead the main goal is to look at the parametrization and optimization.

In Figure 2.2, which is from Casertano et al. (2008), the discovery space of Gaia is plotted. This figure is the result of a double blind test done to asses what Gaia would be able to detect in terms of exoplanets. Of interest here are the blue lines representing a slightly heavier stellar

Table 2.1: Parameters used for the system. The period is not given as it is calculated from Kepler’s 3’rd law using the mass of the star and the mass ratio of the planet to the star. Barnard’s star is used as template for the star. To this a quite massive star is added, roughly as massive as Neptune or a tenth as massive as Jupiter. Also note the subscript on proper motion in right ascension, this α_* is to denote that it is in recti-linear coordinates at the pint (α, δ) , i.e., it includes a factor $\cos \delta$.

Parameter	Symbol	Value	Unit
Right ascension	α	0.8721719219927877	rad
Declination	δ	-0.7517403490455259	rad
Parallax	ϖ	545.4	mas
Proper motion R.A	μ_{α_s}	-798.71	mas/year
Proper motion DEC.	μ_δ	10337.77	mas/year
Radial motion	μ_R	12808.7286843668	mas/year
Magnitude	V	9.54	
Mass of star	$m_{r,*/\odot}$	0.144	
Mass ratio	m_r	1.0/2000.0	
Semi major axis	a	1.5	AU
Eccentricity	e	0.001	
Period	P		yr
Inclination	i	45.0	degree
Argument of periapsis	ω	275.066	degree
Argument of ascending node	Ω	100.492	degree
Time of periapsis passage	t_p	REF_EPOCH_YR+0.5*P	
Mission length		5	yr

mass ($0.5 M_\odot$ vs. $0.144 M_\odot$) but at a larger distance than the template system (25 pc vs. ~ 2 pc). The smaller distance to the template system, and the smaller mass of the host star, imply that the lines for a similar system should be shifted downwards by a factor of ~ 50 . So the template system should not present any problems for detection with Gaia.

2.2 Planetary model

Here follows a summary of how the template system is parameterized and how the orbit of the planet will affect the position of the star. The full derivation of these equations are in the Appendix A, B and C.

To begin, the motion of a planet can be viewed as an ellipse in a xy -plane with position described by

$$\begin{aligned}
 x &= a(\cos E - e) \\
 y &= a(1 - e^2) \sin E
 \end{aligned}$$

from equation A.5a and A.5b.

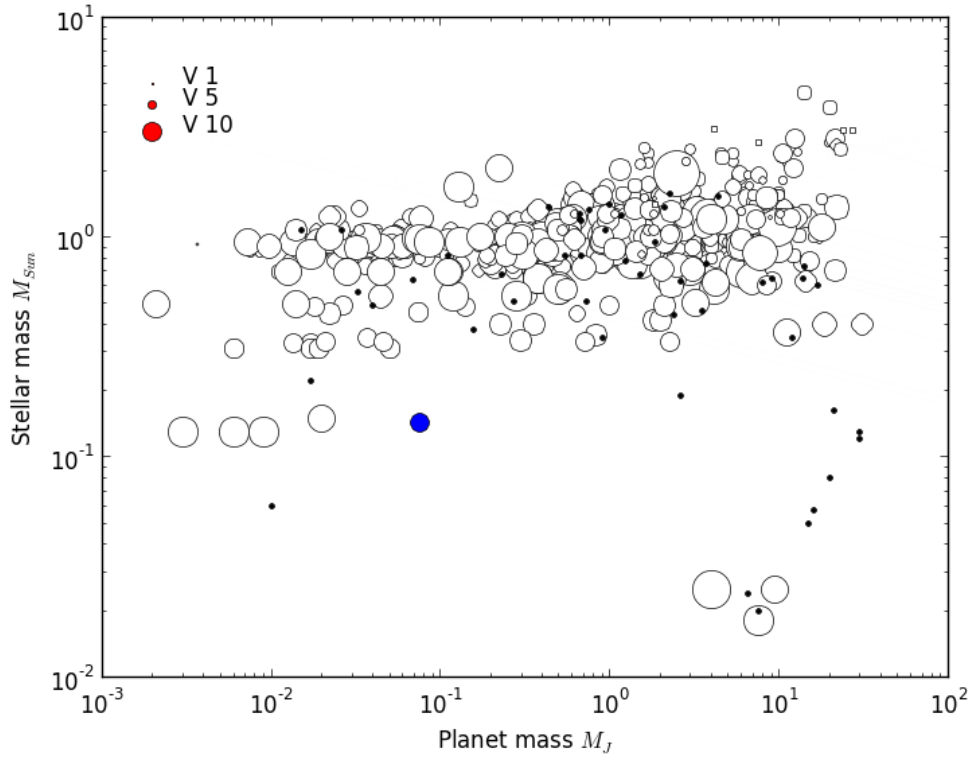


Figure 2.1: Plot of exoplanet mass together with mass of its host star. Size of circle correspond to V-magnitude, filled dots are of stars without listed magnitude. The template system is the blue filled dot ($0.075 M_J$, $0.144 M_\odot$, 9.54 V). This makes the template system sit in an area which is not populated by other detected exoplanets. Source for data: exoplanets.eu (Retrieved on May 1'st)

Or just the radius vector from one of the foci

$$r = a(1 - e \cos E)$$

This describes an ellipse (see Figure A.1) with semi major axis a and eccentricity e . E is the eccentric anomaly or rather an angle related to the position of the planet in its orbit. The eccentric anomaly is calculated by solving Kepler's equation (Equation A.19) at time t

$$E - e \sin E = \frac{2\pi}{P}(t - t_p)$$

where t_p is the time of periapsis, or the point in time where the planet is closest to the barycenter of the system. P is the period. This little equation is the one which ties up three of the parameters e , P and t_p into a non-linear expression.

This is derived by starting out with two bodies orbiting each other and using Newton's laws. From Newton's second law the forces on the bodies are

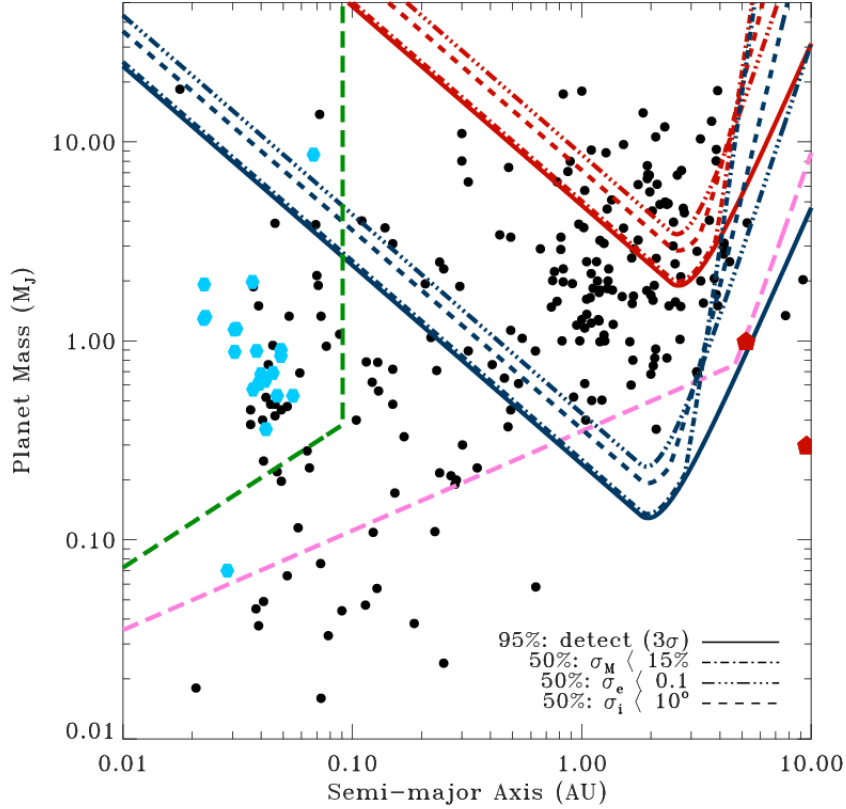


Figure 2.2: In Figure 22 of Casertano et al. (2008) they present the discovery space for planets with Gaia together with two other techniques. The blue lines are for a $0.5 M_{\odot}$ star at 25 pc distance, the red lines are for a $1 M_{\odot}$ at 200 pc distance. Line types correspond to uncertainty in parameter determination. The pink line is for radial velocity and the green line for transit photometry. Other markings correspond to exoplanets detected by different methods and two planets in the solar system (red pentagons). The detectability of the template system can not directly be read of from this plot as the star it is orbiting is a $0.144 M_{\odot}$ at a distance of ~ 2 pc. But as the signal generated by the system (astrometric signature) is $m_r \frac{a}{d}$ where d is the distance to the system, a semi major axis and m_r the mass ratio, the closeness of the template system would increase astrometric signature by a factor ~ 10 bringing the blue lines down by a factor ~ 10 and making detection possible. Also, in addition, there is a factor ~ 5 in the mass ratio of the system. So Gaia would comfortably be able to detect the planet if same methods were employed as for generating this Figure.

$$\mathbf{F}_1 = m_1 \ddot{\mathbf{r}}_1 = G \frac{m_1 m_2}{r^3} \mathbf{r}$$

$$\mathbf{F}_2 = m_2 \ddot{\mathbf{r}}_2 = -G \frac{m_1 m_2}{r^3} \mathbf{r}$$

and from the third law

$$\mathbf{F}_2 = -\mathbf{F}_1$$

Instead of expressing it in terms of direction vectors from the centre of mass (\mathbf{r}_1 and \mathbf{r}_2) it could be expressed as a vector connecting the two bodies

$$\mathbf{r} = \mathbf{r}_2 - \mathbf{r}_1 \quad (2.2)$$

The relation between the bodies and vectors are in Figure A.4.

After a lengthy derivation, which is in Appendix A.2, the result is Kepler's equation for calculating the eccentric anomaly E .

To help visualize how the different coordinate systems are related to each other Figure 2.3 has a depiction. This figure is also reproduced in Figure C.1 with a somewhat longer explanation. The direction to the center of mass for the star and planet is given by the two angles α and δ . The gray coordinate system is placed at the center of mass of the system with the Z -axis pointing back to the observer. The two other coordinate axes are aligned such that Y is in the direction of increasing right ascension α and X in the direction of increasing declination δ . The orbital plane of the planet, xy -plane, can have any orientation in this gray XYZ -coordinate system. This can be thought of as first having the xy -plane aligned with the XY -plane, then rotating the xy -plane into its desired orientation. Three angles are required for this rotation; inclination i , argument of periapsis ω and argument of ascending node Ω . The equations for expressing the coordinates of the xy -system in the gray XYZ -system is given by the three linear equations (Equation B.7a, B.7b and B.7c in the appendix B)

$$\begin{aligned} X &= Ax + Fy \\ Y &= Bx + Gy \\ Z &= Cx + Hy \end{aligned}$$

where the parameters A , B , C , F , G , and H are the Thiele-Innes parameters. They are the matrix elements describing the rotation of the xy -orbit in the gray XYZ -system. Note that they contain a factor a . This is the same factor as in the description of the planets orbit but which due to convenience in the implementation is moved into the Thiele-Innes parameters.

$$\begin{aligned} A &= a(\cos \Omega \cos \omega - \sin \Omega \cos i \sin \omega) \\ B &= a(\sin \Omega \cos \omega + \cos \Omega \cos i \sin \omega) \\ C &= a(\sin i \sin \omega) \\ F &= a(-\cos \Omega \sin \omega - \sin \Omega \cos i \cos \omega) \\ G &= a(-\sin \Omega \sin \omega + \cos \Omega \cos i \cos \omega) \\ H &= a(\sin i \cos \omega) \end{aligned}$$

This describe the orbit of the *planet* in *that* coordinate system. What is needed is the *offset* of the star which is in Equation C.1, C.3 and C.3.

$$\begin{aligned} X^{\text{Offset}} &= -m_r \varpi (Ax + Fy) \\ Y^{\text{Offset}} &= -m_r \varpi (Bx + Gy) \\ Z^{\text{Offset}} &= -m_r \varpi (Cx + Hy) \end{aligned}$$

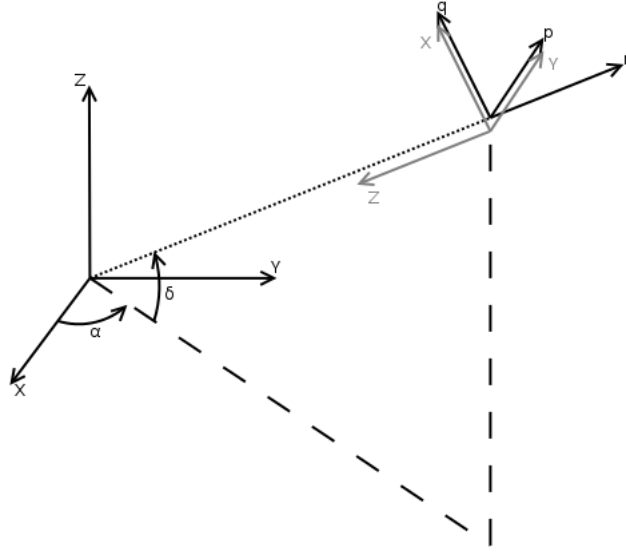


Figure 2.3: Relation of coordinate systems. The observer is in the black XYZ -system with the direction to the star (α, δ) . The star-planet system is described in the gray XYZ -system. What will be observed can be thought of as first drawing an ellipse for the planet in the gray XY -plane. As it can be orientated in any way it has to be rotated. The Thiele-Innes parameters are related to this rotation, so the planetary orbit is described by three coordinates in the gray XYZ -system. The star will have an offset opposite to the position to the planet. What is then measured by astrometry is the star's position including the offset due to a planet. Astrometry can only detect the offsets in the XY -plane which is perpendicular to the radial direction r or tangential to the celestial sphere. Radial velocity on the other hand measures the velocity in the radial direction or the time derivative of the Z -offset. Further the star also has proper motion and radial motion.

The offset in Z can not be measured, but the radial velocity can be measured which is just the time derivative of Z^{Offset} , i.e. Equation C.7

$$\dot{Z}^{\text{Offset}} = -m_r \varpi (C\dot{x} + H\dot{y})$$

with the expressions for \dot{x} and \dot{y} in Equation C.4 and C.5

The X^{Offset} and Y^{Offset} describe the offset in the direction angles δ and α respectively, and \dot{Z}^{Offset} is the negative component of the radial velocity due to an orbiting planet.

Through the parameters e , P , t_p , m_r , A , B , C , F , G , and H both the astrometric offsets and radial velocity can be expressed¹.

2.3 Astrometric data

How the astrometric observations were made is left to AGISLab. Provided the data for the star, a source is created and the measurements are made, taking into account all the details of noise,

¹Note that the Thiele-Innes parameters depend on each other. The optimization, however, did not take this into account which may have contributed to its poor performance.

gating of the CCDs etc. All what is needed is the implementation of how to calculate the α and δ offsets which are given in the expression for Y^{Offset} and X^{Offset} respectively.

If there is more than one planet, then these offsets are just added not considering non-linear terms.

The measurements are however not of α and δ but instead functions of these $\zeta(\alpha, \delta, \dots)$ and $\eta(\alpha, \delta, \dots)$ so taking the derivative of either of these function with respect to a planetary parameters will give slightly expanded expressions.

2.4 Radial velocity data

The radial velocity data was generated as a separate data set, covering a different span in time with different cadence than what Gaia will observe. It was also assumed that the radial velocity had no linear term or any acceleration, that is the radial velocity was described only through the expression for \dot{Z}^{Offset} . Normally the units for radial velocity in m/s or similar whereas here it is internally computed as rad/yr so it assumes some knowledge of the parallax to the system. The only conversion of units is made for the standard deviation of the errors for the measurements which is chosen quite small to 0.1 m/s. The measurements are made ten years back in time from the reference epoch of 2010 for Gaia. To not just have uniformly spaced points in time, the observation time is determined through a Bernoulli process with probability of 0.9 per step, or rather, *“a radial velocity measurement is made daily with the success rate of 90 %”*

2.5 Levenberg-Marquardt

As optimization algorithm Levenberg-Marquardt was chosen. This is a combination of steepest descent (for large updates far from optimum) and Gauss-Newton (smaller updates close to the optimum) approaches to optimization (See appendix C.1 for a fuller explanation). Further it is considered quite stable and likely to converge given good starting conditions, not needing any boundary conditions on the parameters.

Even if good starting conditions were given, it did sometimes give unrealistic results. To avoid this, the planetary parameters were restricted to an interval, e.g.,

$$\tilde{x} = \tan \left\{ \frac{\pi}{2} \left(\frac{2x - b - a}{b - a} \right) \right\}$$

would restrict x to the interval (a, b) .

The goal of the Levenberg-Marquardt optimizer is to find a set of parameters \mathbf{p} such that the difference between the measurements \mathbf{y} and computed values $\hat{\mathbf{y}}(\mathbf{p})$ is minimized, e.g., minimize the merit function

$$\chi^2(\mathbf{p}) = \frac{1}{2}(\mathbf{y} - \hat{\mathbf{y}}(\mathbf{p}))^T \mathbf{W}(\mathbf{y} - \hat{\mathbf{y}}(\mathbf{p}))$$

where \mathbf{W} is a diagonal weight matrix with elements $1/\sigma_i^2$ corresponding to the errors of the i 'th measurement.

To find the update of the parameters, the algorithm solves the equation

$$(\mathbf{J}^T \mathbf{W} \mathbf{J} + \lambda \text{diag}(\mathbf{J}^T \mathbf{W} \mathbf{J})) \mathbf{h}_{\text{LM}} = \mathbf{J}^T \mathbf{W} (\mathbf{y} - \hat{\mathbf{y}})$$

to find \mathbf{h}_{LM} as the update to the parameters \mathbf{p} .

The matrix \mathbf{J} is the Jacobian and consist of the partial derivatives of the functions ζ and η with respect to the parameters

$$\begin{pmatrix} \vdots & \vdots & \vdots & \vdots & \vdots & \vdots & \vdots & \vdots & \vdots & \vdots \\ \frac{\partial \zeta_i}{\partial \alpha_*} & \frac{\partial \zeta_i}{\partial \delta} & \frac{\partial \zeta_i}{\partial \mu_{\alpha_*}} & \frac{\partial \zeta_i}{\partial \mu_\delta} & \cdots & \frac{\partial \zeta_i}{\partial \alpha_*} \frac{\partial Y^{\text{Offset}}}{\partial \tilde{P}_1} + \frac{\partial \zeta_i}{\partial \delta} \frac{\partial X^{\text{Offset}}}{\partial \tilde{P}_1} & \frac{\partial \zeta_i}{\partial \alpha_*} \frac{\partial Y^{\text{Offset}}}{\partial \tilde{e}_1} + \frac{\partial \zeta_i}{\partial \delta} \frac{\partial X^{\text{Offset}}}{\partial \tilde{e}_1} & \cdots & \vdots & \vdots \\ \frac{\partial \eta_j}{\partial \alpha_*} & \frac{\partial \eta_j}{\partial \delta} & \frac{\partial \eta_j}{\partial \mu_{\alpha_*}} & \frac{\partial \eta_j}{\partial \mu_\delta} & \cdots & \frac{\partial \eta_j}{\partial \alpha_*} \frac{\partial Y^{\text{Offset}}}{\partial \tilde{P}_1} + \frac{\partial \eta_j}{\partial \delta} \frac{\partial X^{\text{Offset}}}{\partial \tilde{P}_1} & \frac{\partial \eta_j}{\partial \alpha_*} \frac{\partial Y^{\text{Offset}}}{\partial \tilde{e}_1} + \frac{\partial \eta_j}{\partial \delta} \frac{\partial X^{\text{Offset}}}{\partial \tilde{e}_1} & \cdots & \vdots & \vdots \\ \vdots & \vdots & \vdots & \vdots & \vdots & \vdots & \vdots & \vdots & \vdots & \vdots \\ 0 & 0 & 0 & 0 & \cdots & \frac{\partial \dot{Z}_k^{\text{Offset}}}{\partial \tilde{P}_1} & \frac{\partial \dot{Z}_k^{\text{Offset}}}{\partial \tilde{e}_1} & \cdots & \vdots & \vdots \\ \vdots & \vdots & \vdots & \vdots & \vdots & \vdots & \vdots & \vdots & \vdots & \vdots \end{pmatrix}$$

Appendix A, B and C cover from the description of planetary orbits to how all the partial derivatives with respect to the transformed parameters are calculated. This description of planetary orbits is what had to be implemented in AGISLab to be able to create positional offsets, but also the calculation of the Jacobian and the possibility to either use transformed or non-transformed parameters.

Once the algorithm as converged, or at least stopped updating the parameters, it is assumed that the function $\chi^2(\mathbf{p})$ can be approximated by a quadratic function, and the formal errors can be calculated from the expression

$$\sigma_{\mathbf{p}} = \sqrt{\text{diag}((\mathbf{J}^T \mathbf{W} \mathbf{J})^{-1})}$$

2.6 SVD and Bootstrapping

Even though the Levenberg-Marquardt optimizer can give a set of parameters as a solution, it could be that the matrix $\mathbf{J}^T \mathbf{W} \mathbf{J}$ becomes singular, so no formal errors on the parameters¹ can be calculated. Even if it does not become singular, it could become ill-conditioned giving un-realistic large formal errors on some or the parameters.

Leaving aside the issue of how good a solution is for a moment and looking at what it means that a solution was found. The ideal case is that the set of parameters which give the smallest merit function actually have been found, i.e., the global minima. A less ideal case is that a set of parameters have been found such that any small step away from the point in parameters space will result in a increased merit function, or a local minima. This local minima is equally valid as the global minima in this sense. How good a solution ties in to this through how the merit function changes due to small changes in the parameters. It could be that a set of parameters have been found which give a small merit function. A small change in some of the parameters result in a increased merit function, but a small change in some of the other parameters only

¹To avoid un-realistic solutions transformations of the parameters were used in the optimization, once the optimizer had converged a switch was made to use non-transformed parameters

marginally changes the merit function (imagine a valley, the elevation change more in some directions than others).

By looking at the singular values of $\mathbf{J}^T \mathbf{W} \mathbf{J}$ it can be assessed how well the approximation by a quadratic function is, or at least if some parameters will have a much larger influence than others.

If the magnitude of the different singular values is large, then it might be necessary to try to find the formal errors by other means. The approach taken are two kinds of bootstrapping. First kind is to re-sample the observations, that is pick a random selection from the observations with replacements (one observation could be included more than once), then the optimization is performed to create a set of optimized parameters for each selection of observations. The second kind of bootstrapping is to utilize the errors associate with the measurements and perturb the observation by a Gaussian random number. So, to each observation a random number is added. This random number is a Gaussian with zero mean and standard deviation three times as large as the measurement error associated with the observation. From this set of perturbed observations an optimization is performed to get parameters. Again, this is repeated multiple times to get a set of parameters.

The number of bootstrap draws was chosen empirically to 5000.

3 Results

Here the result of the two bootstrap approaches are presented. The first approach is re-sampling the observations with replacements, and the second is parametric bootstrapping. For each approach, three tests are done; optimize only for astrometric parameters, optimize for astrometric plus some planetary parameters and optimize for astrometric plus all planetary parameters.

The singular values are presented for each case.

Some of the optimizations fail and an attempt to recover is made.

Finally a QQ-plot is made for period and right ascension for censored data to compare to normal distributions.

In Table 3.1 a summary of the three different calculations are given. Each of the three calculations are performed for the case of simple bootstrapping and the case of parametric bootstrapping.

3.1 Simple Bootstrap

This first section deals with only astrometric measurements. The method for bootstrapping is re-sampling the observations and then re-doing the optimization. For each bootstrap iteration a set of parameters is generated and these parameter sets are used for calculating and plotting. As starting parameters in each iteration, the true parameters are selected.

3.1.1 Only astrometric variables

This simulation correspond to having the planetary signal perfectly removed, or rather knowing the planetary parameter and not doing any optimization on them. All which is updated are the astrometric parameters. In Table 3.2 the singular values are summarized, together with the condition number of the matrix $\mathbf{J}^T \mathbf{W} \mathbf{J}$ and the χ^2 -residuals. Note that the singular value decomposition ($\mathbf{J}^T \mathbf{W} \mathbf{J} = \mathbf{U} \mathbf{\Sigma} \mathbf{V}^*$) is calculated starting from the parameters resulting from the optimization and also using the original measurements (not re-sampled).

Singular values can not directly be translated into parameters. Instead a small value indicate that some parameter, or combination of parameters, does not carry much weight in the updating procedure. To disentangle which singular value correspond to which parameters the rotation matrix \mathbf{V}^* from the singular value decomposition has to be investigated. The column vectors of the rotation matrix would then describe how the parameters are combined. For a perfect

Table 3.1: Listing of the different calculations done, what they include and why they were chosen. Each of these three were performed for both the simple bootstrapping and parametric bootstrapping.

Calculation	Motivation
Only astrometric variables in optimization	Included as a baseline of how well the optimization works. The astrometric parameters are those which would have the most influence on the merit function, e.g., compare change the position of the system slightly to changing the mass of the planet. This also assumes the planetary parameters to be known perfectly.
Astrometric and some planetary variables in optimization	In addition to the astrometric parameters, the period, eccentricity, mass ratio and time of periapsis for the planet is included. The Thiele-Innes parameters are not included, i.e., neither the orientation nor the semi major axis of the orbit are included. None of the parameters should be degenerate so it should be possible to calculate formal errors on the parameters.
Astrometric and planetary variables in optimization	All the parameters are included. There might be degeneracy among some parameters, e.g., the parameters which enter in Kepler's third law.

case the condition number should be around 1 roughly translating into that all parameters are equally important in the optimization.

Table 3.2: Singular values for astrometric parameters only and not using radial velocity. The condition number translates roughly into the span between the largest and smallest singular value. χ^2 is the weighted residuals.

SVD Value 1	4.5553394719569866e21
SVD Value 2	3.672016977128855e21
SVD Value 3	219570.0660009152
SVD Value 4	184815.6986945001
SVD Value 5	65462.98322361746
SVD condition number	6.958649373488268e16
χ^2	1769.22

The calculation of the formal errors on the parameters succeeded, i.e., from a normal optimization, and they are summarized in Table 3.3

In Figure 3.1 the five residuals (Computed-True) of the parameters from the bootstrap iterations are plotted together with the χ^2 -residuals. The red dashed line correspond to the

Table 3.3: Parameters resulting from a normal optimization. Note $1.0e - 11 \text{ rad} \sim 2 \mu\text{as}$

Parameter	Value	Formal error	Units
α_*	0.8721719221	1.5987706399e-11	rad
δ	-0.7517403491	1.5795185411e-11	rad
μ_{α_*}	-798.7119789658	0.0023183760	mas/yr
μ_{δ}	10337.7718377825	0.0022522428	mas/yr
ϖ	545.3985337274	0.0035655325	mas

true value, i.e., indicating a zero difference.

From the bootstrapped parameters the mean and standard deviations are calculated and summarized in Table 3.4. Comparing the values to the ones listed in Table 3.3. There is nothing which stands out, both the parameter value and the errors seem to match. Still the χ^2 -residual for the normal optimization is a bit lower than the central peak in Figure 3.1.

Table 3.4: Parameters for bootstrapping on astrometric parameters only

Parameter	Mean	Standard deviation	Units
α_*	0.8721719220	1.6246813882e-11	rad
δ	-0.7517403491	1.6082514297e-11	rad
μ_{α_*}	-798.711995575	0.0020957551	mas/yr
μ_{δ}	10337.7718211	0.0024085249	mas/yr
ϖ	545.398498336	0.0038997273	mas

For the five astrometric parameters the optimization approach seems to work OK, even though the condition number is quite large.

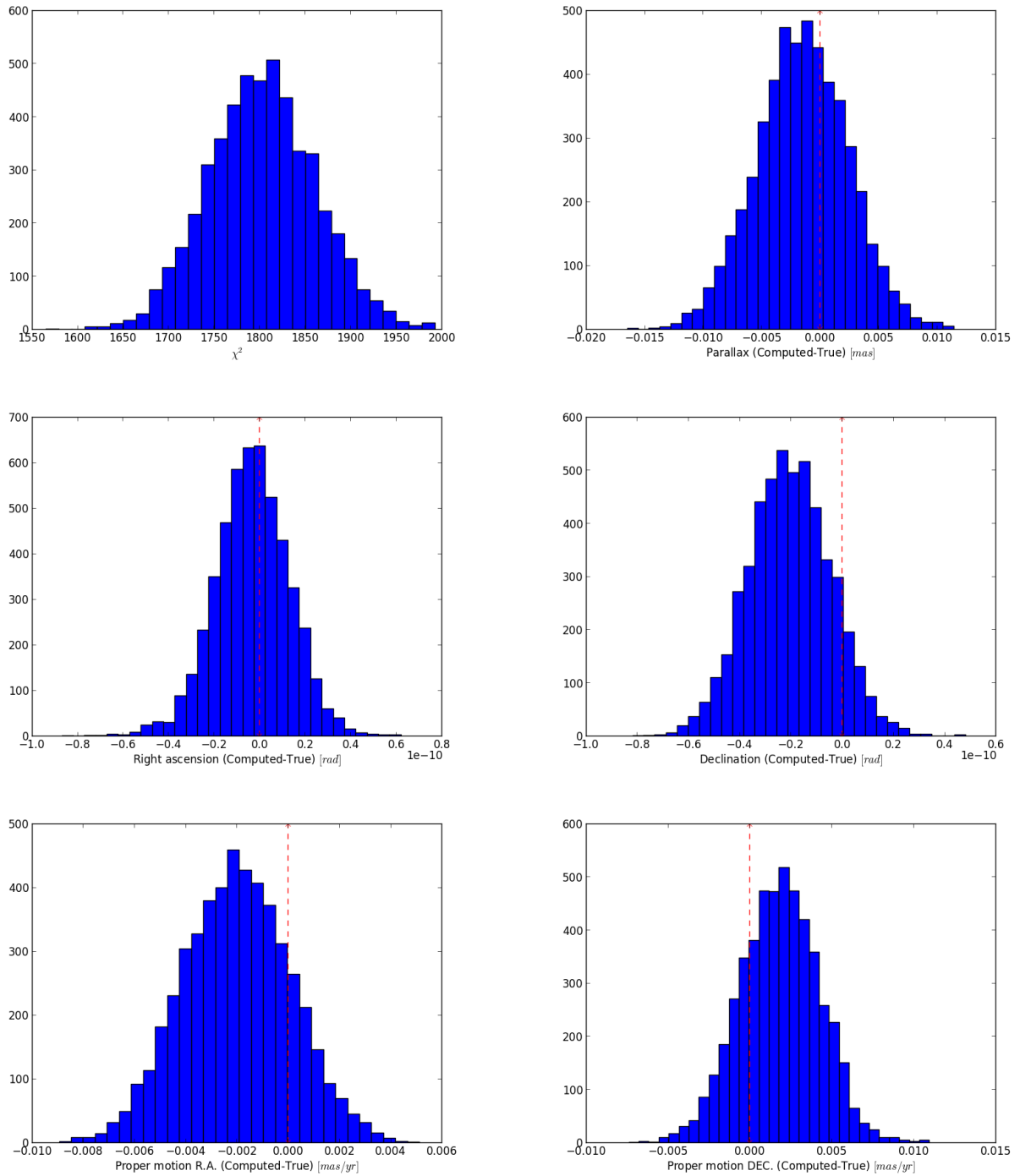


Figure 3.1: Histogram of χ^2 -residuals and only astrometric parameter residuals. Top left - χ^2 -residuals, top right - parallax, middle left - α , middle right - δ , bottom left - μ_{α^*} and bottom right - μ_{δ} . All except χ^2 -residuals are of the computed minus the true parameter, red dashed line indicates true value.

3.1.2 Astrometric and no orientation

Next step is to include some of the parameters describing the planetary orbit. None of the Thiele-Innes parameters are include, so none of the three angles related to the orientation or the semi major axis of the orbit are being updated. Instead, they are assumed to be known perfectly.

In all other regards, the same approach is taken as in the previous.

Table 3.5 contain the summary of the singular value together with the χ^2 -residual. Using the χ^2 -value as indication of how well the optimization succeeded there is no real difference between including some of the planetary parameters or not including any. However, the condition number is *much* larger so things might not work out quite as well.

Table 3.5: Largest and smallest singular values for astrometric and planetary parameters, though not the Thiele-Innes parameters or the semi major axis of the orbit. No radial velocity is included

SVD value 1	4.555339471935343E21
SVD value 9	1.892725865440631E-12
SVD condition number	2.406761356787846E33
χ^2	1766.38

Performing the same normal optimization the resulting parameters and formal errors are in Table 3.6. The astrometric parameters seem well behaved in comparison to only updating the astrometric parameters. Moving on to the planetary parameters it becomes obvious that, even though the optimization succeeded, the formal error on the eccentricity clearly is nonsensical. For the mass ratio the formal error is also very large.

Table 3.6: Parameters resulting from a normal optimization. Note $1.0e - 11 \text{ rad} \sim 2 \mu\text{as}$

Parameter	Value	Formal error	Units
α_*	0.8721719220	2.5404441930e-11	rad
δ	-0.7517403491	4.3020967116e-11	rad
μ_{α_*}	-798.7174411462	0.0046746581	mas/yr
μ_δ	10337.7713998149	0.0031530891	mas/yr
ϖ	545.3990159336	0.0036103264	mas
P	4.7919670188	0.0212121855	yr
e	4.0135015045e-07	8.7275185793e+10	
m_r	4.9341627436e-04	0.8227709260	
t_p	2012.4750746353	0.0046565361	yr

In Figure 3.2 the astrometric parameters together with the χ^2 -residuals for the bootstraps are shown. The χ^2 histogram does not show anything standing out, but looking at any of the other histograms something clearly did not work. The bar standing out always include the true value, the true value was also the starting value for the optimization. So either the optimization did not change from the initial value or it decided that the true value was, statistically speaking, better. A bit interesting to note is the lack of any feature in the χ^2 histogram. Even though many of the bootstrap iterations came to similar optimized parameters there is enough variation to give a un-remarkable χ^2 histogram.

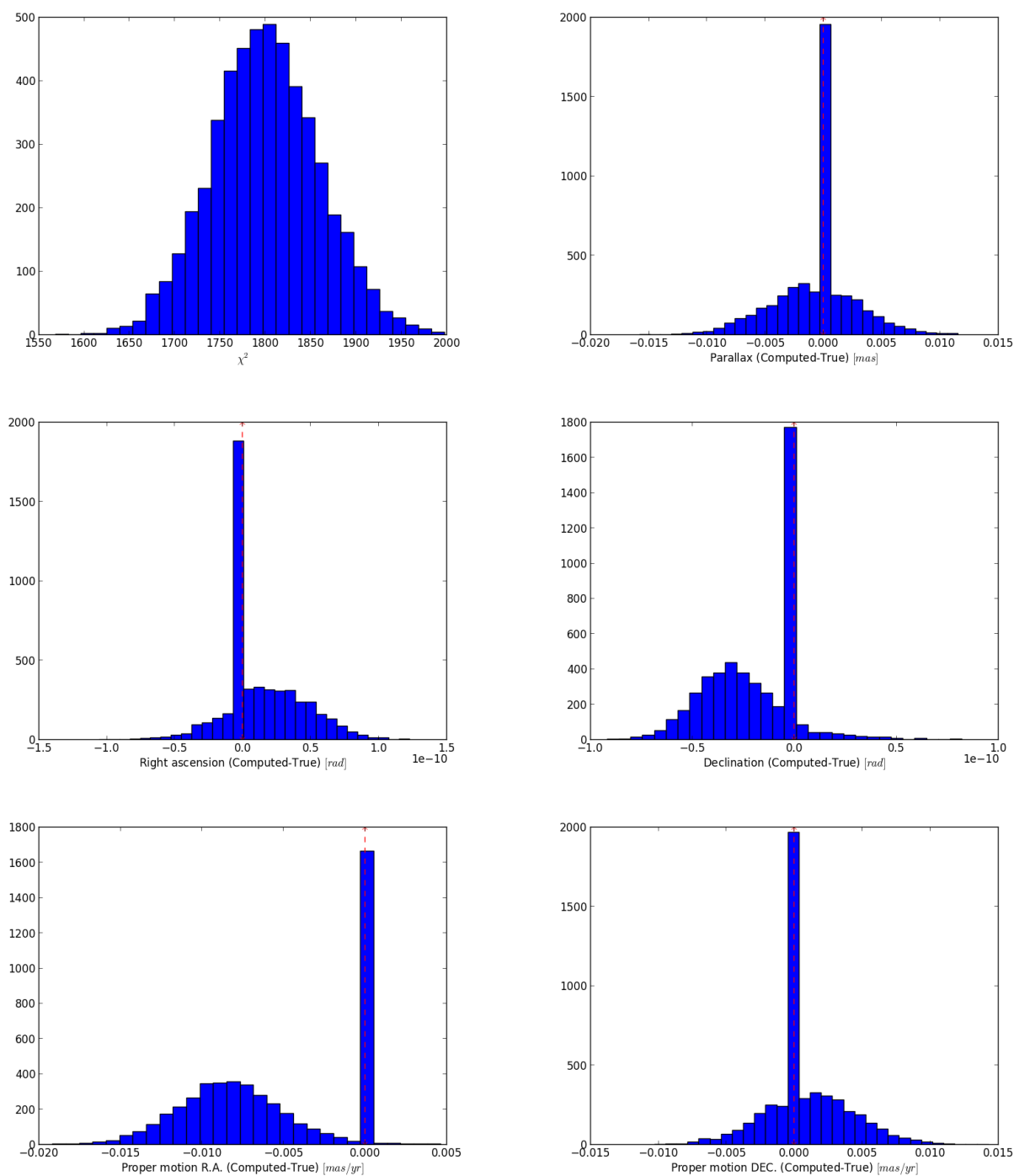


Figure 3.2: Histogram of χ^2 -residuals and only astrometric parameter residuals. Top left - χ^2 -residuals, top right - parallax, middle left - α , middle right - δ , bottom left - μ_{α^*} and bottom right - μ_{δ} . All except χ^2 -residuals are of the computed minus the true parameter, red dashed line indicates true value.

Taking a closer look at one of the planetary parameters, the period, to see if it possible to determine what went wrong and if there is some way to rectify this. Top left in Figure 3.3 the cumulative number of bootstraps is plotted as function of computed minus true period. A very big jump takes place closely to zero offset, as expected from the histograms of the astrometric parameters. The top right of the same figure shows the same plot, but now each line correspond to a given number of internal iterations for the optimizer. One line stands out, namely when the optimizer spent two internal iterations before “converging”. Assuming that it seems un-realistic to make such a good guess that the optimizer would converge in less than three iterations, the top left figure can be redrawn but with censored data. Bottom row is the result, left the cumulative number of bootstraps, and right the histogram. The other parameters result in similar plots.

Calculating the mean and standard deviation for the parameters of these censored bootstraps, the result is tabulated in Table 3.7. The formal errors do look a bit more realistic using the censored data.

Table 3.7: Parameters for astrometric and some planetary parameters. Censored data to only include those bootstrap iteration which had more than two iteration in the optimization step.

Parameter	Mean	Standard deviation	Units
α_*	0.8721719220	3.1384685808e-11	rad
δ	-0.7517403491	1.8453516072e-11	rad
μ_{α_*}	-798.71829975	0.0031946494	mas/yr
μ_δ	10337.7710959	0.0034150001	mas/yr
ϖ	545.399134103	0.0039919358	mas
P	4.7801687529	0.0486837395	yr
e	4.7204886325e-05	0.0004200413	
m_r	0.0004927209	5.6686353301e-06	
t_p	2012.48638853	0.0415953808	yr

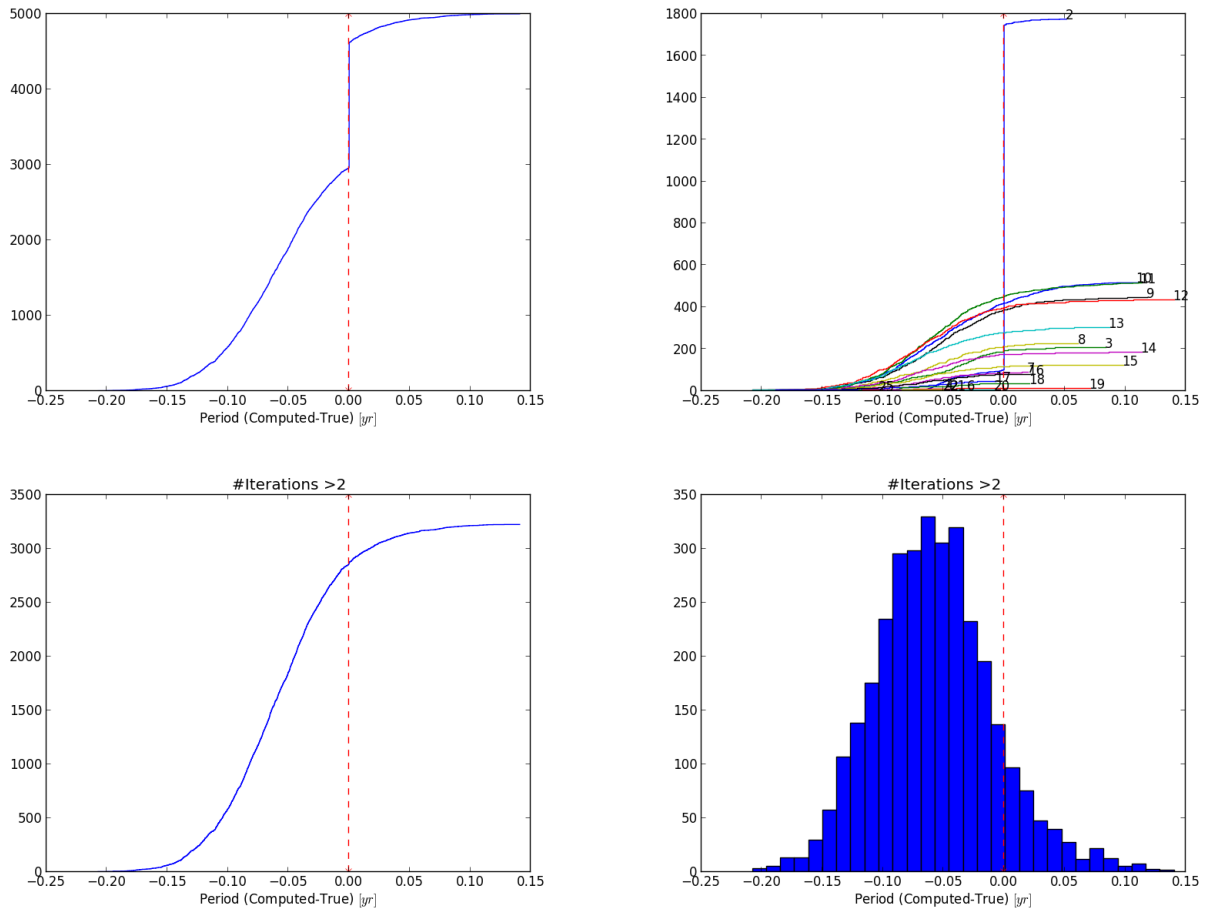


Figure 3.3: A closer look at how the period behaves after bootstrapping. Top left is the normal cumulative plot of the computed minus true values. At zero it makes a clear jump, i.e. the optimizer does not alter the parameters. Top right gives a somewhat better explanation to what is going on. Same thing is plotted, the cumulative plot of the computed minus true value, but this time each line correspond to the specific number of iterations the optimizer performed. When the optimizer performs only two iterations, the period does not get updated. (Same applies to other parameters). In the bottom left, the data has been censored to only include those bootstrap iterations which had more than two iterations in the internal optimization. The cumulative plot looks much cleaner. Bottom right the histogram is plotted for the censored bootstraps.

3.1.3 Astrometric and orientation

Performing the same action with singular value decomposition as the two previous, but this time including the Thiele-Innes parameters, a summary of the singular values are tabulated in Table 3.8. Even though the condition number has not change much there are now two additional very small singular values.

Table 3.8: Largest and two smallest singular values for astrometric and planetary parameters. No radial velocity is included

SVD value 1	4.5553394719385217E21
SVD value 12	3.728711504521402E-12
SVD value 13	1.095296345668235E-12
SVD condition number	4.1590017988778474E33
χ^2	1766.30

In Figure 3.4, the same kind of plot as Figure 3.3, there are some small changes. The number of internal iterations of the optimizer has increased, and now the jump occurs at either 13 or 14 iterations. There is also something happening for 15 iterations, but not where it is expected to happen. However lacking the distinct feature for a specific value this more likely reflects a feature in the merit function. Also the jump for 13 or 14 iterations is less pronounced as some of them seem to converge to values other than the true one. The same censoring is done, but now any iteration performing less than 15 internal optimization iterations are excluded. In the bottom row of Figure 3.4 there is no jump at zero offset any longer. There seem to be some extra features but nothing remarkable.

Once again the mean and standard deviation for the parameters can be calculated and are in Table 3.9. Again they are in line with previous values, though the standard deviations have increase ever so slightly for some of the parameters.

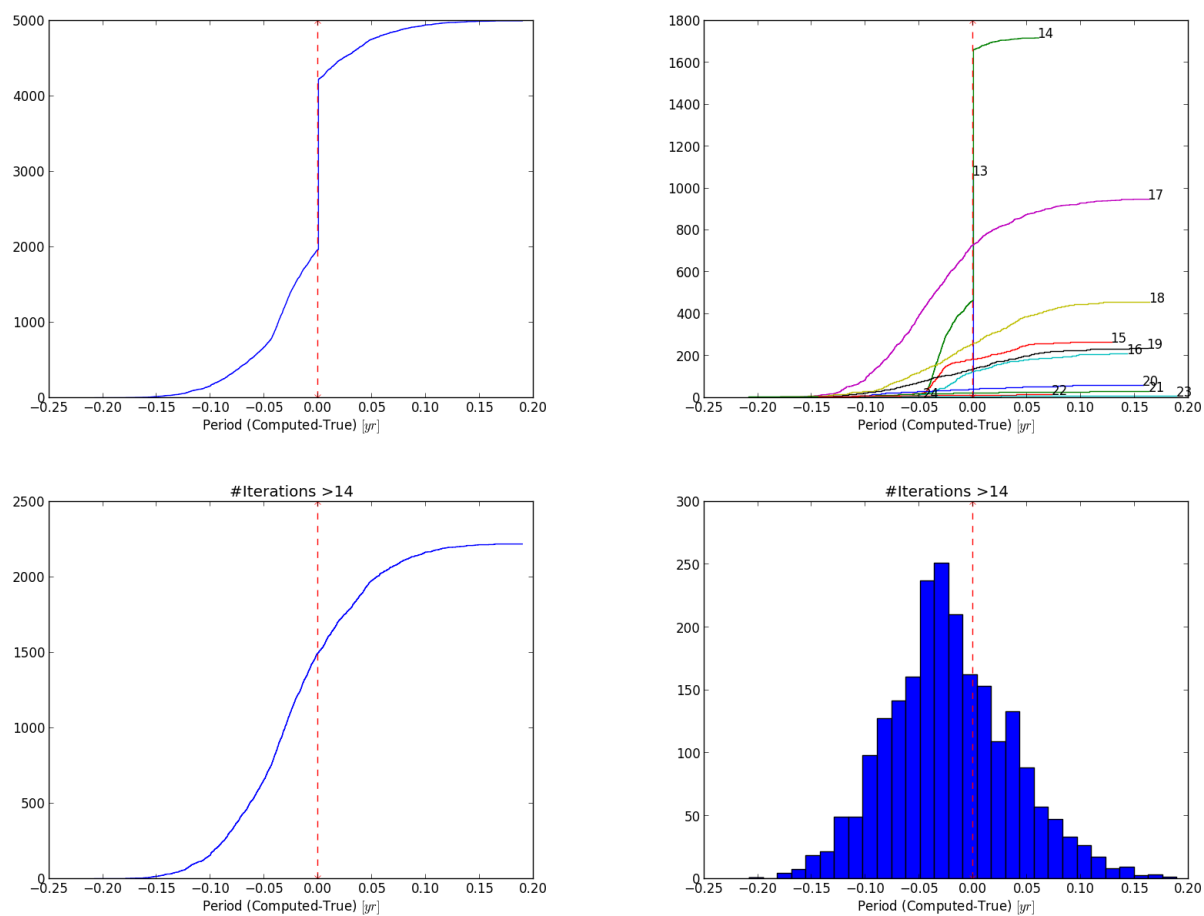


Figure 3.4: Similar as Figure 3.3 but this time the Thiele-Innes parameters are also included. The clear step seem to be associated with those bootstraps which had 13 or 14 iterations in the optimization step. There is something happening for those which had 15 iterations in the optimization also, but the step is not at the same position so it has some other reason behind it.

Table 3.9: Parameters for astrometric and planetary parameters. No radial velocity is included. The data has been censored to exclude those bootstrap iterations which had less than 15 iterations in the optimization step.

Parameter	Mean	Standard deviation	Units
α_*	0.8721719220	3.2519653100e-11	rad
δ	-0.7517403491	2.0174751570e-11	rad
μ_{α_*}	-798.714439424	0.0045400936	mas/yr
μ_δ	10337.7726249	0.0047303293	mas/yr
ϖ	545.398703712	0.0040395640	mas
P	4.8163449913	0.0571854315	yr
e	9.7335568535e-05	0.0005300715	
m_r	0.0004980586	1.1048241194e-05	
t_p	2012.41343429	0.0439229275	yr
A	1.0181397183	0.0262358236	AU
B	-0.1254568583	0.0262358236	AU
F	-0.2947694959	0.0469444056	AU
G	1.4850366504	0.02391310904	AU

3.2 Parametric bootstrap

Instead of just re-sampling the measurements as previously done, a somewhat more elaborate scheme can be employed utilizing the errors of the measurements. For each measurement there is an associated error σ_i . This is then used for adding Gaussian noise to the observations, the noise has zero mean but with a scale parameter chosen as three times σ_i . Also, instead of starting from the true parameters the true parameters are slightly offset by another random number with zero mean and $1.0e - 11$ as scale parameter. The formal errors from the previous section could have been used but it was opted instead for this smaller disturbance for the start parameters.

Other than that, this follows the same approach as previously.

3.2.1 Only astrometric variables

Once again it begins with only the astrometric parameters and a singular value decomposition. The result is in Table 3.10. What is different here is mainly the value of χ^2 -residuals which is much larger. This is expected as noise has been added to the observations. As the noise had three times the error of the measurements, the χ^2 -value should roughly go up by a factor nine. Though the χ^2 -value here seem to be roughly a factor ten larger. The condition number and the singular values pretty much behave as in the previous so the same minima is being investigated.

Table 3.10: Singular values for astrometric parameters only and not using radial velocity. Parametric bootstrapping was employed

SVD Value 1	4.5553394719568434e21
SVD Value 2	3.6720169771288945e21
SVD Value 3	219570.0660009041
SVD Value 4	184815.69869434627
SVD Value 5	65462.983222604475
SVD condition number	6.9586493735957288e16
χ^2	18178.94

Performing a normal optimization succeeds and also calculating the formal errors, the result is in Table 3.11 and they are similar to the result from Table 3.3.

Table 3.11: Parameters resulting from a normal optimization. The start values were perturbed by a Gaussian random number with zero mean and $1.0e - 11$ as scale parameter

Parameter	Value	Formal error	Units
α_*	0.8721719219	1.536906201520050e-11	rad
δ	-0.7517403490	1.607703195427514e-11	rad
μ_{α_*}	-798.7119789658	0.0021670658	mas/yr
μ_δ	10337.7718377825	0.0023674626	mas/yr
ϖ	545.3985337273	0.0038652174	mas

Performing the bootstrapping and plotting the histograms of the astrometric parameters

results in the plots of Figure 3.5. Again, no surprises. The distributions do look a bit wider than in Figure 3.1

The mean and standard deviations of the parameters are calculated in Table 3.12. Comparing to the result in Table 3.4 the mean values seem to agree but the standard deviations are somewhat larger.

Table 3.12: Parameters for parametric bootstrapping on astrometric parameters only

Parameter	Mean	Standard deviation	Units
α_*	0.8721719220	5.8414277712e-11	rad
δ	-0.7517403491	4.8409623422e-11	rad
μ_{α_*}	-798.712017513	0.0064335461	mas/yr
μ_δ	10337.7717154	0.0071945788	mas/yr
ϖ	545.39850958	0.0115631639	mas

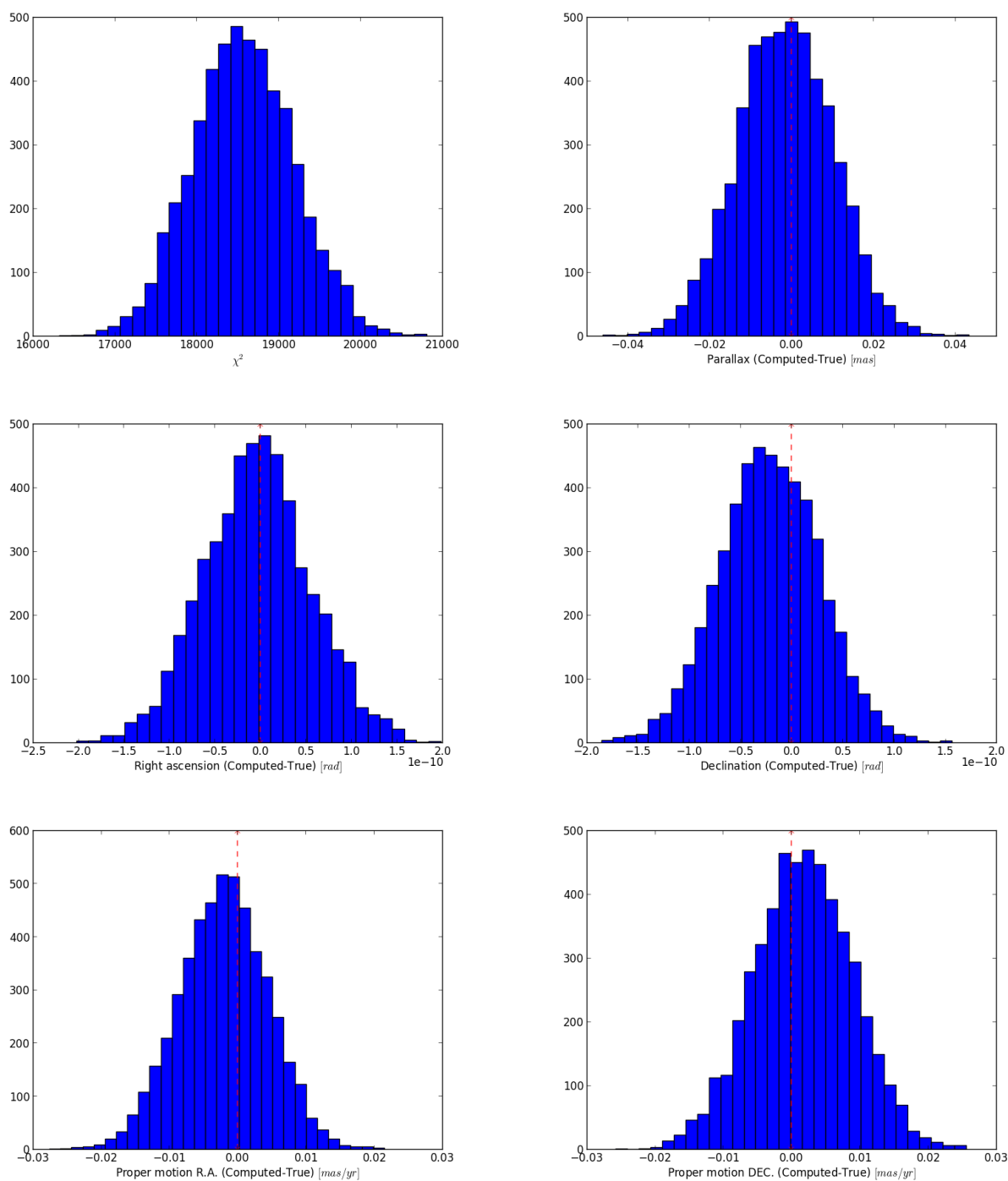


Figure 3.5: Histogram of χ^2 -residuals and only astrometric parameter residuals. Top left - χ^2 -residuals, top right - parallax, middle left - α , middle right - δ , bottom left - μ_{α^*} and bottom right - μ_{δ} . All except χ^2 -residuals are of the computed minus the true parameter, red dashed line indicates true value. Parametric bootstrapping.

3.2.2 Astrometric and no orientation

Also performing the optimization for some of the planetary parameters and doing a singular value decomposition indicate that the condition number is a bit worse, $\sim 2.4e33$ compared to $\sim 1.3e34$. The singular values are in Table 3.13

Table 3.13: Singular values for astrometric no planetary parameters, though not the Thiele-Innes parameters. No radial velocity is included. Parametric bootstrapping

SVD value 1	4.5553394721394267e21
SVD value 9	3.125994192425261e-13
SVD condition number	1.4572450208569413e34
χ^2	18118.95

It is possible to perform a normal optimization, but not compute the formal errors as the matrix become singular.

So moving straight ahead and plotting (Figure 3.6) what is happening to the period, it looks like once again the bootstrap iterations which have few step internally in the optimizer is causing some problem. Censoring the data the cumulative plot (lower left) look quite OK. The histogram does clearly look skewed though.

Calculating the mean and standard deviation and comparing the result in Table 3.14 to the old result in Table 3.7. Again, the mean values compare OK, but the standard deviations are larger.

Table 3.14: Censoring the result to only include bootstrap iterations with more than two internal optimization iterations the mean and standard deviation of the parameters can be calculated

Parameter	Mean	Standard deviation	Units
α_*	0.8721719220	9.8205375851e-11	rad
δ	-0.7517403491	5.875017744e-11	rad
μ_{α_*}	-798.717664582	0.0113966152	mas/yr
μ_δ	10337.7711113	0.0102272160	mas/yr
ϖ	545.399047511	0.0116846658	mas
P	4.7904436579	0.1624169708	yr
e	6.7638749680e-10	3.66191941e-09	
m_r	0.0004943957	1.9001347818e-05	
t_p	2012.47659982	0.1426400405	yr

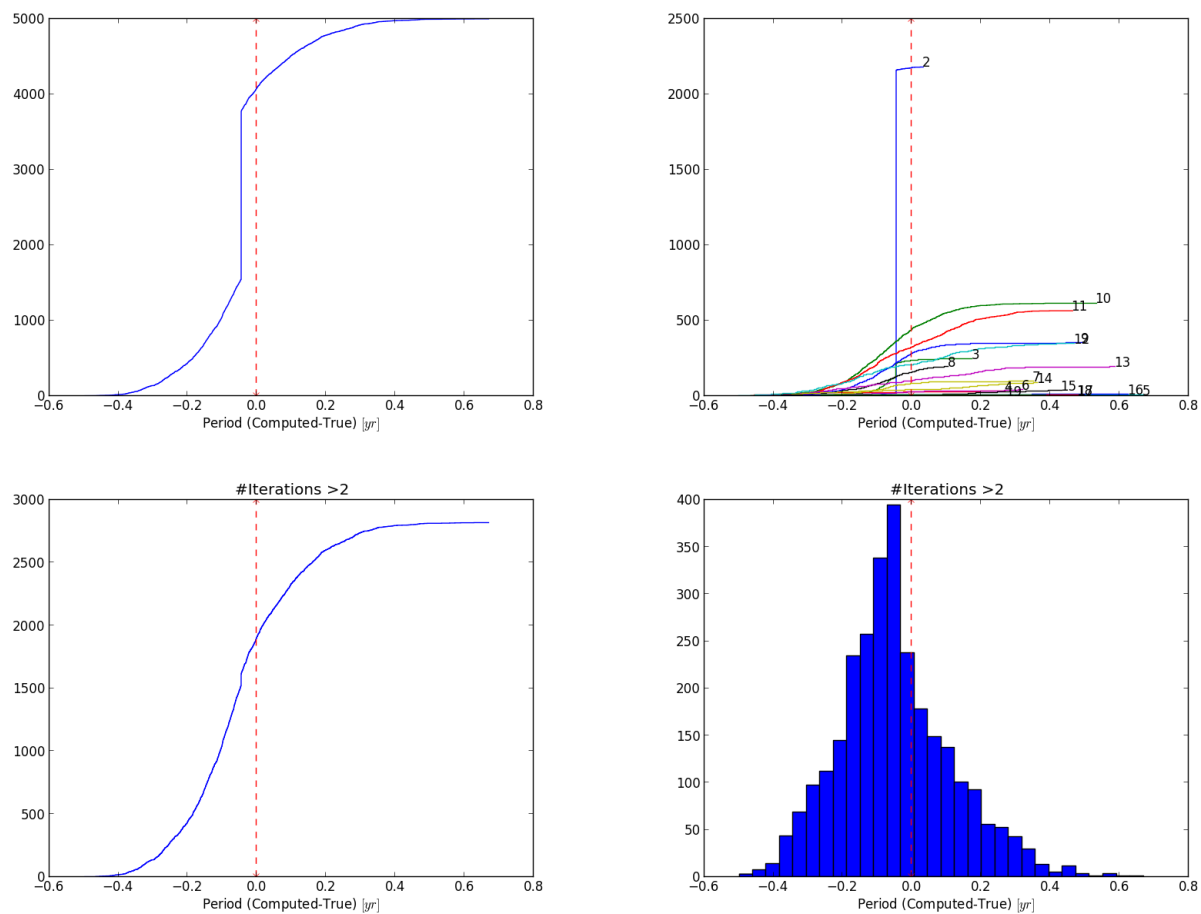


Figure 3.6: Similar as Figure 3.3, but here parametric bootstrapping is employed. Those optimization steps which only have two iterations seem to produce abnormal results and are censored.

3.2.3 Astrometric and orientation

And finally including all the parameters for the parametric bootstrapping. The singular values are in Table 3.15. Again the matrix is ill conditioned and a few of the values are very small.

Table 3.15: Singular values for astrometric and planetary parameters. No radial velocity is included. Parametric bootstrapping

SVD value 1	4.5553394719415374E21
SVD value 12	3.823209712162227E-12
SVD value 13	3.3234491148364225E-13
SVD condition number	1.3706662309363347E34
χ^2	1806.04

In Figure 3.7 the period is plotted the same way as before and the limit for censoring data is set at 14 iterations. Still, the cumulative plot of the censored data for the period does show some extra features than what would be expected had it been something resembling a Gaussian. Also in the bottom right of Figure 3.7 the histogram does not look like what would be expected from a Gaussian distribution. At best it would resemble a leptokurtic Gaussian.

Still the mean and standard deviation of the parameters can be calculated and are Table 3.16. Clearly the Thiele-Innes parameters are not the same as in Table 3.9

Table 3.16: Parameters for astrometric and planetary parameters calculated from censoring the data to only include bootstrap iterations with more than 14 iterations in the optimization step. No radial velocity is included. Parametric bootstrapping

Parameter	Mean	Standard deviation	Units
α_*	0.8721719220	1.0814998385e-10	rad
δ	-0.7517403491	6.1801051353e-11	rad
μ_{α_*}	-798.710665141	0.0162602989	mas/yr
μ_δ	10337.7745086	0.0148389232	mas/yr
ϖ	545.398518977	0.0113284003	/mas
P	4.8600783095	0.1951325435	yr
e	1.0171092743e-06	1.0691781371e-05	
m_r	0.0004461087	1.3038683148e-05	
t_p	2011.88008444	0.2447280522	yr
A	1.0889187465	0.1250904152	AU
B	-1.0774607545	0.1250904152	AU
F	0.4122186752	0.3021354484	AU
G	1.2283745851	0.3042639942	AU

The period looked a bit too narrow in Figure 3.7 to be a normal distribution. So, in Figure 3.8 to the left the QQ-plot is shown, that is the quantiles of the normal theoretical distribution with the same mean and standard deviation is plotted against the quantiles of the data. If the distribution would be normal then it should follow the dashed red line. It does not follow the straight line and the shape indicate that indeed the data is narrower than what would be expected from a normal distribution. In the same figure, but to the right, the same distribution

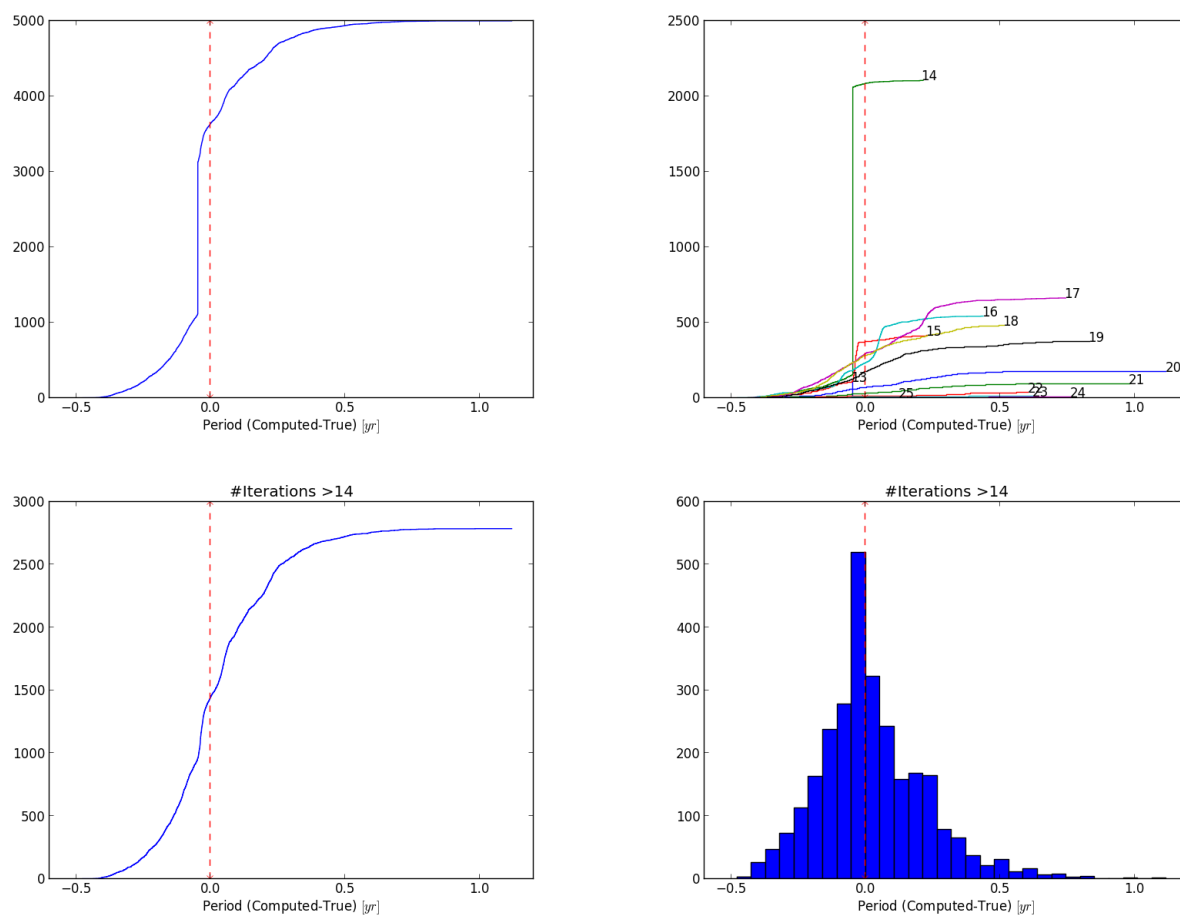


Figure 3.7: Similar as Figure 3.4 but this time using parametric bootstrapping.

for the right ascension is also plotted. This time the data seem to be wider than what would be expected.

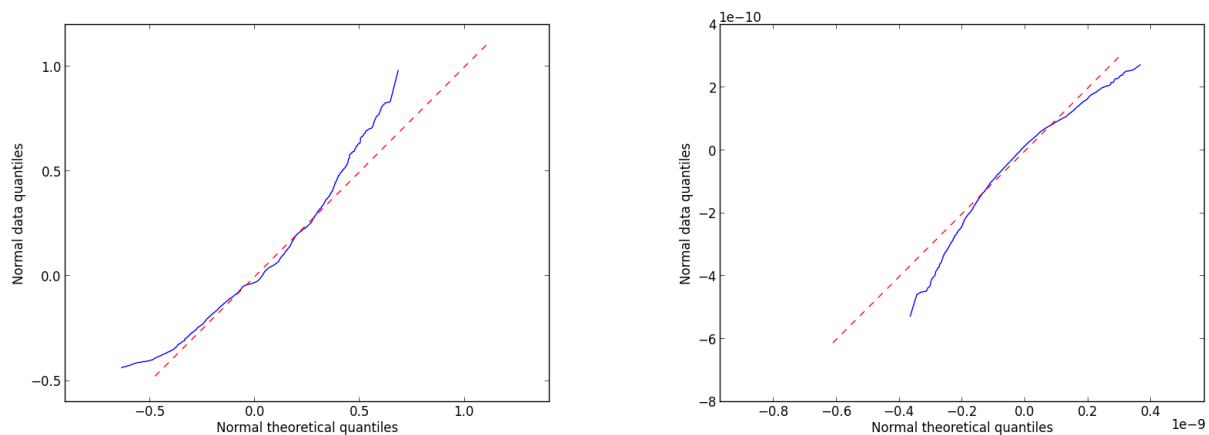


Figure 3.8: QQ-plot for censored data from parametric bootstrapping. To the left the period is plotted and to the right the right ascension is plotted. The period show a narrower distribution and the right ascension show a wider distribution than what would be expected from a Gaussian distribution using parameters from Table 3.16.

3.3 Bootstrapping and including radial velocity

Unfortunately the same procedure did not succeed when including radial velocity as no clear distinction could be made for censoring the data.

4 Conclusion

Solving for only the astrometric parameters proved possible. Using the inverse of the weighted Hessian as co-variance matrix to calculate the formal error also prove possible.

Including some of the Keplerian parameters in the optimization made the problem less well conditioned. For low eccentricity orbits the time of periapsis passage become less well defined. But it was not the time of periapsis passage which had a large formal error when performing a normal optimization and using the inverse of the Hessian as co-variance matrix as above. Instead it was the eccentricity which had a very large formal error indicating that a good solution was not possible. Bootstrapping and censoring the data to only include iterations which seemed to work did bring down the standard deviation of the eccentricity.

Even though the combined and simultaneous solution of the astrometric and all the Keplerian parameters is very appealing in its simplicity, it might not be a good idea. Looking at the SVD-values the problem become quite ill-conditioned so the assumption that the target function/merit function can be approximated with a quadratic function at a minima is maybe not a very sound one. This ill-conditioning also leads to the optimization becoming insensitive to some parameter, or a combination of parameters. One way to fail a bit more gracefully is to do bootstrapping on the optimized parameters. This is a bit computationally expensive considering that a different parametrization(e.g. Wright and Howard (2009) Pourbaix and Jancart (2008) or Catanzarite (2010)) might not lead to this ill-conditioning.

A different solution strategy, e.g., employing a hierarchical strategy might prove more efficient and drift less from the starting parameters.

This change in how to solve the problem is, on the other hand, not something which would pose too much of a problem. The machinery for calculating the derivatives etc. is already in place and could be adapted without too much work¹.

Calculating the parameters from bootstrapping leads to the parameters being biased compared to the true ones. This is not necessarily a consequence of the bad parametrization. There is noise on the observations and a different set of parameters than the true ones may indeed give a better fit. One way to investigate this could have been to have more random systems to see if the bias is from the data or from the optimization procedure.

Also the parametric bootstrapping should maybe be a bit closer scrutinized and see how good the choice $3\sigma_i$ was for the added noise. If could be this was the reason for larger standard deviation of the parameters compared to the re-sampling bootstrap.

The bootstrapping did prove useful in the sense that standard deviations could be provided on the parameters. On the other hand, the standard deviations were calculated from a censored set and the censoring could be argued to be invalid.

¹Of course, what might look like a simple problem with a straightforward solution might be, and usually is, harder to solve in reality. A frequently recurrent theme during this course of work.

A bit disappointing is that the addition of radial velocity did not prove useful. This however is likely not due to its inherent usefulness but on some other factor, such as the parametrization of the problem.

Bibliography

- Casertano, S., Lattanzi, M. G., Sozzetti, A., Spagna, A., Jancart, S., Morbidelli, R., Pannunzio, R., Pourbaix, D., and Queloz, D. (2008). Double-blind test program for astrometric planet detection with Gaia. , 482:699–729.
- Catanzarite, J. H. (2010). A new algorithm for fitting orbits of multiple-planet systems to combined RV and astrometric data. *ArXiv e-prints*.
- Dumusque, X., Pepe, F., Lovis, C., Ségransan, D., Sahlmann, J., Benz, W., Bouchy, F., Mayor, M., Queloz, D., Santos, N., and Udry, S. (2012). An Earth-mass planet orbiting α Centauri B. , 491:207–211.
- Goldin, A. and Makarov, V. V. (2006). Unconstrained Astrometric Orbits for Hipparcos Stars with Stochastic Solutions. , 166:341–350.
- Holl, B. (2011). Astrometric planet detectability with Gaia, a short AGISLab study. *Gaia Technical Note GAIA-C3-TN-LU-BH-003-01*.
- Holl, B. and Lindegren, L. (2012). Error characterization of the Gaia astrometric solution. I. Mathematical basis of the covariance expansion model. , 543:A14.
- Holl, B., Lindegren, L., and Hobbs, D. (2009). AGISLab - A facility for experimental astrometric solutions. *Gaia Technical Note GAIA-C3-TN-LU-BH-002-01*.
- Holl, B., Lindegren, L., and Hobbs, D. (2012). Error characterization of the Gaia astrometric solution. II. Validating the covariance expansion model. , 543:A15.
- Kepler, S. O., Costa, J. E. S., Castanheira, B. G., Winget, D. E., Mullally, F., Nather, R. E., Kilic, M., von Hippel, T., Mukadam, A. S., and Sullivan, D. J. (2005). Measuring the Evolution of the Most Stable Optical Clock G 117-B15A. , 634:1311–1318.
- Klioner, S. (2011). Lecture Notes on Basic Celestial Mechanics.
- Lindegren, L., Lammers, U., Hobbs, D., O’Mullane, W., Bastian, U., and Hernández, J. (2012). The astrometric core solution for the Gaia mission. Overview of models, algorithms, and software implementation. , 538:A78.
- Mayor, M. and Queloz, D. (1995). A Jupiter-mass companion to a solar-type star. , 378:355–359.
- Nesvorný, D., Kipping, D. M., Buchhave, L. A., Bakos, G. Á., Hartman, J., and Schmitt, A. R. (2012). The Detection and Characterization of a Nontransiting Planet by Transit Timing Variations. *Science*, 336:1133–.

- Perryman, M. (2011). *The Exoplanet Handbook*.
- Perryman, M. A. C., Lindegren, L., and Turon, C. (1997). The Scientific Goals of the GAIA Mission. In Bonnet, R. M., Høg, E., Bernacca, P. L., Emiliani, L., Blaauw, A., Turon, C., Kovalevsky, J., Lindegren, L., Hassan, H., Bouffard, M., Strim, B., Heger, D., Perryman, M. A. C., and Woltjer, L., editors, *Hipparcos - Venice '97*, volume 402 of *ESA Special Publication*, pages 743–748.
- Pourbaix, D. and Jancart, S. (2008). Reductio of the astrometric binaires. *Gaia Technical Note GAIA-C4-TN-ULB-DP-002-031*.
- Seager, S. (2011). *Exoplanets*.
- Strand, K. A. (1943). 61 Cygni as a Triple System. , 55:29–32.
- Struve, O. (1952). Proposal for a project of high-precision stellar radial velocity work. *The Observatory*, 72:199–200.
- Traub, W. A., Beichman, C., Boden, A. F., Boss, A. P., Casertano, S., Catanzarite, J., Fischer, D., Ford, E. B., Gould, A., Halverson, S., Howard, A., Ida, S., Kasdin, N. J., Laughlin, G. P., Levison, H. F., Lin, D., Makarov, V., Marr, J., Muterspaugh, M., Raymond, S. N., Savransky, D., Shao, M., Sozzetti, A., and Zhai, C. (2010). Detectability of Earth-like Planets in Multi-Planet Systems: Preliminary Report. In Goździewski, K., Niedzielski, A., and Schneider, J., editors, *EAS Publications Series*, volume 42 of *EAS Publications Series*, pages 191–199.
- Williams, D. R. (2004). *Sun Fact Sheet*.
- Wolszczan, A. and Frail, D. A. (1992). A planetary system around the millisecond pulsar PSR1257 + 12. , 355:145–147.
- Wright, J. T. and Gaudi, B. S. (2013). *Exoplanet Detection Methods*, page 489.
- Wright, J. T. and Howard, A. W. (2009). Efficient Fitting of Multiplanet Keplerian Models to Radial Velocity and Astrometry Data. , 182:205–215.

A Kepler's Laws

In this chapter *Kepler's laws* are derived;

1. *Planets move on ellipses*

$$r = \frac{a(1 - e^2)}{1 + e \cos \nu}$$

2. *The radius vector will sweep out equal area in equal time*

$$\dot{A} = \frac{1}{2}r^2\dot{\theta} = \frac{1}{2}h$$

3. *Orbital period squared is proportional to the semi-major axis cubed*

$$P^2 = \frac{4\pi^2}{G(m_1 + m_2)}a^3$$

A very useful expression for the planets position in a plane is also derived

$$\begin{aligned}x &= a(\cos E - e) \\y &= a(1 - e^2) \sin E\end{aligned}$$

where E is obtained from solving *Kepler's equation*

$$E - e \sin E = n(t - t_p)$$

This chapter starts out with two threads; one about ellipses and one about Newton's laws. The first part derive some of the basic equations for the relation of angles and radius for ellipses. All of that might seem a bit unrelated to the subject in general, but as the track changes to Newton's laws the formulas come in handy as it turns out that *the orbit of a planet is an ellipse with the Sun at one focus*^a. This makes the connection back to the discussion of ellipses and the derivation of Kepler's laws.

The equations for describing the position of the planet in its orbit are necessary when adding planetary signals to astrometric observations. Kepler's equation, has to be solved when calculating an angle related to the orbital position. Kepler's third law is used for calculating either the orbital or the semi-major axis when knowing the other parameters.

The derivations are done by following Perryman (2011), Seager (2011) and Klioner (2011) but keeping the notation consistent throughout.

^aIn this case the reference is made to the Solar system, the general case is for a body in orbit around a central mass

A.1 Ellipses

This section establish the notation and goes through some basic details for ellipses. Later on, they are used in connection with Newton's laws to produce Kepler's laws.

Most useful is the parametrization of an ellipse in the plane by the equations

$$\begin{aligned}x &= a(\cos E - e) \\y &= a(1 - e^2) \sin E\end{aligned}$$

Starting out with the general equation for an ellipse in *Cartesian* coordinates

$$\frac{x^2}{a^2} + \frac{y^2}{b^2} = 1$$

where a is the *semi-major axis*¹ and b is the *semi-minor axis*. A depiction of the ellipse is in Figure A.1, of which only one quarter is shown with the solid line being the ellipse referred to.

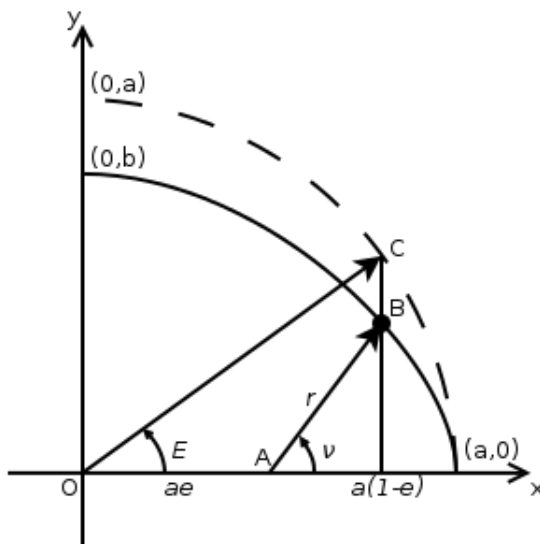


Figure A.1: The solid line represents the ellipse in the first quadrant. The ellipse intercepts the x-axis at $x = a$ and the y-axis at $y = b$, these are the semi-major and semi-minor axis respectively in this case. The point “A” is at one of the foci, and from this point the arrow r is drawn representing the radius of the ellipse after a move of the origin to point “A”. Note that the distance “O-A” is equal to ea where e is the eccentricity of the ellipse. The dashed circle is called the *auxiliary circle*. The angle E is the *eccentric anomaly* and v is the *true anomaly*.

Adapted from http://en.wikipedia.org/wiki/Kepler's_laws_of_planetary_motion

Shifting the origin to the right focus, point “A” in the FigureA.1, this expression is altered to

¹In some texts this is also called *semi-axis major*, but they refer to the same object

$$\frac{(x + ae)^2}{a^2} + \frac{y^2}{b^2} = 1 \quad (\text{A.2})$$

The reason is, as stated earlier in this section, that planets move on ellipses with the star at one focus. That planets do indeed move this way will be derived but after the discussion of ellipses.

The semi-minor axis can be expressed through the *eccentricity* e and the semi-major axis.

$$b^2 = a^2(1 - e^2) \quad (\text{A.3})$$

The eccentricity is a measure of how elliptical it is. If $e = 0$ the result is a circle, if $0 < e < 1$ it is an ellipse. Other possibilities which are related but not treated further are if $e = 1$ it is a parabola and for $e > 1$ the result is a hyperbola.

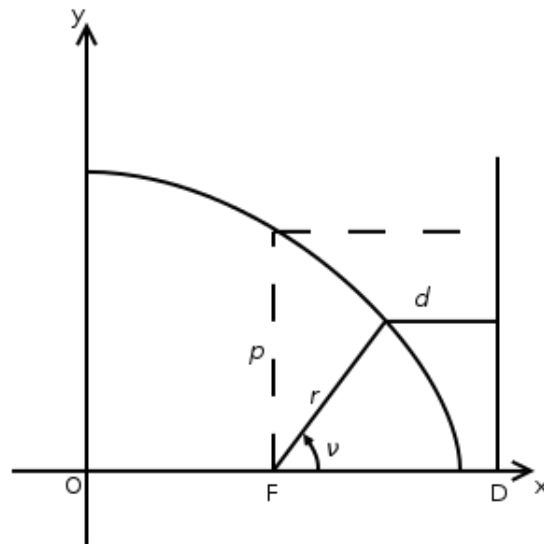


Figure A.2: The ellipse in Figure A.1 is a special case of a conic section(see Figure A.3). What this refers to is basically a intersection of a plane and a cone. Depending on the angle of the intersection it will produce different conic sections. If the normal of the plane is parallel to the rotational axis of the cone the conic section will be a circle. A slight variation from this and the conic section will be an ellipse. If the angle increases even further the intersection will not form a closed loop on the cone and will become a parabola. When the normal of the plane is perpendicular to the rotational axis of the cone it will be a hyperbola.

Adapted from <http://mathworld.wolfram.com/Ellipse.html>

The equation, Equation A.2, for the ellipse can now be re-written replacing b^2 through Equation A.3

$$\frac{(x + ae)^2}{a^2} + \frac{y^2}{a^2(1 - e^2)} = 1$$

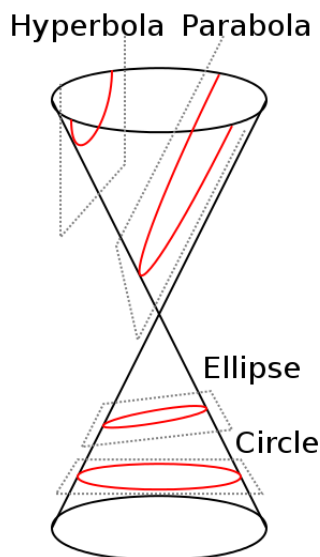


Figure A.3: Conic sections in relation to a cone. The conic sections are the intersections of a cone and a infinite plane. What makes the hyperbola different from the parabola is that the hyperbola will intersect “both of the cones” even though only one intersection is shown here. Here only the two cases of ellipse and circle, $0 \leq e < 1$, are considered as they are the only which form a closed orbit.

Adapted from <http://mathworld.wolfram.com/ConicSection.html>

this expression can the be re-written and cleaned up to give an expression for the radius from point A to the ellipse.

$$r^2 = x^2 + y^2 = \dots = (a(1 - e^2) - ex)^2$$

Using *polar* coordinates instead of Cartesian, the x - *coordinate* can be replaced with the equivalent $x = r \cos \nu$ which gives

$$r = a(1 - e^2) - er \cos \nu$$

The length r of the radial vector can be expressed trough

$$r = \frac{a(1 - e^2)}{1 + e \cos \nu} \quad (\text{A.4})$$

Note that the angle ν is the angle the radial vector \mathbf{r} makes with the x-axis, and is called the *true anomaly*.

Instead of using the true anomaly another anomaly¹ can be used, namely the *eccentric anomaly* E , related through

¹Anomalies translate into angles

$$\cos \nu = \frac{e - \cos E}{1 - e \cos E}$$

or

$$\tan\left(\frac{\nu}{2}\right) = \left(\frac{1+e}{1-e}\right)^{1/2} \tan\left(\frac{E}{2}\right)$$

This can be used to re-write the expression for the Cartesian x and y coordinates.

$$x = a(\cos E - e) \tag{A.5a}$$

$$y = a(1 - e^2) \sin E \tag{A.5b}$$

And similarly for the radius

$$r = a(1 - e \cos E)$$

As planets, or particles, move in their orbits the true and eccentric anomaly changes. A third anomaly can then be defined through the orbital period. Namely the *mean anomaly* which is the angle of a fictitious particle moving on a circular orbit having the same period, P .

$$M = \frac{2\Pi}{P}(t - t_p) = n(t - t_p)$$

This angle is the same as true anomaly for two points of the orbit, namely the periapsis and apoapsis points.

A.1.1 Cylindrical coordinates

Here follows a little side note on *cylindrical* coordinates as a supplement to the polar coordinates. The reason for this section is to get the time derivatives of the radial vectors and take the step into 3D.

The notation is slightly different with θ representing the angle as the subject discussed after this will use this angle to set it apart slightly from the discussion about the ellipse.

So let $\hat{\mathbf{r}}$ be a unit vector parameterize by θ in a plane, eg. $(\cos \theta, \sin \theta, 0)$. Let $\hat{\mathbf{z}}$ be a unit vector normal to the plane in which $\hat{\mathbf{r}}$ lies, eg. $(0, 0, 1)$.

Then the unit vector $\hat{\theta}$ can be defined to create a right handed coordinate system by $\hat{\theta} = \hat{\mathbf{z}} \times \hat{\mathbf{r}}$ so that the local triad is formed by $[\hat{\mathbf{r}}, \hat{\theta}, \hat{\mathbf{z}}]$

$$\hat{\theta} = \hat{\mathbf{z}} \times \hat{\mathbf{r}} = \begin{vmatrix} \mathbf{e}_1 & \mathbf{e}_2 & \mathbf{e}_3 \\ 0 & 0 & 1 \\ \cos \theta & \sin \theta & 0 \end{vmatrix} = (-\sin \theta, \cos \theta, 0)$$

Furthermore, as the local triad is normalized and right-handed $\hat{\mathbf{r}} = \hat{\theta} \times \hat{\mathbf{z}}$

The derivatives of $\hat{\mathbf{r}}$ and $\hat{\theta}$ with respect to θ are in component form

$$\begin{aligned}\frac{d}{d\theta}\hat{\mathbf{r}} &= (-\sin\theta, \cos\theta, 0) = \hat{\theta} \\ \frac{d}{d\theta}\hat{\theta} &= (-\cos\theta, -\sin\theta, 0) = -\hat{\mathbf{r}}\end{aligned}$$

The differential with respect to time, if θ is a function of time¹, can then be calculated using the chain rule

$$\begin{aligned}\dot{\hat{\mathbf{r}}} &= \dot{\theta}\hat{\theta} \\ \dot{\hat{\theta}} &= -\dot{\theta}\hat{\mathbf{r}}\end{aligned}$$

A radial vector together with its first and second time derivatives is

$$\begin{aligned}\mathbf{r} &= r\hat{\mathbf{r}} \\ \dot{\mathbf{r}} &= \dot{r}\hat{\mathbf{r}} + r\dot{\theta}\hat{\theta} \\ \ddot{\mathbf{r}} &= \ddot{r}\hat{\mathbf{r}} + 2\dot{r}\dot{\theta}\hat{\theta} + r\ddot{\theta}\hat{\theta} - r\dot{\theta}^2\hat{\mathbf{r}} \\ &= (\ddot{r} - r\dot{\theta}^2)\hat{\mathbf{r}} + (2\dot{r}\dot{\theta} + r\ddot{\theta})\hat{\theta} \\ &= (\ddot{r} - r\dot{\theta}^2)\hat{\mathbf{r}} + \left\{ \frac{1}{r} \frac{d}{dt}(r^2\dot{\theta}) \right\} \hat{\theta}\end{aligned}$$

A.2 A two body system

Starting from Newton's laws, Kepler's three laws are derived together with Kepler's equation.

It is assumed that the center of mass, "CM", is stationary with respect to the observer which makes the expressions a bit simpler.

Starting out with two point masses (see Figure A.4) the forces acting on each of the masses are

$$\begin{aligned}\mathbf{F}_1 &= m_1\ddot{\mathbf{r}}_1 = G\frac{m_1m_2}{r^3}\mathbf{r} \\ \mathbf{F}_2 &= m_2\ddot{\mathbf{r}}_2 = -G\frac{m_1m_2}{r^3}\mathbf{r}\end{aligned}$$

The vector connecting the two points are, together with its second derivative of time

$$\begin{aligned}\mathbf{r} &= \mathbf{r}_2 - \mathbf{r}_1 \\ \ddot{\mathbf{r}} &= \ddot{\mathbf{r}}_2 - \ddot{\mathbf{r}}_1\end{aligned}$$

Re-writing the force acting on one particle

¹Later on it will be

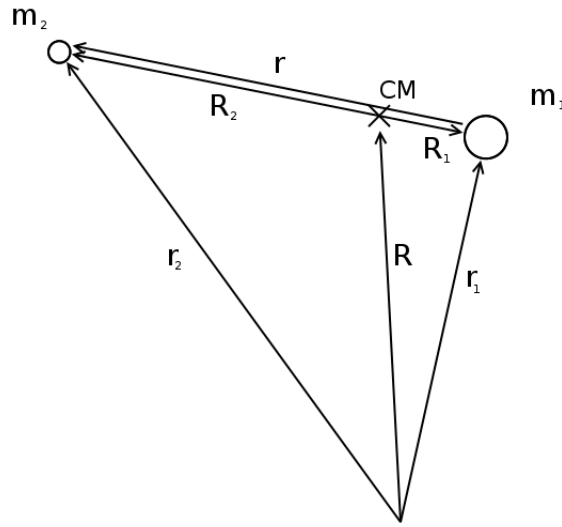


Figure A.4: Point masses at different positions together with the vectors pointing out their positions. The vectors \mathbf{R}_1 and \mathbf{R}_2 are drawn from the center of mass, “CM”.

$$\mathbf{F}_2 = m_2 \ddot{\mathbf{r}}_2 = m_2 (\ddot{\mathbf{r}} + \ddot{\mathbf{r}}_1) = m_2 \ddot{\mathbf{r}} + m_2 \ddot{\mathbf{r}}_1 = m_2 \ddot{\mathbf{r}} + \frac{m_2}{m_1} \mathbf{F}_1$$

and that the forces are in opposite direction¹

$$\mathbf{F}_2 = -\mathbf{F}_1$$

then, after some more re-writing and simplification an expression of the vector connecting the two points are

$$\begin{aligned} -\mathbf{F}_1 &= m_2 \ddot{\mathbf{r}} + \frac{m_1}{m_1} \mathbf{F}_1 \\ \Rightarrow 0 &= m_2 \ddot{\mathbf{r}} + \left(1 + \frac{m_1}{m_1}\right) \mathbf{F}_1 \\ \Rightarrow 0 &= m_2 \left(\ddot{\mathbf{r}} + \frac{1}{m_1 m_2} (m_1 + m_2) G \frac{m_1 m_2}{r^3} \mathbf{r} \right) \\ \Rightarrow 0 &= \ddot{\mathbf{r}} + G \frac{m_1 + m_2}{r^3} \mathbf{r} \end{aligned} \tag{A.6}$$

Taking the vector product of \mathbf{r} with 0 gives for the expression above

$$0 = \mathbf{r} \times 0 = \mathbf{r} \times \left(\ddot{\mathbf{r}} + G \frac{m_1 + m_2}{r^3} \mathbf{r} \right) = \mathbf{r} \times \ddot{\mathbf{r}}$$

So the second time derivative of \mathbf{r} is parallel to \mathbf{r} .

¹For every action, there is an equal and opposite reaction.

The time derivative of the vector product $\mathbf{r} \times \dot{\mathbf{r}}$

$$\frac{d}{dt}(\mathbf{r} \times \dot{\mathbf{r}}) = \dot{\mathbf{r}} \times \dot{\mathbf{r}} + \mathbf{r} \times \ddot{\mathbf{r}} = \mathbf{r} \times \ddot{\mathbf{r}}$$

which is the same as the expression above, so that

$$\mathbf{r} \times \dot{\mathbf{r}} = \mathbf{h}$$

where \mathbf{h} is constant with time. This is then a vector perpendicular to both \mathbf{r} and $\dot{\mathbf{r}}$, the angular momentum vector.

The radial vector \mathbf{r} can be written as the unit normal vector

$$\mathbf{r} = r\hat{\mathbf{r}}$$

so

$$\mathbf{r} \times \dot{\mathbf{r}} = r\hat{\mathbf{r}} \times (\dot{r}\hat{\mathbf{r}} + r\dot{\theta}\hat{\theta}) = r\dot{r}\hat{\mathbf{r}} \times \hat{\mathbf{r}} + r^2\dot{\theta}\hat{\mathbf{r}} \times \hat{\theta} = r^2\dot{\theta}\hat{\mathbf{z}}$$

or

$$\mathbf{h} = r^2\dot{\theta}\hat{\mathbf{z}} \tag{A.7}$$

so that $r^2\dot{\theta}$ is constant in time.

The small triangle spanned by r and $d\theta$ can be seen as a sum of squares sized dr times $rd\theta$ (Figure A.5).

$$dA = \int_0^r r' dr' d\theta = \frac{1}{2}r^2 d\theta$$

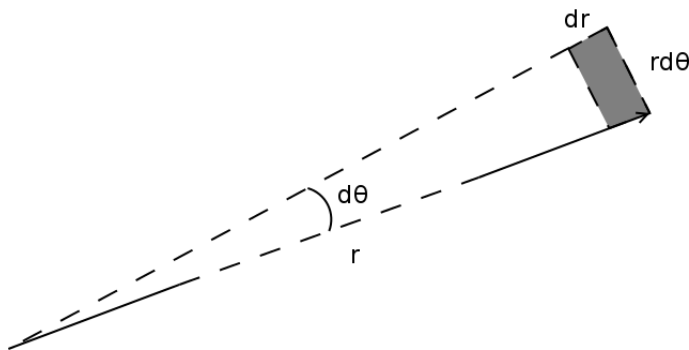


Figure A.5: The area swept out by the radius vector. The change of angle is $d\theta$ giving the small area swept out as the integral over $r' dr' d\theta$

which mean that the small area change over a short interval in time is

$$\dot{A} = \frac{dA}{dt} = \frac{1}{2}r^2\dot{\theta} \quad (\text{A.8})$$

or the area that the radius vector sweeps out in a given time interval is constant
The center of mass is defined through

$$\mathbf{R} = \frac{\sum_i m_i \mathbf{r}_i}{\sum_i m_i}$$

for the two masses in Figure A.4 this mean

$$\mathbf{R} = \frac{m_1 \mathbf{r}_1 + m_2 \mathbf{r}_2}{m_1 + m_2}$$

If there are no external forces acting on the system the center of mass will not experience any acceleration¹ so

$$\ddot{\mathbf{R}} = \frac{m_1 \ddot{\mathbf{r}}_1 + m_2 \ddot{\mathbf{r}}_2}{m_1 + m_2} = 0$$

The two vectors \mathbf{r}_1 and \mathbf{r}_2 can be expressed through

$$\begin{aligned} \mathbf{r}_1 &= \mathbf{R} + \mathbf{R}_1 \\ \mathbf{r}_2 &= \mathbf{R} + \mathbf{R}_2 \end{aligned}$$

so the center of mass can be written

$$\mathbf{R} = \frac{m_1(\mathbf{R} + \mathbf{R}_1) + m_2(\mathbf{R} + \mathbf{R}_2)}{m_1 + m_2} = \left(\frac{m_1 + m_2}{m_1 + m_2} \right) \mathbf{R} + \frac{m_1 \mathbf{R}_1 + m_2 \mathbf{R}_2}{m_1 + m_2}$$

or canceling the \mathbf{R} from both sides

$$m_1 \mathbf{R}_1 + m_2 \mathbf{R}_2 = 0$$

As \mathbf{R}_1 and \mathbf{R}_2 are in opposite directions (eg. $\mathbf{R}_2 = R_2 \left(\frac{-\mathbf{R}_1}{|\mathbf{R}_1|} \right)$) only their magnitude can be used to write

$$m_1 R_1 = m_2 R_2$$

continuing along the same lines, only using the magnitudes

¹The acceleration of a body is parallel and proportional to the force acting on the body

$$\begin{aligned}
R_1 + R_2 &= r \\
\Rightarrow m_1 R_2 &= m_2(r - R_1) \\
\Rightarrow (m_1 + m_2)R_1 &= m_2 r \\
\Rightarrow R_1 &= \frac{m_2}{m_1 + m_2} r
\end{aligned}$$

$$R_1 = \left(\frac{m_2}{m_1 + m_2} \right) r \quad (\text{A.10a})$$

$$R_2 = \left(\frac{m_1}{m_1 + m_2} \right) r \quad (\text{A.10b})$$

So depending on the mass of the object the distance from the center of mass is scaled with the mass ratio.

Then Equation A.8 can be rewritten, for say R_1

$$\begin{aligned}
\dot{A} &= \frac{1}{2} r^2 \dot{\theta} = \frac{1}{2} (R_1 + R_2)^2 \dot{\theta} \\
&= \frac{1}{2} \left(R_1 + \frac{m_1}{m_2} R_1 \right)^2 \dot{\theta} \\
&= \frac{1}{2} \left(1 + \frac{m_1}{m_2} \right)^2 R_1^2 \dot{\theta}
\end{aligned} \quad (\text{A.11})$$

$$(\text{A.12})$$

which means that also the are swept out by either R_1 or R_2 are constant in time, as could be expected. The vector \mathbf{r} is from the center of the star to the planet, whereas \mathbf{R}_1 and \mathbf{R}_2 are from the center of mass to the star and planet respectively.

Starting from Equation A.6

$$\ddot{\mathbf{r}} + G(m_1 + m_2) \frac{1}{r^3} \mathbf{r} = 0$$

$$\ddot{\mathbf{r}} = (\ddot{r} - r\dot{\theta}^2) \hat{\mathbf{r}} + \left(\frac{1}{r} \frac{d}{dt} (r^2 \dot{\theta}) \right) \hat{\theta}$$

$$\left((\ddot{r} - r\dot{\theta}^2) + G(m_1 + m_2) \frac{1}{r^2} \right) \hat{\mathbf{r}} + \left(\frac{1}{r} \frac{d}{dt} (r^2 \dot{\theta}) \right) \hat{\theta} = 0$$

$$\ddot{r} - r\dot{\theta}^2 = -G(m_1 + m_2) \frac{1}{r^2}$$

Substitute $u = 1/r$

$$\begin{aligned}
\ddot{r} &= \frac{d}{dt} \left(\frac{d}{dt} r \right) \\
&= \frac{d}{dt} \left(\frac{d\theta}{dt} \frac{d}{d\theta} \frac{1}{u} \right) \\
&= \frac{d}{dt} \left(\dot{\theta} \frac{-1}{u^2} \frac{du}{d\theta} \right) \\
&= \frac{d}{dt} \left(-h \frac{du}{d\theta} \right) \\
&= -h \frac{d\theta}{dt} \frac{d}{d\theta} \left(\frac{du}{d\theta} \right) \\
&= -h \dot{\theta} \frac{d^2 u}{d\theta^2}
\end{aligned}$$

$$r \dot{\theta}^2 = (r^2 \dot{\theta})^2 \frac{1}{r^3} = h^2 u^3$$

$$-h^2 u^2 \left(\frac{d^2 u}{d\theta^2} + u \right) = -G(m_1 + m_2) u^2$$

$$\frac{d^2 u}{d\theta^2} + u = \frac{G(m_1 + m_2)}{h^2}$$

This is Binet's equation and it has the solution

$$u = \frac{G(m_1 + m_2)}{h^2} (1 + e \cos(\theta - \varpi))$$

or back into more recognizable form

$$r = \frac{h^2}{G(m_1 + m_2)} \frac{1}{1 + e \cos(\theta - \varpi)}$$

This can be compared to the equation for an ellipse (Equation A.4)

$$r = \frac{a(1 - e^2)}{1 + e \cos \nu} \tag{A.13}$$

This can be used to equate

$$a(1 - e^2) = \frac{h^2}{G(m_1 + m_2)} \tag{A.14}$$

The area of an ellipse is πab where $b = a\sqrt{1 - e^2}$ or $b^2 = a^2(1 - e^2)$. Also, as stated before the area the radius vector sweeps out over a give time is constant $\dot{A} = \frac{1}{2}h$, so the area of the whole ellipse is swept out over one period or $A = \frac{1}{2}hP$ where P is the orbital period.

$$A^2 = \frac{1}{4}h^2P^2$$

$$A^2 = \pi^2a^4(1 - e^2)$$

these two together give

$$\frac{1}{4}h^2P^2 = \pi^2a^4(1 - e^2)$$

$$\Rightarrow \frac{1}{4}a(1 - e^2)G(m_1 + m_2)P^2 = \pi^2a^4(1 - e^2)$$

$$\Rightarrow P^2 = \frac{4\pi^2}{G(m_1 + m_2)}a^3$$

Define the *mean motion* through a particle moving on a circular orbit with period P

$$n = \frac{2\pi}{P}$$

Using the expression relating the period to semi major axis

$$P^2 = \frac{4\pi^2}{n^2}$$

$$P^2 = \frac{4\pi^2}{G(m_1 + m_2)}a^3 \tag{A.16}$$

which gives

$$n^2a^3 = G(m_1 + m_2)$$

Re-writing Equation A.14

$$h = \sqrt{a(1 - e^2)G(m_1 + m_2)} = \sqrt{n^2a^4}\sqrt{1 - e^2} = na^2\sqrt{1 - e^2}$$

$$r = \frac{a(1 - e^2)}{1 + e \cos \theta}$$

$$\begin{aligned}
\dot{r} &= \frac{a(1-e^2)}{(1+e\cos\theta)^2} (-1)(-e\dot{\theta}\sin\theta) \\
&= \frac{a(1-e^2)}{1+e\cos\theta} \frac{e\dot{\theta}\sin\theta}{1+e\cos\theta} \\
&= r\dot{\theta} \frac{e\sin\theta}{1+e\cos\theta} \\
&= \frac{h}{r} \frac{e\sin\theta}{1+e\cos\theta} & h = r^2\dot{\theta} \\
&= \frac{h(1+e\cos\theta)}{a(1-e^2)} \frac{e\sin\theta}{1+e\cos\theta}
\end{aligned} \tag{A.17}$$

and also from $h = r^2\dot{\theta}$

$$r\dot{\theta} = \frac{h}{r} = \frac{h(1+e\cos\theta)}{a(1-e^2)} \tag{A.18}$$

The velocity is

$$\mathbf{v} = \dot{\mathbf{r}} = \dot{r}\hat{\mathbf{r}} + r\dot{\theta}\hat{\boldsymbol{\theta}}$$

and so from Equation A.17 and A.18

$$\begin{aligned}
v^2 &= \dot{\mathbf{r}} \cdot \dot{\mathbf{r}} = \dot{r}^2 + (r\dot{\theta})^2 \\
&= \left(\frac{h(1+e\cos\theta)}{a(1-e^2)} \right)^2 + \left(\frac{h(1+e\cos\theta)}{a(1-e^2)} \frac{e\sin\theta}{1+e\cos\theta} \right)^2 \\
&= \frac{h^2}{a^2(1-e^2)^2} \{e^2\sin^2\theta + 1 + 2e\cos\theta + e^2\cos^2\theta\} \\
&= \frac{h^2}{a^2(1-e^2)^2} \{2 + 2e\cos\theta + e^1 - 1\} \\
&= \frac{h^2}{a^2(1-e^2)} \left\{ \frac{2a(1-e^2)}{r} - (1-e^2) \right\} \\
&= \frac{h^2}{a(1-e^2)} \left\{ \frac{2}{r} - \frac{1}{a} \right\} \\
&= G(m_1 + m_2) \left\{ \frac{2}{r} - \frac{1}{a} \right\}
\end{aligned}$$

in the last few steps the following was used

$$\begin{aligned}
h^2 &= n^2 a^4 (1-e^2) \\
n^2 a^3 &= G(m_1 + m_2)
\end{aligned}$$

to re-write

$$\frac{h^2}{a(1-e^2)} = n^2 a^3 = G(m_1 + m_2)$$

The expression for v^2 can be used to re-write

$$\begin{aligned} \dot{r}^2 &= v^2 - r^2 \dot{\theta}^2 \\ &= G(m_1 + m_2) \left\{ \frac{2}{r} - \frac{1}{a} \right\} - \left(\frac{h}{r} \right)^2 \\ &= G(m_1 + m_2) \left\{ \frac{2}{r} - \frac{1}{a} \right\} - \frac{n^2 a^4 (1-e^2)}{r^2} \\ &= n^2 a^3 \left[\left\{ \frac{2}{r} - \frac{1}{a} \right\} - \frac{a(1-e^2)}{r^2} \right] \\ &= \frac{n^2 a^3}{r^2} [2ra - r^2 - a^2 + a^2 e^2] \\ &= \frac{n^2 a^2}{r^2} [(ae)^2 - (r-a)^2] \end{aligned}$$

so that

$$\dot{r} = \frac{na}{r} \sqrt{(ae)^2 - (r-a)^2}$$

Using the expression for r as a function of the eccentric anomaly E

$$r = a(1 - e \cos E)$$

$$\dot{r} = ae \sin E \dot{E}$$

$$\begin{aligned} ae \sin E \dot{E} &= \frac{na}{a(1-e \cos E)} \sqrt{(ae)^2 - \{a(1-e \cos E) - a\}^2} \\ &= \frac{na^2 e}{a(1-e \cos E)} \sqrt{1 - \cos^2 E} \\ &= \frac{nae}{1-e \cos E} \sin E \end{aligned}$$

which a bit simplified gives

$$\dot{E}(1 - e \cos E) = n$$

with a solution

$$E - e \sin E = n(t - t_p) \tag{A.19}$$

This is Kepler's equation and it is used by solving for the eccentric anomaly E given a time t .

A.3 Kepler's Laws

Here Kepler's three laws are summarized from the section above.

A short note is made on using orbital parameters from Jupiter and the Sun to calculate period for a artificial system. This because it more convenient to express star and planet masses in terms of Sun an Jupiter masses.

A.3.1 First Law

Stated earlier in the introduction is "the orbit of a planet is an ellipse with the Sun at one focus". This is Kepler's first law but there needs to be a slight modification to it. Namely that the center of mass is at one focus. Equation A.13 describe the separation of two bodies orbiting each other, but this has to be corrected to describe the radius vector of *one* body to the center of mass and this is done through Equation A.10a.

$$R_1 = \left(\frac{m_2}{m_1 + m_2} \right) \frac{a(1 - e^2)}{1 + e \cos \nu} \simeq \frac{a(1 - e^2)}{1 + e \cos \nu} \quad \text{if } m_2 \gg m_1$$

So the planet move on an elliptical orbit around the center of mass with a separation close to the separation between the Sun and the planet if the Sun is assumed to be much heavier.

For the Sun the same applies but with a factor of $\left(\frac{m_1}{m_1 + m_2} \right) \simeq \frac{m_1}{m_2}$ instead. If taken for the Sun and Earth it would mean that the Sun barely¹ moves. Even if taken for the Sun and Jupiter the center of mass would only be slightly outside² the Sun.

So in reality the orbit of a planet is an ellipse around the center of mass of the system, but the Sun is much heavier and does almost not move due to its much larger mass so it stays put at the center of mass.

If more planets are tugging on the Sun their contributions will not add linearly but as their individual contributions are small they can be taken as perturbations and added linearly.

A.3.2 Second Law

The second law states that the area the radial vector sweeps out over a given time is constant. Equation A.8 and A.7 together state that

$$\dot{A} = \frac{1}{2}h$$

which then is re-written in Equation A.11 so that the area a the radial vector for one planet sweeps out over a given time is constant.

Also, the closer the orbiting body is to the center of mass, the faster it will go in its orbit.

A.3.3 Third Law

The thrid and final law states that the cube of the semi major axis is proportional to the square of the period.

All this is derived above giving Equation A.16

¹ $m_{\oplus}/M_{\odot} * a_{\oplus} \simeq 150 * 10^6 / 333000 \text{ km} \simeq 450 \text{ km}$ (Williams, 2004)

² $m_{\text{J}}/M_{\odot} * a_{\text{J}}/\text{radius}_{\odot} \simeq 780 * 10^6 * 318 / 333000 / 6.96 * 10^5 \simeq 1.07$

A.3.4 Calculations of orbital period for artificial systems

When creating a system (planet and star) not all parameters are independent. For example the period is connected to the semi-major axis and mass of both the planet and star through Kepler's third law. Therefore if the a system is created (mass of planet and star, semi major axis) then the orbital period has to be calculated.

Using the orbital parameters of the Sun and Jupiter it is possible to express the orbital period of the planet directly in year.

$$\begin{aligned}
 P_{\mathcal{J}}^2 &= \frac{4\pi^2}{G(m_{\odot} + m_{\mathcal{J}})} a_{\mathcal{J}}^3 \\
 P_p^2 &= \frac{4\pi^2}{G(m_* + m_p)} a_p^3 \\
 \Rightarrow P_p &= P_{\mathcal{J}} \left(\frac{a_p}{a_{\mathcal{J}}} \right)^{3/2} \left(\frac{m_{\odot} + m_{\mathcal{J}}}{m_* + m_p} \right)^{1/2} \\
 &= P_{\mathcal{J}} \left(\frac{a_p}{a_{\mathcal{J}}} \right)^{3/2} \left(\frac{(1 + m_{r,\mathcal{J}/\odot})m_{\odot}}{(1 + m_{r,p/*})m_{r,*/\odot}m_{\odot}} \right)^{1/2} \\
 &= P_{\mathcal{J}} \left(\frac{a_p}{a_{\mathcal{J}}} \right)^{3/2} \left(\frac{1 + m_{r,\mathcal{J}/\odot}}{(1 + m_{r,p/*})m_{r,*/\odot}} \right)^{1/2}
 \end{aligned}$$

where $m_{r,p/*}$ denote the mass ratio of the planet to the star, $m_{r,\mathcal{J}/\odot}$ the mass ratio of Jupiter to the Sun and $m_{r,*/\odot}$ the mass ratio of the star to the Sun.

The reason for this somewhat more complicated expression, instead of just using the ratio of the semi major axis of the planet relative to Jupiter, comes from the mass ratio of the star to the Sun. For example Barnard's star which is roughly one tenth of the mass of the Sun would give a factor three too long period ($\sqrt{1/0.1} \simeq 3$)

B Thiele-Innes Parameters

In this chapter, expressions are derived describing the position of a planet in a coordinate system tangential to the celestial sphere

$$X = Ax + Fy$$

$$Y = Bx + Gy$$

$$Z = Cx + Hy$$

where X and Y are related to declination and right ascension respectively.

Also, the time derivative of the offset in the radial direction is derived, which is used if radial velocity measurements are included in addition to the offset, or astrometric measurements.

$$\dot{Z} = C\dot{x} + H\dot{y}$$

This transformation is described through the Thiele-Innes parameters, which can be thought of as the elements in a rotation matrix together with a scaling

$$A = a(\cos \Omega \cos \omega - \sin \Omega \cos i \sin \omega)$$

$$B = a(\sin \Omega \cos \omega + \cos \Omega \cos i \sin \omega)$$

$$C = a(\sin i \sin \omega)$$

$$F = a(-\cos \Omega \sin \omega - \sin \Omega \cos i \cos \omega)$$

$$G = a(-\sin \Omega \sin \omega + \cos \Omega \cos i \cos \omega)$$

$$H = a(\sin i \cos \omega)$$

B.1 Rotations

This section discusses rotations of ellipses as what will be observed is basically the components of a rotated ellipse. The reflex motion of a star due to an orbiting planet will, as shown in Kepler's first law, be an ellipse. But as the orientation of the planetary orbit relative to the observer is random a few more parameters are needed to describe what the observer will see. These parameters are not connected directly to the Keplerian parameters but describe the *orientation*

of the orbit relative to the observer.

Three parameters, or angles, are needed to describe the orbit and not only two as could be expected. To see this imagine the normal to the orbital plane. This normal can be orientated in any way with only *two* angles, but the orbit is not necessarily circular so a third angle is needed to orient or rotate the orbit around the normal.

The sequence of rotations and around which axis does not matter that much in reality, but convention has it that they are described in a particular order so the angles get particular names and meanings. In the end it all amounts three parameters for the orientation of the orbit, and below is a particular choice of angles and order of rotations.

One way to describe an ellipse in the xy -plane is through the parametrization

$$\begin{cases} x = (\cos E - e) \\ y = \sqrt{1 - e^2} \sin E \\ z = 0 \end{cases} \quad (\text{B.3})$$

where E is the eccentric anomaly describing the position on the ellipse and e is the eccentricity describing the shape

Another way to parameterize the ellipse is through

$$\begin{cases} x = r \cos \nu = \frac{(1 - e^2)}{1 + e \cos \nu} \cos \nu \\ y = r \sin \nu = \frac{(1 - e^2)}{1 + e \cos \nu} \sin \nu \\ z = 0 \end{cases} \quad (\text{B.4})$$

where

$$r = r(\nu) = \frac{(1 - e^2)}{1 + e \cos \nu}$$

They are used in different context, the second one mostly in radial velocity. However, they do describe the same thing just in different ways.

Note: There is no a in these equations as opposed to the in the section about ellipses. The reason for this is that the equations get a bit simpler if we start out with an ellipse having a semi major axis $a = 1$. The scaling, or giving the orbit a realistic semi major axis with correct units, is included later in the Thiele-Innes parameters.

Rotations are then described as multiplication of a rotation matrix and the vector $(x, y, z)^T$. Rotation around the x -axis by an angle ϕ can be described by the matrix

$$P_x(\phi) = \begin{pmatrix} 1 & 0 & 0 \\ 0 & \cos \phi & -\sin \phi \\ 0 & \sin \phi & \cos \phi \end{pmatrix}$$

Rotation around the z -axis

$$P_z(\phi) = \begin{pmatrix} \cos \phi & -\sin \phi & 0 \\ \sin \phi & \cos \phi & 0 \\ 0 & 0 & 1 \end{pmatrix}$$

Three rotations can then transform the points on the ellipse $(x, y, z)^T$ to what will actually be seen by an observer $(X, Y, Z)^T$.

$$\begin{pmatrix} X \\ Y \\ Z \end{pmatrix} \propto P_z(\Omega)P_x(i)P_z(\omega) \begin{pmatrix} x \\ y \\ z \end{pmatrix}$$

What these transformations look like is shown in Figure B.1.

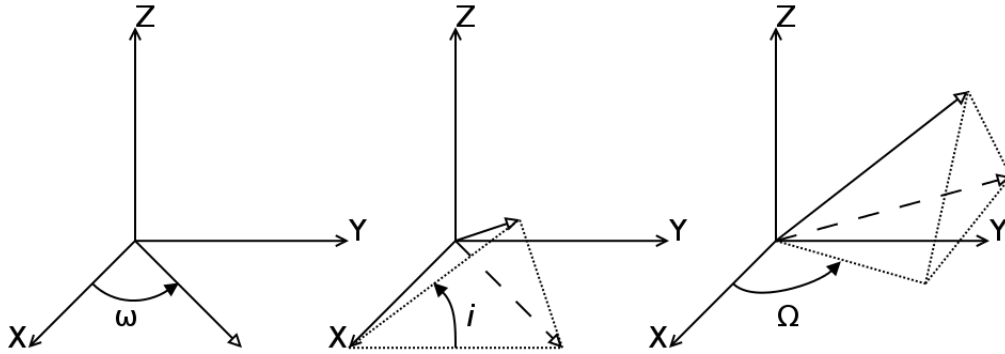


Figure B.1: Three rotations describing the orientation. The sequence is from left to right; 1. Rotate an angle ω around the z -axis $P_z(\omega)$, 2. Rotate an angle i around the x -axis $P_x(i)$, 3. Rotate an angle Ω around the z -axis $P_z(\Omega)$. Three angles are needed to fully describe the orientation of an orbit if the orbit does not possess a rotation symmetry, i.e. non zero eccentricity. If the orbit is circular then the first rotation ($P_z(\omega)$) does not have any effect.

Note the order of the rotations: **z x z**. The first rotation $P_z(\omega)$ is as stated above a rotation of an angle ω around the z -axis. If the orbit is circular this rotation does not have any actual effect, but for elliptical orbits this will change the *argument of periapsis*. The second rotation $P_x(i)$ refers to the inclination of the orbit. The third, and last, rotation $P_z(\Omega)$ is again a rotation around the z -axis, but this time the orbit has already been rotated out of the xy -plane and so this angle corresponds to where the orbit will “move through” the xy -plane.

Multiplying the three matrices and writing out the components

$$P_z(\Omega)P_x(i)P_z(\omega) = \begin{pmatrix} \cos \Omega \cos \omega - \sin \Omega \cos i \sin \omega & -\cos \Omega \sin \omega - \sin \Omega \cos i \cos \omega & \sin \Omega \sin i \\ \sin \Omega \cos \omega + \cos \Omega \cos i \sin \omega & -\sin \Omega \sin \omega + \cos \Omega \cos i \cos \omega & -\cos \Omega \sin i \\ \sin i \sin \omega & \sin i \cos \omega & \cos i \end{pmatrix} \quad (\text{B.5})$$

This is the rotation matrix describing how the orbit is transformed.

So transforming the orbit amounts to, for a given set of angles $\{\omega, \Omega, i\}$, multiplication by nine numbers.

Now define the *Thiele-Innes parameters* which are related to the elements in the full rotation matrix by

$$\begin{aligned} A &= a(\cos \Omega \cos \omega - \sin \Omega \cos i \sin \omega) \\ B &= a(\sin \Omega \cos \omega + \cos \Omega \cos i \sin \omega) \\ C &= a(\sin i \sin \omega) \\ F &= a(-\cos \Omega \sin \omega - \sin \Omega \cos i \cos \omega) \\ G &= a(-\sin \Omega \sin \omega + \cos \Omega \cos i \cos \omega) \\ H &= a(\sin i \cos \omega) \end{aligned}$$

Note: Now the semi-major axis is included in the above expressions

So the rotation matrix can be re-written somewhat more compactly using the Thiele-Innes parameters

$$P_z(\Omega)P_x(i)P_z(\omega) = \frac{1}{a} \begin{pmatrix} A & F & a(\sin \Omega \sin i) \\ B & G & a(-\cos \Omega \sin i) \\ C & H & a(\cos i) \end{pmatrix}$$

and the components of the rotated orbit can be calculated from the matrix multiplication

$$\begin{pmatrix} X \\ Y \\ Z \end{pmatrix} = \begin{pmatrix} A & F & a(\sin \Omega \sin i) \\ B & G & a(-\cos \Omega \sin i) \\ C & H & a(\cos i) \end{pmatrix} \begin{pmatrix} x \\ y \\ z \end{pmatrix}$$

or more in component form

$$X = Ax + Fy \tag{B.7a}$$

$$Y = Bx + Gy \tag{B.7b}$$

$$Z = Cx + Hy \tag{B.7c}$$

This also explains why the rightmost column in the rotation matrix is not re-written with Thiele-Innes parameters; As $z = 0$ for the initial ellipse the rightmost column does not have any effect.

The two components X and Y are then related to the offset in the position of the star due to the planet by being in the opposite direction and corrected for the much lower mass of the star, i.e. the offset of the star will be $-\frac{m_P}{M_*}X$ and $-\frac{m_P}{M_*}Y$ respectively. This will be clarified further down.

The expression for Z can be written with expanded Thiele-Innes parameters

$$\begin{aligned} Z &= Cx + Hy \\ &= ar \cos \nu \sin i \sin \omega + ar \sin \nu \sin i \cos \omega \\ &= ar \sin(\nu + \omega) \sin i \end{aligned}$$

The expression for the radial distance was (Equation B.4)

$$r = \frac{(1 - e^2)}{1 + e \cos \nu}$$

so the time derivative of r becomes

$$\begin{aligned} \dot{r} &= \frac{(1 - e^2)}{(1 + e \cos \nu)^2} e \dot{\nu} \sin \nu \\ &= \frac{1}{(1 + e \cos \nu)} r e \dot{\nu} \sin \nu \\ &= r^2 \dot{\nu} \frac{e \sin \nu}{(1 - e^2)} \end{aligned}$$

So then the time derivative of the Z-component

$$\begin{aligned} \dot{Z} &= a \dot{r} \sin(\nu + \omega) \sin i + a r \cos(\nu + \omega) \dot{\nu} \sin i \\ &= a \dot{r} \sin(\nu + \omega) \sin i + a r \dot{\nu} \cos(\nu + \omega) \sin i \\ &= a \frac{1}{(1 + e \cos \nu)} r e \dot{\nu} \sin \nu \sin(\nu + \omega) \sin i + a r \dot{\nu} \cos(\nu + \omega) \sin i \\ &= a \frac{r \dot{\nu}}{(1 + e \cos \nu)} \{e \sin \nu \sin(\nu + \omega) + (1 + e \cos \nu) \cos(\nu + \omega)\} \sin i \\ &= a \frac{r \dot{\nu}}{(1 + e \cos \nu)} \{e(\sin \nu \sin(\nu + \omega) + \cos \nu \cos(\nu + \omega)) + \cos(\nu + \omega)\} \sin i \\ &= a \frac{r \dot{\nu}}{(1 + e \cos \nu)} \{e \cos \omega + \cos(\nu + \omega)\} \sin i \\ &= a \frac{r^2 \dot{\nu}}{(1 - e^2)} \{e \cos \omega + \cos(\nu + \omega)\} \sin i \end{aligned}$$

Note: The expression $r^2 \dot{\nu}$ does not simplify to h as the r in here is the unit-less expression above. So to get the correct expression $r^2 \dot{\nu} \rightarrow \frac{1}{a^2} (ar)^2 \dot{\nu} = \frac{1}{a^2} h$

$$\dot{Z} = \frac{h}{a(1 - e^2)} \{e \cos \omega + \cos(\nu + \omega)\} \sin i$$

(B.8)

To get the expression for the radial velocity of the star this has to be corrected by a factor $\frac{-m_2}{m_1 + m_2}$, but as the Z-axis and the radial vector are anti-parallel the negative sign disappears

$$\begin{aligned} v_{r,1} &= \frac{m_2}{m_1 + m_2} \frac{h}{a(1 - e^2)} \{e \cos \omega + \cos(\nu + \omega)\} \sin i \\ &= \frac{m_2}{m_1 + m_2} \frac{\sqrt{(m_1 + m_2) G a (1 - e^2)}}{a(1 - e^2)} \{e \cos \omega + \cos(\nu + \omega)\} \sin i \\ &= \sqrt{\frac{G m_2^2}{m_1 + m_2}} \frac{1}{a(1 - e^2)} \{e \cos \omega + \cos(\nu + \omega)\} \sin i \end{aligned}$$

This is the radial velocity component from the orbital motion and can be compared to Equation 1.1. This can be measured in contrast to just the Z-component of the reflex motion.

However, the time derivative of the Z component could be expressed through the time derivatives of x and y instead

$$\begin{aligned}\dot{Z} &= C\dot{x} + H\dot{y} \\ &= Ca\dot{E}\sin E - Ha\sqrt{1-e^2}\dot{E}\cos E \\ &= Ca\dot{E}\sin E - Ha\sqrt{1-e^2}\dot{E}\cos E \\ &= Ca\frac{2\pi}{P}\frac{1}{1-e\cos E}\sin E - Ha\sqrt{1-e^2}\frac{2\pi}{P}\frac{1}{1-e\cos E}\cos E\end{aligned}$$

As the radial velocity component has parameters in common with the position offset, a combination of the data from astrometry and radial velocity can help constrain the solution or give better initial guesses of the parameters.

B.1.1 Random points on the sphere

To generate a random orientation of a planetary system, the vector normal to the orbital plane has to be uniformly distributed over the sphere. The three angles used are ω , Ω and i . Of these three the argument of periapsis ω does not change the vector normal to the orbital plane of the planet. Only the argument of ascending node Ω and inclination i change the orientation.

So why is this important? If the distribution¹ for the random angles would be chosen as uniformly distributed over $[0, 2\pi]$ and $[0, \pi]$ for Ω and i respectively, then this would result in too many points close to the poles. This can be nicely visualized with looking at a globe having uniformly distributed markings of longitude and latitude. Clearly one of these patches is smaller closer to the pole than at the equator, so if each patch had equally many points the patches close to the poles would have a higher density of points.

Writing the infinitesimal area element with usual notation for the two angles (θ here correspond to Ω and ϕ to i) as $d\Omega = \sin\phi d\theta d\phi$ there is a dependence on ϕ through the $\sin\phi$ term. This can be slightly changed to $d\Omega = -d\theta d(\cos\phi)$. If the number of points per area element is to be constant it would also mean that $d\theta$ and $d(\cos\phi)$ should be constant. θ is to be in the range $[0, 2\pi]$ and ϕ in the range $[0, \pi]$. If independent uniform distributions are used for generating the random numbers, a good guess for the transformation is $\theta = 2\pi u$ and $\cos\phi = 2v - 1$ where u and v are two uniformly distributed random variables in the range $[0, 1]$.

Calculating the density for these two transformations

$$\begin{aligned}P_\theta d\theta P_\phi d\phi &= P_u \left| \frac{du}{d\theta} \right| d\theta P_v \left| \frac{dv}{d\phi} \right| d\phi \\ &= \frac{1}{2\pi} d\theta \frac{\sin\phi}{2} d\phi \\ &= \frac{1}{4\pi} \sin\phi d\theta d\phi\end{aligned}$$

¹This is adapted from <http://mathworld.wolfram.com/SpherePointPicking.html>

where the last line can be compared to the infinitesimal area element above. So this transformation will produce uniformly distributed points on the sphere (having solid angle 4π) given two uniformly distributed random variables on $[0, 1]$.

Re writing it in terms of the notation for argument of ascending node and inclination

$$\begin{aligned}\Omega &= 2\pi u & u &\sim \text{U}(0, 1) \\ i &= \arccos(2v - 1) & v &\sim \text{U}(0, 1)\end{aligned}$$

will be the transformation used for picking random points on the sphere.

C Levenberg-Marquardt

The offsets of a stars position due to an orbiting planet are calculated

$$\begin{aligned}X^{\text{Offset}} &= -m_r \varpi (Ax + Fy) \\Y^{\text{Offset}} &= -m_r \varpi (Bx + Gy) \\Z^{\text{Offset}} &= -m_r \varpi (Cx + Hy)\end{aligned}$$

in addition, the time derivatives of these offsets are calculated. Furthermore all partial derivatives with respect to the parameters are calculated.

Transformations of the parameters are defined to map a range of realistic parameters onto the full line, i.e., the transformed parameters correspond to restrictions or boundary conditions. The partial derivatives of the parameters with respect to the transformed partial derivatives are also calculated.

The end result is the possibility to construct the Jacobian which is then used both for calculating the updates in the optimization procedure and for estimating the formal errors of the optimized parameters.

Often in here, there are references made to a solution of non-linear least squares in one way or another. The reason for not only using a linear least square solution when doing the optimization for the Keplerian parameters is, as might be guessed, that some of the parameters do not appear in linear expressions. The parameters; eccentricity, time of periapsis passage and orbital period are those which are not in linear expressions. The other Keplerian parameters, such as the three angles related to the orientation of the orbit in relation to the observer are linear, or could at least be made linear by expressing them through the Thiele Innes parameters.

C.1 The problem

Two ways of optimizing, or in this case find the minimum of a function, are to either take steps in the direction where the function is decreasing the most (steepest descent) or approximate the function with a quadratic function and find the minimum (Gauss-Newton). These two methods have quite complementary strengths and weaknesses and can be combined into the Levenberg-Marquardt method for solving non-linear equations.

The problem¹ of optimizing is to find a set of parameters such that the function values

¹This is based on notes from Gavin, H. *The Levenberg-Marquardt method for nonlinear least squares curve-*

get close to the measured values in some sense. One widespread way to define this closeness is the sum of the weighted square residuals. Which if the residuals were normally distributed with standard deviation equal to the weight would give a χ^2 -value, thus it is called the χ^2 -error criterion

$$\chi^2(\mathbf{p}) = \frac{1}{2} \sum_i \left(\frac{y(t_i) - \hat{y}(t_i; \mathbf{p})}{w_i} \right)^2$$

where $y(t_i)$ is the measured value at time t_i (field angle of the star image or radial velocity), w_i the associated standard deviation of the measurement and $\hat{y}(t_i; \mathbf{p})$ is the function value at t_i for the parameters \mathbf{p} .

This can be written in matrix notation instead

$$\begin{aligned} \chi^2(\mathbf{p}) &= \frac{1}{2} (\mathbf{y} - \hat{\mathbf{y}}(\mathbf{p}))^\top \mathbf{W} (\mathbf{y} - \hat{\mathbf{y}}(\mathbf{p})) \\ &= \frac{1}{2} \mathbf{y}^\top \mathbf{W} \mathbf{y} + \frac{1}{2} \hat{\mathbf{y}}^\top \mathbf{W} \hat{\mathbf{y}} - \mathbf{y}^\top \mathbf{W} \hat{\mathbf{y}} \end{aligned}$$

where \mathbf{W} is a diagonal matrix with elements $1/w_i^2$.

So as said above the two different methods are to update the parameters \mathbf{p} by \mathbf{h} either to find the minimum of a local quadratic approximation or in the direction which gives the largest decrease in the χ^2 -error criterion.

C.1.1 Gauss-Newton

The Gauss-Newton update assumes that the χ^2 -error criterion, or function, can be approximated by a quadratic function, that is to say that the parameter is relatively close to the true value and by taking a step $\mathbf{h}_{\text{Gauss-Newton}}$ in parameter space will give the true value. The χ^2 -error criterion is Taylor expanded around the minimum

$$\hat{\mathbf{y}}(\mathbf{p} + \mathbf{h}_{\text{GN}}) \simeq \hat{\mathbf{y}}(\mathbf{p}) + \left(\frac{\partial \hat{\mathbf{y}}}{\partial \mathbf{p}} \right) \mathbf{h}_{\text{GN}} = \hat{\mathbf{y}} + \mathbf{J} \mathbf{h}_{\text{GN}}$$

where \mathbf{J} is the Jacobian, i.e. the partial derivatives of the function $\hat{\mathbf{y}}(t_i; \mathbf{p})$ for all function arguments t_i with respect to the parameters \mathbf{p}

This then gives

$$\begin{aligned} \chi^2(\mathbf{p} + \mathbf{h}_{\text{GN}}) &= \frac{1}{2} \mathbf{y}^\top \mathbf{W} \mathbf{y} + \frac{1}{2} (\hat{\mathbf{y}} + \mathbf{J} \mathbf{h}_{\text{GN}})^\top \mathbf{W} (\hat{\mathbf{y}} + \mathbf{J} \mathbf{h}_{\text{GN}}) - \mathbf{y}^\top \mathbf{W} (\hat{\mathbf{y}} + \mathbf{J} \mathbf{h}_{\text{GN}}) \\ &= \frac{1}{2} \mathbf{y}^\top \mathbf{W} \mathbf{y} + \frac{1}{2} \hat{\mathbf{y}}^\top \mathbf{W} \hat{\mathbf{y}} - \mathbf{y}^\top \mathbf{W} \hat{\mathbf{y}} \\ &\quad - (\mathbf{y} - \hat{\mathbf{y}})^\top \mathbf{W} (\mathbf{J} \mathbf{h}_{\text{GN}}) + \frac{1}{2} (\mathbf{J} \mathbf{h}_{\text{GN}})^\top \mathbf{W} (\mathbf{J} \mathbf{h}_{\text{GN}}) \end{aligned}$$

the update should then be chosen such that the derivative become zero

fitting problems

¹In the case of measurements with estimated standard deviations of σ_i then $w_i = \sigma_i^2$

$$\frac{\partial \chi^2}{\partial \mathbf{h}_{\text{GN}}}(\mathbf{p} + \mathbf{h}_{\text{GN}}) = 0$$

or

$$0 = \frac{\partial \chi^2}{\partial \mathbf{h}_{\text{GN}}}(\mathbf{p} + \mathbf{h}_{\text{GN}}) \simeq -(\mathbf{y} - \hat{\mathbf{y}})^T \mathbf{W} \mathbf{J} + (\mathbf{J} \mathbf{h}_{\text{GN}})^T \mathbf{W} \mathbf{J}$$

So the Gauss-Newton update is then found by solving

$$(\mathbf{J}^T \mathbf{W} \mathbf{J}) \mathbf{h}_{\text{GN}} = \mathbf{J}^T \mathbf{W} (\mathbf{y} - \hat{\mathbf{y}})$$

C.1.2 Gradient descent

The gradient descent method is slightly easier as it only involves taking a step in negative gradient which can be calculated from

$$\begin{aligned} \frac{\partial \chi^2}{\partial \mathbf{p}} &= \frac{\partial}{\partial \mathbf{p}} \left(\frac{1}{2} \mathbf{y}^T \mathbf{W} \mathbf{y} + \frac{1}{2} \hat{\mathbf{y}}^T \mathbf{W} \hat{\mathbf{y}} - \mathbf{y}^T \mathbf{W} \hat{\mathbf{y}} \right) \\ &= \hat{\mathbf{y}}^T \mathbf{W} \frac{\partial \hat{\mathbf{y}}}{\partial \mathbf{p}} - \mathbf{y}^T \mathbf{W} \frac{\partial \hat{\mathbf{y}}}{\partial \mathbf{p}} \\ &= -(\mathbf{y} - \hat{\mathbf{y}})^T \mathbf{W} \mathbf{J} \end{aligned}$$

so the step in the negative gradient is

$$\mathbf{h}_{\text{gradient descent}} = \frac{1}{\lambda} \mathbf{J}^T \mathbf{W} (\mathbf{y} - \hat{\mathbf{y}})$$

where λ is related to the step size.

C.1.3 Levenberg-Marquardt

If the two methods, Gauss-Newton and gradient descent, are combined the result is called Levenberg-Marquardt

$$(\mathbf{J}^T \mathbf{W} \mathbf{J} + \lambda \mathbf{I}) \mathbf{h}_{\text{Levenberg-Marquardt}} = \mathbf{J}^T \mathbf{W} (\mathbf{y} - \hat{\mathbf{y}})$$

The motivation for this comes from the choice of step size (λ) in relation to how “close” the parameters are to the optimum. Close to the optimum the Gauss-Newton method gives a fast convergence but farther away the quadratic approximation may not be too good. On the other hand, far away from the optimum the gradient descent gives a fast convergence but once it get close to the optimum it may have trouble settling down. So, if the step size is chosen such that far away a large step size is chosen the method behaves like a gradient descent, but as it closes in on the optimum the step size is reduced behaving more like a Gauss-Newton method.

Usually the identity matrix \mathbf{I} is replaced by the diagonal of $\mathbf{J}^T \mathbf{W} \mathbf{J}$

$$(\mathbf{J}^T \mathbf{W} \mathbf{J} + \lambda \text{diag}(\mathbf{J}^T \mathbf{W} \mathbf{J})) \mathbf{h}_{\text{LM}} = \mathbf{J}^T \mathbf{W} (\mathbf{y} - \hat{\mathbf{y}})$$

In addition to finding the parameters minimizing the χ^2 -error function it is of interest to find a formal errors on the parameters to be able to say something about how the solution depend on the parameters or if some of the parameters have such a large formal error that they can not be relied upon.

The formal errors are calculated from

$$\sigma_{\mathbf{p}} = \sqrt{\text{diag}((\mathbf{J}^T \mathbf{W} \mathbf{J})^{-1})}$$

the possibility to perform this operation¹ depend the matrix $\mathbf{J}^T \mathbf{W} \mathbf{J}$ not being singular, i.e. it must have full rank.

So what is needed for solving with the Levenberg-Marquardt algorithm is an expression for the function $\hat{\mathbf{y}}(t_i; \mathbf{p})$, the observations \mathbf{y} and the weights w_i of the observations. The derivatives of the function with respect to the parameters, the Jacobian \mathbf{J} , is not necessary as the numerical derivatives can be formed. However, if the derivatives are possible to calculate analytically the number of function evaluations can be reduced and also any numerical errors can be avoided. If the weights are homoscedastic the expressions can be simplified, but the inclusion of them in the χ^2 -error criterion has another good consequence. Each term in the sum is dimensionless! So different sets of measurements can be added freely, eg. radial velocity and astrometry, as long as both are parameterized by the same parameters.

C.2 Partial derivatives

In this section all the partial derivatives of the offsets with respect to the parameters are calculated. In addition, the same partial derivatives are calculated but for the time derivatives of the offsets.

Depending on which algorithm is chosen for an optimization, a number of auxiliary quantities are needed. The choice for the algorithm to do the optimization is the Levenberg-Marquardt algorithm which, if it is possible to calculate, take the partial derivative of the target function with respect to the parameters. The analytical derivatives are not explicitly needed as they can be substituted with the numerical counterparts. However, if they are possible to calculate it will help both computationally and also numerical errors can be avoided.

The target function is in this case the position of the star at a given time, and of particular interest are the seven Keplerian parameters. The derivatives with respect to the five astrometric parameters have already been implemented so only the derivatives of the seven Keplerian parameters are needed. Also remember that going from the offset of the star to the position of the planet, all that is required is a change of sign and correction for the mass.

The merit function, the measure of how close the target function is to the observations, is already implemented in the Levenberg-Marquardt algorithm. The last part which is needed are the *weights* for each observations which are used when calculating the merit function.

¹In the *Commons Math: The Apache Commons Mathematics Library* the inverse of the matrix $(\mathbf{J}^T \mathbf{W} \mathbf{J})$ is calculated by QR-decomposition

$$\begin{aligned}x &= \cos E - e \\y &= \sqrt{1 - e^2} \sin E \\z &= 0\end{aligned}$$

The two expressions for the position of the planet in the orbit are as previously stated

$$\begin{aligned}X &= Ax + Fy \\Y &= Bx + Gy \\Z &= Cx + Hy\end{aligned}$$

where E is the eccentric anomaly which is calculated from Kepler's equation:

$$M = 2\pi \frac{t - t_p}{P} = E - e \sin E$$

This has to be corrected for the distance to the system

$$\begin{aligned}\bar{X} &= \varpi(Ax + Fy) \\ \bar{Y} &= \varpi(Bx + Gy) \\ \bar{Z} &= \varpi(Cx + Hy)\end{aligned}$$

However, this is the position of the planet so there has to be a further correction to get the position of the *star*

$$X^{\text{Offset}} = -m_r \varpi(Ax + Fy) \tag{C.1}$$

$$Y^{\text{Offset}} = -m_r \varpi(Bx + Gy) \tag{C.2}$$

$$Z^{\text{Offset}} = -m_r \varpi(Cx + Hy) \tag{C.3}$$

These are the offsets in the units of whatever ϖ is measured in so that X^{Offset} and Y^{Offset} are the angular offsets in position.

While discussing the position offsets, the time derivatives of the offsets can also be included.

$$\dot{x} = -\dot{E} \sin E \tag{C.4}$$

$$\dot{y} = \sqrt{1 - e^2} \dot{E} \cos E \tag{C.5}$$

$$\dot{z} = 0 \tag{C.6}$$

The time derivative of the Z^{Offset} is related to the radial velocity, the two other components can be included in the calculations of proper motion as offsets.

$$\dot{X}^{\text{Offset}} = -m_r \varpi (A\dot{x} + F\dot{y}) \quad (\text{C.7})$$

$$\dot{Y}^{\text{Offset}} = -m_r \varpi (B\dot{x} + G\dot{y}) \quad (\text{C.8})$$

$$\dot{Z}^{\text{Offset}} = -m_r \varpi (C\dot{x} + H\dot{y}) \quad (\text{C.9})$$

The three partial derivatives of the eccentric anomaly with respect to the three parameter; period, eccentricity and time of periapsis passage.

$$\begin{aligned} \frac{\partial E}{\partial t_p} &= \frac{-2\pi}{P(1 - e \cos E)} \\ \frac{\partial E}{\partial P} &= \frac{2\pi(t - t_p)}{P^2(e \cos E - 1)} \\ \frac{\partial E}{\partial e} &= \frac{\sin E}{1 - e \cos E} \end{aligned}$$

The partial derivative of the elliptical coordinates with respect to the time of periapsis passage, period and eccentricity

$$\begin{aligned} \frac{\partial x}{\partial t_p} &= -\sin E \frac{\partial E}{\partial t_p} \\ \frac{\partial y}{\partial t_p} &= \sqrt{1 - e^2} \cos E \frac{\partial E}{\partial t_p} \end{aligned}$$

$$\begin{aligned} \frac{\partial x}{\partial P} &= -\sin E \frac{\partial E}{\partial P} \\ \frac{\partial y}{\partial P} &= \sqrt{1 - e^2} \cos E \frac{\partial E}{\partial P} \end{aligned}$$

$$\begin{aligned} \frac{\partial x}{\partial e} &= -\sin E \frac{\partial E}{\partial e} - 1 \\ \frac{\partial y}{\partial e} &= \frac{-e}{\sqrt{1 - e^2}} \sin E + \sqrt{1 - e^2} \cos E \frac{\partial E}{\partial e} \end{aligned}$$

If a parameter is transformed, e.g. $S \rightarrow \tilde{S}$, then the partial derivative with respect to the transformed variable will naturally follow the chain rule for differentiation

$$\begin{aligned} \frac{\partial S^{\text{Offset}}}{\partial \tilde{S}} &= \frac{\partial S^{\text{Offset}}}{\partial S} \frac{\partial S}{\partial \tilde{S}} \\ \frac{\partial \dot{S}^{\text{Offset}}}{\partial \tilde{S}} &= \frac{\partial \dot{S}^{\text{Offset}}}{\partial S} \frac{\partial S}{\partial \tilde{S}} \end{aligned}$$

The eccentric anomaly is dependent on three parameters as before, in addition it has a time derivative which is also dependent on the same three parameters

$$\begin{aligned}\frac{\partial \dot{E}}{\partial t_p} &= \frac{-\partial \dot{E}}{\partial E} \frac{\partial E}{\partial t_p} \\ \frac{\partial \dot{E}}{\partial P} &= \frac{-2\pi}{P^2(1-e \cos E)} + \frac{\partial \dot{E}}{\partial E} \frac{\partial E}{\partial P} \\ \frac{\partial \dot{E}}{\partial e} &= \frac{2\pi \cos E}{P(1-e \cos E)^2} \frac{\partial \dot{E}}{\partial E} \frac{\partial E}{\partial e}\end{aligned}$$

The partial derivative of the time derivatives of the elliptical coordinates for time of periapsis, period and eccentricity

$$\begin{aligned}\frac{\partial \dot{x}}{\partial t_p} &= -\frac{\partial \dot{E}}{\partial t_p} \sin E - \dot{E} \frac{\partial E}{\partial t_p} \cos E \\ \frac{\partial \dot{y}}{\partial t_p} &= \sqrt{1-e^2} \frac{\partial \dot{E}}{\partial t_p} \cos E - \sqrt{1-e^2} \dot{E} \frac{\partial E}{\partial t_p} \sin E\end{aligned}$$

$$\begin{aligned}\frac{\partial \dot{x}}{\partial P} &= -\frac{\partial \dot{E}}{\partial P} \sin E - \dot{E} \frac{\partial E}{\partial P} \cos E \\ \frac{\partial \dot{y}}{\partial P} &= \sqrt{1-e^2} \frac{\partial \dot{E}}{\partial P} \cos E - \sqrt{1-e^2} \dot{E} \frac{\partial E}{\partial P} \sin E\end{aligned}$$

$$\begin{aligned}\frac{\partial \dot{x}}{\partial e} &= -\frac{\partial \dot{E}}{\partial e} \sin E - \dot{E} \frac{\partial E}{\partial e} \cos E \\ \frac{\partial \dot{y}}{\partial e} &= \frac{-e}{\sqrt{1-e^2}} \dot{E} \cos E + \sqrt{1-e^2} \frac{\partial \dot{E}}{\partial e} \cos E - \sqrt{1-e^2} \dot{E} \frac{\partial E}{\partial e} \sin E\end{aligned}$$

The partial derivatives of the tangential coordinates can now start being formed. First the three non-linear parameters

$$\begin{aligned}\frac{\partial X^{\text{Offset}}}{\partial t_p} &= -m_r \varpi \left(A \frac{\partial x}{\partial t_p} + F \frac{\partial y}{\partial t_p} \right) \\ \frac{\partial Y^{\text{Offset}}}{\partial t_p} &= -m_r \varpi \left(B \frac{\partial x}{\partial t_p} + G \frac{\partial y}{\partial t_p} \right) \\ \frac{\partial Z^{\text{Offset}}}{\partial t_p} &= -m_r \varpi \left(C \frac{\partial x}{\partial t_p} + H \frac{\partial y}{\partial t_p} \right)\end{aligned}$$

$$\begin{aligned}\frac{\partial X^{\text{Offset}}}{\partial e} &= -m_r \varpi \left(A \frac{\partial x}{\partial e} + F \frac{\partial y}{\partial e} \right) \\ \frac{\partial Y^{\text{Offset}}}{\partial e} &= -m_r \varpi \left(B \frac{\partial x}{\partial e} + G \frac{\partial y}{\partial e} \right) \\ \frac{\partial Z^{\text{Offset}}}{\partial e} &= -m_r \varpi \left(C \frac{\partial x}{\partial e} + H \frac{\partial y}{\partial e} \right)\end{aligned}$$

$$\begin{aligned}\frac{\partial X^{\text{Offset}}}{\partial P} &= -m_r \varpi \left(A \frac{\partial x}{\partial P} + F \frac{\partial y}{\partial P} \right) \\ \frac{\partial Y^{\text{Offset}}}{\partial P} &= -m_r \varpi \left(B \frac{\partial x}{\partial P} + G \frac{\partial y}{\partial P} \right) \\ \frac{\partial Z^{\text{Offset}}}{\partial P} &= -m_r \varpi \left(C \frac{\partial x}{\partial P} + H \frac{\partial y}{\partial P} \right)\end{aligned}$$

and then for all the Thiele-Innes parameters

$$\begin{aligned}\frac{\partial X^{\text{Offset}}}{\partial A} &= -m_r \varpi x \\ \frac{\partial Y^{\text{Offset}}}{\partial A} &= 0 \\ \frac{\partial Z^{\text{Offset}}}{\partial A} &= 0\end{aligned}$$

$$\begin{aligned}\frac{\partial X^{\text{Offset}}}{\partial B} &= 0 \\ \frac{\partial Y^{\text{Offset}}}{\partial B} &= -m_r \varpi x \\ \frac{\partial Z^{\text{Offset}}}{\partial B} &= 0\end{aligned}$$

$$\begin{aligned}\frac{\partial X^{\text{Offset}}}{\partial C} &= 0 \\ \frac{\partial Y^{\text{Offset}}}{\partial C} &= 0 \\ \frac{\partial Z^{\text{Offset}}}{\partial C} &= -m_r \varpi x\end{aligned}$$

$$\begin{aligned}\frac{\partial X^{\text{Offset}}}{\partial F} &= -m_r \varpi y \\ \frac{\partial Y^{\text{Offset}}}{\partial F} &= 0 \\ \frac{\partial Z^{\text{Offset}}}{\partial F} &= 0\end{aligned}$$

$$\begin{aligned}\frac{\partial X^{\text{Offset}}}{\partial G} &= 0 \\ \frac{\partial Y^{\text{Offset}}}{\partial G} &= -m_r \varpi y \\ \frac{\partial Z^{\text{Offset}}}{\partial G} &= 0\end{aligned}$$

$$\begin{aligned}\frac{\partial X^{\text{Offset}}}{\partial H} &= 0 \\ \frac{\partial Y^{\text{Offset}}}{\partial H} &= 0 \\ \frac{\partial Z^{\text{Offset}}}{\partial H} &= -m_r \varpi y\end{aligned}$$

$$\begin{aligned}\frac{\partial X^{\text{Offset}}}{\partial m_r} &= -\varpi(Ax + Fy) \\ \frac{\partial Y^{\text{Offset}}}{\partial m_r} &= -\varpi(Bx + Gy) \\ \frac{\partial Z^{\text{Offset}}}{\partial m_r} &= -\varpi(Cx + Hy)\end{aligned}$$

And for completeness, all the previous partial derivatives can be calculated for the time derivatives of the tangential coordinates.

$$\begin{aligned}\frac{\partial \dot{X}^{\text{Offset}}}{\partial t_p} &= -m_r \varpi \left(A \frac{\partial \dot{x}}{\partial t_p} + F \frac{\partial \dot{y}}{\partial t_p} \right) \\ \frac{\partial \dot{Y}^{\text{Offset}}}{\partial t_p} &= -m_r \varpi \left(B \frac{\partial \dot{x}}{\partial t_p} + G \frac{\partial \dot{y}}{\partial t_p} \right) \\ \frac{\partial \dot{Z}^{\text{Offset}}}{\partial t_p} &= -m_r \varpi \left(C \frac{\partial \dot{x}}{\partial t_p} + H \frac{\partial \dot{y}}{\partial t_p} \right)\end{aligned}$$

$$\begin{aligned}\frac{\partial \dot{X}^{\text{Offset}}}{\partial e} &= -m_r \varpi \left(A \frac{\partial \dot{x}}{\partial e} + F \frac{\partial \dot{y}}{\partial e} \right) \\ \frac{\partial \dot{Y}^{\text{Offset}}}{\partial e} &= -m_r \varpi \left(B \frac{\partial \dot{x}}{\partial e} + G \frac{\partial \dot{y}}{\partial e} \right) \\ \frac{\partial \dot{Z}^{\text{Offset}}}{\partial e} &= -m_r \varpi \left(C \frac{\partial \dot{x}}{\partial e} + H \frac{\partial \dot{y}}{\partial e} \right)\end{aligned}$$

$$\begin{aligned}\frac{\partial \dot{X}^{\text{Offset}}}{\partial P} &= -m_r \varpi \left(A \frac{\partial \dot{x}}{\partial P} + F \frac{\partial \dot{y}}{\partial P} \right) \\ \frac{\partial \dot{Y}^{\text{Offset}}}{\partial P} &= -m_r \varpi \left(B \frac{\partial \dot{x}}{\partial P} + G \frac{\partial \dot{y}}{\partial P} \right) \\ \frac{\partial \dot{Z}^{\text{Offset}}}{\partial P} &= -m_r \varpi \left(C \frac{\partial \dot{x}}{\partial P} + H \frac{\partial \dot{y}}{\partial P} \right)\end{aligned}$$

$$\begin{aligned}\frac{\partial \dot{X}^{\text{Offset}}}{\partial A} &= -m_r \varpi \dot{x} \\ \frac{\partial \dot{Y}^{\text{Offset}}}{\partial A} &= 0 \\ \frac{\partial \dot{Z}^{\text{Offset}}}{\partial A} &= 0\end{aligned}$$

$$\begin{aligned}\frac{\partial \dot{X}^{\text{Offset}}}{\partial B} &= 0 \\ \frac{\partial \dot{Y}^{\text{Offset}}}{\partial B} &= -m_r \varpi \dot{x} \\ \frac{\partial \dot{Z}^{\text{Offset}}}{\partial B} &= 0\end{aligned}$$

$$\begin{aligned}\frac{\partial \dot{X}^{\text{Offset}}}{\partial C} &= 0 \\ \frac{\partial \dot{Y}^{\text{Offset}}}{\partial C} &= 0 \\ \frac{\partial \dot{Z}^{\text{Offset}}}{\partial C} &= -m_r \varpi \dot{x}\end{aligned}$$

$$\begin{aligned}\frac{\partial \dot{X}^{\text{Offset}}}{\partial F} &= -m_r \varpi \dot{y} \\ \frac{\partial \dot{Y}^{\text{Offset}}}{\partial F} &= 0 \\ \frac{\partial \dot{Z}^{\text{Offset}}}{\partial F} &= 0\end{aligned}$$

$$\begin{aligned}\frac{\partial \dot{X}^{\text{Offset}}}{\partial G} &= 0 \\ \frac{\partial \dot{Y}^{\text{Offset}}}{\partial G} &= -m_r \varpi \dot{y} \\ \frac{\partial \dot{Z}^{\text{Offset}}}{\partial G} &= 0\end{aligned}$$

$$\begin{aligned}\frac{\partial \dot{X}^{\text{Offset}}}{\partial H} &= 0 \\ \frac{\partial \dot{Y}^{\text{Offset}}}{\partial H} &= 0 \\ \frac{\partial \dot{Z}^{\text{Offset}}}{\partial H} &= -m_r \varpi \dot{y}\end{aligned}$$

$$\begin{aligned}\frac{\partial \dot{X}^{\text{Offset}}}{\partial m_r} &= -\varpi(A\dot{x} + F\dot{y}) \\ \frac{\partial \dot{Y}^{\text{Offset}}}{\partial m_r} &= -\varpi(B\dot{x} + G\dot{y}) \\ \frac{\partial \dot{Z}^{\text{Offset}}}{\partial m_r} &= -\varpi(C\dot{x} + H\dot{y})\end{aligned}$$

C.3 Optimization with boundary conditions

The Levenberg-Marquard (LM) algorithm does not allow for an easy way to apply boundary conditions on the solution.

A simple and crude way is to just allow for one optimization step within the algorithm. After the one iteration has finished, the optimized values can be judged whether they are inside or outside the boundaries. If they are outside the boundaries, they can be reset or set to the boundary or given some other value. The parameters which did not end up outside the boundary can be kept. A new iteration is then undertaken with the new and constrained parameter values. This loop is broken up once the maximum number of iteration have been reached or if convergence has been achieved.

The simplest way to implement this is probably to just write a wrapper for the LM optimization. It will then take care of enforcing the constraints and checking for convergence. Within it, different approaches could then be taken as to how values which fall outside the boundaries are to be reset. Maybe start over from the initial values, but with the other parameters which did not result in values outside the boundaries being kept. Or the values could be slightly fuzzed, say with some arbitrary value but keeping it inside the boundary conditions.

Additional parameters which have to be provided to the wrapper method are the boundary conditions. Even better would be to provide some distribution of where a likely initial value should be. This could then be reminiscent of using priors.

C.4 Optimization with penalties

Another way to constrain the parameters in the optimization is to introduce penalties on the objective function being optimized. This is similar to the above method but the algorithm becomes aware of the boundary through the added penalty as the parameter move away from the allowed region. It is also implemented readily in the Levenberg-Marquardt algorithm.

Eventually however, this method was not used as at the time it seemed simpler to use another method. The parameters were assumed to be possible in certain intervals with the extreme values no less possible than any other¹.

C.5 How it was implemented

The previous section discussed a way to introduce boundary conditions by just resetting the values being optimized when the optimizer passed the boundaries. It would lead to the problem

¹This decision might have been a bad one as it turned out that the implementation got a bit complicated settling for the other method

that the optimizer is “unaware” that it has reached a boundary and it could be that it would end up in “corner” wanting to pass through the corner but by resetting the values each time it would not be able to reach a minimum and eventually the number of optimization iterations would get large enough that any sensible implementation would stop.

Another way to implement boundary conditions is to transform the variable, so that even though the transformed variable could have any value, the real value would still be in an interval. That is, map the interval defined by the boundary conditions for each variable to cover the full line.

From the set of all possible mapping, the tan (tangent) function was chosen. It will map the interval $(\pi/2, \pi/2)$ to cover the full line and at the same time it will also have a unique inverse and its first derivative is well defined. Why this is important will be touched upon shortly.

What is left then is to map the interval specified by the boundary conditions, let it be (a, b) to the interval $(-\pi/2, \pi/2)$.

This transformation has at least one flaw, it will map the interval boundaries to $\pm\infty$. If the optimum has a parameter which is at the boundary, the optimizer will never be able to reach it. However, it should not be too much of a problem as a large enough transformed variable will be close to the boundary. One thing which could cause problem is if it would take the optimizer many iterations to reach a large enough transformed variable.

So the first step is going from (a, b) to $(-\pi/2, \pi/2)$

$$\begin{aligned} e \in (a, b) &\rightarrow (-\pi/2, \pi/2) \\ f_{\text{Temporary}}(x) &= \left(x - a - \frac{b-a}{2} \right) \frac{2}{b-a} \frac{\pi}{2} \\ &= \frac{\pi}{b-a} \left(x - \frac{a+b}{2} \right) \end{aligned}$$

and then the full (a, b) to $(-\infty, \infty)$

$$\begin{aligned} x \in (a, b) &\rightarrow (-\infty/2, \infty/2) \\ f(x) &= \tan \left(\frac{\pi}{b-a} \left(x - \frac{a+b}{2} \right) \right) \end{aligned}$$

The Levenberg-Marquardt optimization uses the Jacobian for computing the update of the target function. In this case the target function is the offset of the stars position due to a planet; or the position of the star. This is expressed in the parameters which need to be constrained, so the transformation is made to constrain them. In the following parameters without a superset tilde will be consider the constrained/un-transformed parameter and parameters with a superset tilde will be consider the un-constrained/transformed paramters, e.g. for period with some constraints on P and without constraints \tilde{P}

So that means for the above

$$\begin{aligned} \tilde{x} &= \tan \left\{ \frac{\pi}{b-a} \left(x - \frac{a+b}{2} \right) \right\} \\ &= \tan \left\{ \frac{\pi}{2} \left(\frac{2x - b - a}{b-a} \right) \right\} \end{aligned}$$

The inverse transformation is then

$$\begin{aligned} x &= \frac{a+b}{2} + \frac{b-a}{\pi} \arctan \tilde{x} \\ &= \frac{1}{2} \left\{ a+b + \frac{2(b-a)}{\pi} \arctan(\tilde{x}) \right\} \end{aligned}$$

with the derivative (needed for computing the Jacobian)

$$\frac{dx}{d\tilde{x}} = \frac{b-a}{\pi} \frac{1}{1+\tilde{x}^2}$$

Also, instead of using the orbital elements (the angles Ω , i and ω) the problem is transformed to solve in the Thiele-Innes parameters directly. As the Thiele-Innes parameters contain both the semi-major axis and the parallax in addition to the orbital elements, so these two parameters have to be brought outside and instead define the Thiele-Innes parameters as only consisting of the orbital elements.

This will then become for the offset in the tangential plane due to a planet

$$\begin{aligned} X^{\text{offset}} &= -m_r a \varpi (Ax + Fy) \\ Y^{\text{offset}} &= -m_r a \varpi (Bx + Gy) \end{aligned}$$

where m_r is the ratio of the planet to star mass. The elliptical coordinate (x, y) are the same as previously.

Previously the mass ratio had not been included but just assumed to have a fixed value. However, not all planets will have the same mass as can be seen in most listing of exo-planet data. In addition fixing the mass ratio to be Jupiter/Sun like would mean that potential brown dwarfs would be excluded¹.

C.5.1 Boundaries for eccentricity

Probably the most straightforward boundary is the eccentricity. The orbits should not have negative eccentricity, as it is quite customary to have it positive and at the same time this will get rid of some ambiguities on the planetary motion. At the same time, the eccentricity should not be greater than one as this otherwise would imply that the planets are unbound. That is an interval of $(0, 1)$

The lower boundary for the eccentricity is a slight concern. An eccentricity of zero is a very real possibility, but this point is not included in the allowed range. This would then mean that the optimization would never be able to reach this point. However, a *very* small eccentricity is not that different from zero, and depending on the question asked it could be considered zero. Note though that this would introduce a slight bias for positive values.

Eccentricities greater than one would mean that the planets are unbound and the situation would be more described along the lines of a close encounter with a free floating planet. It is possible that it would happen but as the main interest here is for orbiting planets these events are grouped into eccentricities just below one.

¹1 up for the brown dwarf desert

$$\begin{aligned}
e &\in (0, 1) \\
\tilde{e} &= \tan \left\{ \frac{\pi}{2} (2e - 1) \right\} \\
e &= \frac{1}{2} \left\{ 1 + \frac{2}{\pi} \arctan(\tilde{e}) \right\} \\
\frac{\partial e}{\partial \tilde{e}} &= \frac{1}{\pi} \frac{1}{1 + \tilde{e}^2}
\end{aligned}$$

C.5.2 Semi-major axis

Convention has it that the semi major axis is positive (nothing prohibits negative semi-major axes as it could be combined with, say, a negative period to give a realistic situation). The lifetime of the mission is limited so it would not make sense to have an orbit with an period many times the mission lifetime. So this upper bound is set to a_{\max} and decided when running a simulation giving an interval of $(0, a_{\max})$ for the semi-major axis. Note that the semi-major axis is not directly used in the optimization but comes in through the Thiele-Innes parameters.

C.5.3 Thiele-Innes parameters

The Thiele-Innes parameters in their common form describe a rotation plus a scaling. To simplify things, the scaling (semi major axis and parallax) can be taken out from the Thiele-Innes parameters so they should just describe a rotation. This would then mean that they will have a value in the range of negative one to one¹. This is then an interval of $(-1, 1)$. Together with the semi-major axis this interval is $(-a_{\max}, a_{\max})$ for the Thiele-Innes parameters.

For the Thiele-Innes parameters $(A, B, C, F, G$ and $H)$ only A is used to denote any of them as they have the same boundaries and transform the same.

$$\begin{aligned}
A &\in (-a_{\max}, a_{\max}) \\
\tilde{A} &= \tan \left\{ \frac{\pi}{2} \frac{A}{a_{\max}} \right\} \\
A &= \frac{2a_{\max}}{\pi} \arctan(\tilde{A}) \\
\frac{\partial A}{\partial \tilde{A}} &= \frac{2a_{\max}}{\pi} \frac{1}{1 + \tilde{A}^2}
\end{aligned}$$

C.5.4 Period

The same reasoning as for semi-major axis applies to the orbital period. After all, they are related through Kepler's third law. So an interval of $(0, P_{\max})$ is chosen.

This period boundary could have been calculated from the semi-major axis boundary but then some assumptions would have to be made on the central mass, so instead it was just set to a reasonable value.

¹Imagine taking a unit vector, rotating it and looking at its components. None of the components should be outside the range of negative one to one unless an effort is made to construct a special coordinate system(?)

$$\begin{aligned}
P &\in (0, P_{\max}) \\
\tilde{P} &= \tan \left\{ \frac{\pi}{2} \left(\frac{2P - P_{\max}}{P_{\max}} \right) \right\} \\
P &= \frac{1}{2} \left\{ P_{\max} + \frac{2P_{\max}}{\pi} \arctan(\tilde{P}) \right\} \\
\frac{\partial P}{\partial \tilde{P}} &= \frac{P_{\max}}{\pi} \frac{1}{1 + \tilde{P}^2}
\end{aligned}$$

C.5.5 Time of periapsis passage

The time of periapsis passage is the point in time when the planet is closest to its host star, the periapsis/periastron passage. So picking an “arbitrary” point, in this case the time of mission mid point, the plane will within one period cover all its possible positions of the orbit. So the time of periapsis can be set as “time of mission mid point” plus or minus “a maximum period”, i.e. in the interval $(t_m - P_{\max}, t_m + P_{\max})$

$$\begin{aligned}
t_p &\in (t_m - P_{\max}, t_m + P_{\max}) \\
\tilde{t}_p &= \tan \left\{ \frac{\pi}{2} \left(\frac{t_p - t_m}{P_{\max}} \right) \right\} \\
t_p &= t_m + \frac{2P_{\max}}{\pi} \arctan(\tilde{t}_p) \\
\frac{\partial t_p}{\partial \tilde{t}_p} &= \frac{2P_{\max}}{\pi} \frac{1}{1 + \tilde{t}_p^2}
\end{aligned}$$

C.5.6 Mass ratio

Again it is restricted to positive values (unconstrained optimization would find negative mass with some extra rotation to be just as good). Upper limit could then be the lower limit for deuterium burning or somewhere around there, $m_{r,\max}$. This then gives the interval $(0, m_{r,\max})$

$$\begin{aligned}
m_r &\in (0, m_{r,\max}) \\
\tilde{m}_r &= \tan \left\{ \frac{\pi}{2} \left(\frac{2m_r - m_{r,\max}}{m_{r,\max}} \right) \right\} \\
m_r &= \frac{1}{2} \left\{ m_{r,\max} + \frac{2m_{r,\max}}{\pi} \arctan(\tilde{m}_r) \right\} \\
\frac{\partial m_r}{\partial \tilde{m}_r} &= \frac{m_{r,\max}}{\pi} \frac{1}{1 + \tilde{m}_r^2}
\end{aligned}$$

C.6 Construction of the Jacobian

With all the partial derivatives the Jacobian can be constructed. In the optimization procedure the Jacobian is used to determine the update of the parameters and also, one the optimizer has converged, to calculate an estimate of the standard errors on the parameters.

What is measured by Gaia are not the X^{Offset} etc, instead two field angles are measured η and ζ for what is called the “along scan” and “across scan” respectively. These two angles are functions of the astrometric parameters, and through that also functions of the planetary parameters if they are included.

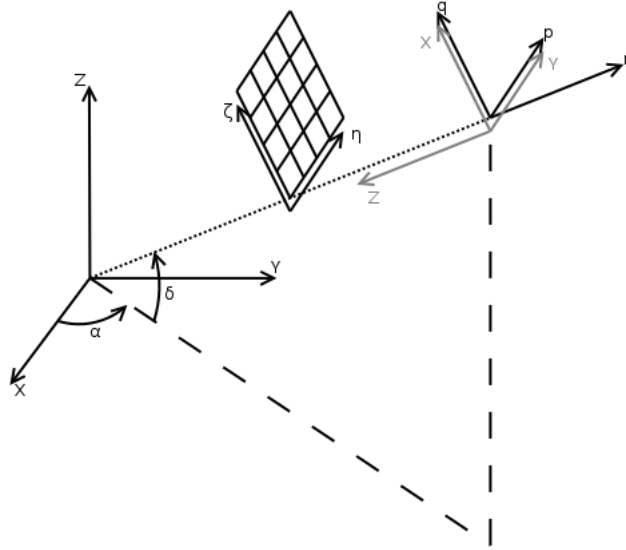


Figure C.1: The relation between some different coordinate systems used. The black (X, Y, Z) refer to the equatorial coordinate system with X pointing towards the Vernal equinox and Z the north polar axis. In this system a star position is given by the right ascension (α) and declination (δ). Related is the normal triad (p, q, r) on the celestial sphere such that p is in the direction of increasing right ascension and q in direction of increasing declination. The vector r is normal to the celestial sphere. Partially aligned with this is what in here is called the “tangential coordinate system”, the gray (X, Y, Z) in the Figure. The third system is what Gaia will measure (ζ, η) , where ζ and η will be function of α and δ among other parameters, i.e., $\zeta = \zeta(\alpha, \delta) = \zeta(\alpha_0 + \alpha^{\text{Offset}}, \delta_0 + \delta^{\text{Offset}}) = \zeta(\alpha_0 + Y^{\text{Offset}}, \delta_0 + X^{\text{Offset}})$ and likewise for η where X^{Offset} and Y^{Offset} are the positional offsets of a star due to a planet.

Let $f_1, f_2 \dots f_n$ be a functions of some parameters $x_1, x_2 \dots x_m$, then the (i, j) 'th element of the Jacobian is

$$J_{i,j} = \frac{\partial f_i}{\partial x_j}$$

which then, for say the along scan ζ and the astrometric parameters give a row in the Jacobian

$$\frac{\partial \zeta_i}{\partial \alpha_*}, \frac{\partial \zeta_i}{\partial \delta}, \frac{\partial \zeta_i}{\partial \mu_{\alpha_*}}, \frac{\partial \zeta_i}{\partial \mu_{\delta}} \dots$$

that is to say the partial derivatives of the i 'th measurement (or at time t_i) of ζ . If the planetary parameters are included then this row has to be expanded

D Testing of Code

D.1 Spread of observations points in time

Much of the testing and experimenting is done with points uniformly spaced in time. This is not necessarily representative of the points in time that Gaia will do an observations. The reason for this is that it takes some time to generate the attitude spline etc. Doing the optimization for the orbital parameters is a small step so it takes a much shorter time. To get an overview of the spread over time of observations for Gaia a small test was done in which the position was noted down for the observations. This is a particular case in which the star has zero declination so it might not be that representative for all stars as the sky coverage is not uniform. In Figure D.1 the result is plotted. So uniformly spaced points in time for testing is probably acceptable, at least if the star has zero declination.

D.2 Residuals when knowing the period

What would happen if for example the period was known before the optimization started? It seems probable that it would really help as it would mean one less parameter to optimize but also that it might help if the initial guesses for the other parameters were not that good.

This could be somewhat explored by doing two optimizations; one with known period and one where the period is not known. The other parameters are the same for both tries. Repeating this procedure many times over will then give a somewhat more bases argument if knowing the period is good.

First thing to decide is how to select the initial parameter. To keep it simple, the initial parameter is taken as the true parameter with a random offset. If the true parameter is x , the offset is limited to 12% and u a uniformly distributed random variable over $(-1, 1)$ then $x_{\text{initial}} = x(1 + 0.12u)$.

This also means that the true parameter has to be restricted such that $x(1 \pm 0.12)$ still is in the allowable range for the parameter, other than that the true parameter is chosen uniformly over the restricted allowable range.

For the period, it is calculated using Kepler's third law by assuming that the central mass is as massive as the Sun.

Then the optimization is performed once for the known period and once for unknown period. The sum of the squared weighted residuals, in this case called χ^2 in the optimization routine, is recorded as well as the number of iteration it took to reach convergence. This is then in this case repeated 5000 times. What the result of one of these simulations might look like is in Figure D.2. In the same picture the two different optimization results are also plotted and it looks like both of them converged.

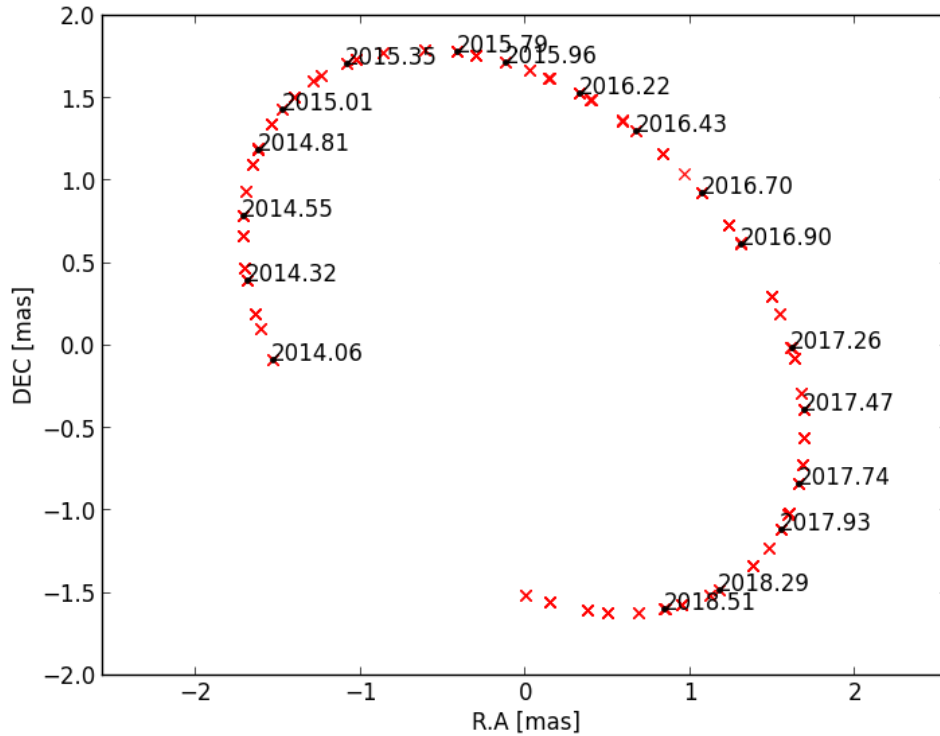


Figure D.1: This is how observations are spread out over time. The system consists of a Jupiter-sized planet orbiting a star in a nearly face on orbit. Semi major axis is ~ 3 AU and the system has a parallax of ~ 544 mas. On the axis are position (α_0, δ_0) in milli-arc seconds. The red 'x'-s are the observations. What looks like a single 'x' is in reality a group of about 10 observations. Every 50 observation is marked with a black dot and year. Note that these observations are at the same times as Gaia would do the observations.

To decide if there is a difference between the two situations a two sample Kolmogorov-Smirnov test is used. That is, compute the maximum absolute difference between the two empirical cumulative distribution functions

$$D = \max_{-\infty < x < \infty} |S_{N_1}(x) - S_{N_2}(x)|$$

where the χ^2 value of the residuals is used as the free parameter.

The null hypothesis in this case is that the two functions are the same which can be rejected if either the Kolmogorov-Smirnov statistic above is large, or if the p-value is low.

Using the statistics routine `scipy.stats.ks_2samp`¹ the computed p-value is $8.43e - 13$ and the Kolmogorov-Smirnov statistic is 0.078. So the null hypothesis can be rejected.

In Figure D.3 the empirical cumulative distribution functions are shown. The blue line is the case with known period and the red line is when the period is not known. So not knowing the period looks like it would result in slightly larger residuals.

¹Python SciPy routine

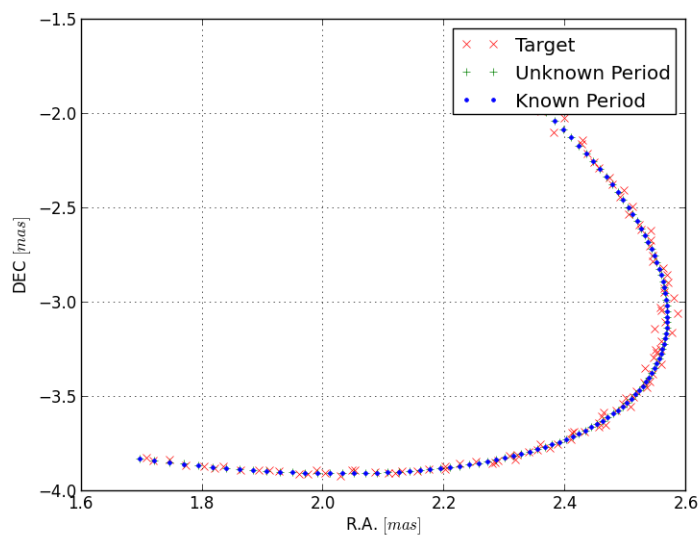


Figure D.2: Typical orbit for one of the iterations in the simulations. The dots representing start from un-known period are hidden behind the dots for the known period. So both have been optimized to the same parameters.

That the residuals are larger could be the result of fewer iterations in the optimization routine. This, however, is probably not the case. In figure D.4 the \log_{10} of the number of iterations performed until convergence is shown. Again the blue line is for known period and the red is for un-known period. Clearly the number of iterations performed when knowing the period are fewer.

So knowing the period do seem to help.

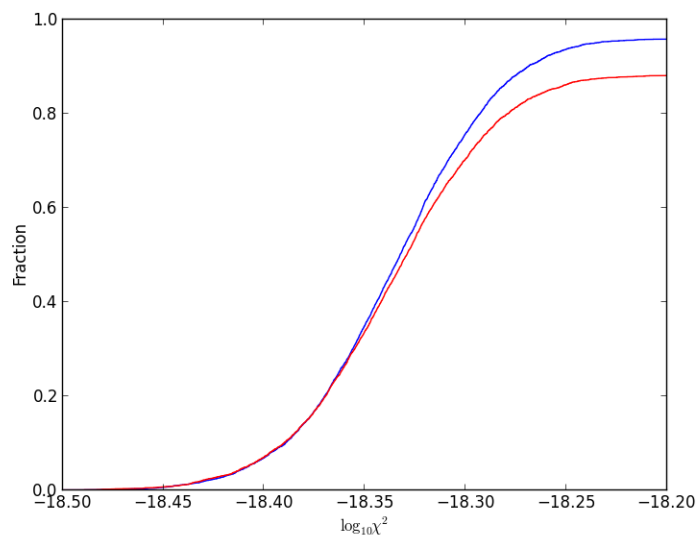


Figure D.3: Empirical cumulative distribution function of the weighted residuals. The red line is for optimizing all parameters, i.e. they are all unknown in the beginning. Blue line correspond to a *known* period, that is fix the period to its true value in the beginning of the optimization procedure. Knowing the period result in smaller residuals. Note that the x-axis is truncated.

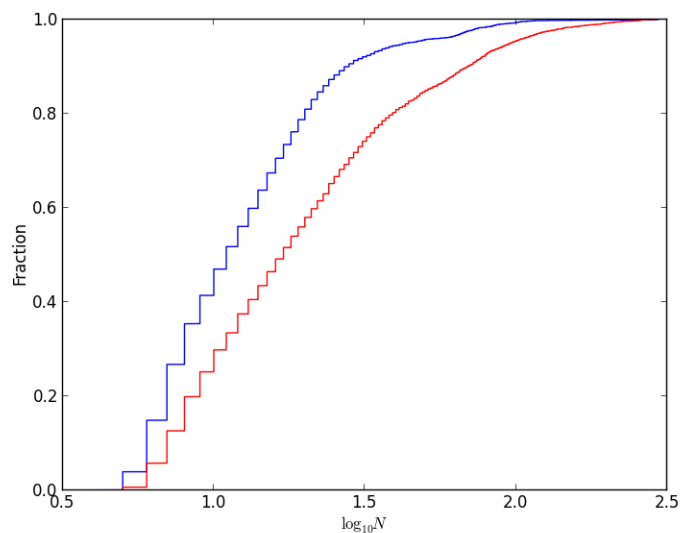


Figure D.4: Empirical cumulative distribution function for the number of iterations until convergence. The red line is for optimizing all parameters, i.e. they are all unknown in the beginning. Blue line correspond to a *known* period.